DIGITAL ACCESS TO SCHOLARSHIP AT HARVARD
DASH.HARVARD.EDU

HARVARD LIBRARY

Amine-mediated CO2 hydration as a potential carbonic anhydrase alternative in marine Thaumarchaeota

Citation

Kocharian, Elida. 2021. Amine-mediated CO2 hydration as a potential carbonic anhydrase alternative in marine Thaumarchaeota. Bachelor's thesis, Harvard College.

Link

https://nrs.harvard.edu/URN-3:HUL.INSTREPOS:37368567

Terms of use

This article was downloaded from Harvard University's DASH repository, and is made available under the terms and conditions applicable to Other Posted Material (LAA), as set forth at

https://harvardwiki.atlassian.net/wiki/external/NGY5NDE4ZjgzNTc5NDQzMGIzZWZhMGFlOWI2M2EwYTg

Accessibility

https://accessibility.huit.harvard.edu/digital-accessibility-policy

Share Your Story

The Harvard community has made this article openly available.
Please share how this access benefits you. Submit a story

Amine-mediated CO_2 hydration as a potential carbonic anhydrase alternative in marine Thaumarchaeota

A Thesis Presented
by
Elida Kocharian
to
The Department of Earth and Planetary Sciences
and
The John A. Paulson School of Engineering and Applied Sciences
Area of Environmental Science and Engineering
in partial fulfilment of the requirements
for a degree with honors
of Bachelor of Arts

Harvard University
Cambridge, MA
March 2021

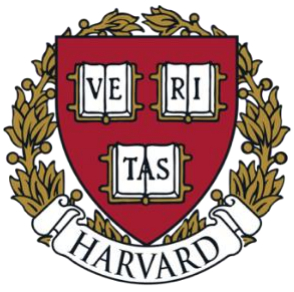

Abstract

Marine Thaumarchaeota are ammonia-oxidizing archaea that make up the predominant group of nitrifiers in the global N cycle and fix bicarbonate (HCO_3^-) autotrophically via the highly efficient 3-HP/4-HB pathway. Most autotrophs produce intracellular bicarbonate via the ubiquitous enzyme carbonic anhydrase (CA), which catalyzes CO_2 hydration. However, the common Thaumarchaeota species *Nitrosopumilus maritimus* lacks CA, and it is unknown how this organism produces sufficient intracellular bicarbonate to satisfy its anabolic requirement without this enzyme. One hypothesis is the autocatalytic addition of water to CO_2 mediated by free intracellular amines, in the form of protein N-termini, via a carbamate intermediate at physiological pH. In order to determine the viability of this bicarbonate pathway as a potential CA alternative in *N. maritimus*, the reaction kinetics of 12 aqueous primary and secondary amine solutions buffered to pH 7.2 were measured via ^{13}C NMR spectroscopy and compared to a novel chemical kinetic model of intracellular carbon dynamics in *N. maritimus*. The experimental observations showed that amine reactivity generally increases with increasing pKa of the amine group, but is heavily influenced by the amine structure; primary and secondary amines form carbamate and bicarbonate through a two-step mechanism involving formation and decarboxylation of a carbamate zwitterion, while sterically hindered and tertiary amines form bicarbonate via a base-catalysis mechanism in which the nitrogen abstracts a proton from water to drive CO_2 hydroxylation. The measured 1^{st}-order reaction rate constants of carbamate formation and dissociation are 1.1×10^{-2} s^{-1} and 4.88×10^{-3} s^{-1} respectively, yielding intracellular fluxes of carbamate and bicarbonate of 4.4×10^{-4} mM s^{-1} and 1.46×10^{-4} to 1.46×10^{-2} mM s^{-1}, respectively. The bicarbonate-fixing enzyme of the 3-HP/4-HB pathway, acetyl-CoA/propionyl-CoA carboxylase, has a turnover rate of 2.168×10^{-1} mM s^{-1}, and the modeled fluxes required to sustain

this rate are 5.067 x 10^{-1} mM s^{-1} for carbamate formation and 2.153 x 10^{-1} mM s^{-1} for carbamate dissociation/bicarbonate formation. Thus, the flux of bicarbonate supplied by amine-mediated CO_2 hydration is insufficient to drive autotrophy in *N. maritimus*. Future work to determine the reaction kinetics of tertiary amines could shed light on the potential activity of the base-catalysis pathway of amine-mediated CO_2 hydration; however, it is suggested that the true hydration mechanism may be driven by the generation of hydroxide ions *in situ* coupled to redox potentials present in copper-containing oxidoreductase enzymes responsible for electron transfer at the cell membrane that could double as CA alternatives or antecedents.

Table of Contents

Abstract ii

List of Figures vi

Acknowledgements vii

Introduction and Background 1

1. Introduction 1

2. Marine Thaumarchaeota Play an Important Role in the Evolution of Ancient Archaeal Autotrophy 3

3. Amine-Mediated CO_2 Hydration Has Potential to Act as an Autocatalytic Carbonic Anhydrase Alternative or Antecedent 6

4. Amine-Mediated CO_2 Hydration: Mechanisms & Kinetics 10

a. Experimental Techniques in Quantifying Carbamate Kinetics 12
b. Carbamate Chemistry in Biology: What Is Known Thus Far 13
c. Carbamate-Driven Methanogenesis in M. barkeri is the Closest Biological Analogue for the Comparative Study of N. maritimus 15

5. Goals & Objectives 16

Methods 18

1. Experimental Procedure for the Use of ^{13}C NMR Spectroscopy to Measure Reaction Kinetics of Amine-Mediated CO_2 Equilibration in Aqueous Solution 19

a. Experimental Amines 19
b. Sample Preparation 19
c. ^{13}C NMR Spectroscopy 21

2. Kinetic Analyses & Modeling 24

a. Extracting Kinetic Parameters from NMR Spectra 24

Results 28

1. Amine Reactivity 28

a. Amino Acids 32
b. Protected Amino Acids & Mixtures 33
c. Abiotic Solvents 35
d. Peptides and Proteins: Glutathione and Cytochrome C 36

2. Kinetic Analyses of Carbamate- and Bicarbonate-Producing Reactions 39

a. Ethanolamine 39
b. Piperidine 42

3. Modeling Amine-Mediated CO_2 Hydration Chemistry in N. maritimus 46

Discussion 49

1. Amine-CO_2 Reactivity is Determined by Amine pKa and Structure 49

a. Amino Acids, Protecting Groups, and Mixtures 49
b. Ethanolamine 51
c. Diethanolamine 52
d. Piperidine 53
e. 2-amino-2-methyl-1-propanol 54
f. Peptides and Proteins 56

2. Experimental & Model Results Suggest Low Viability of Amine-Mediated CO_2 Hydration in N. maritimus 56

a. Carbamate Dissociation Could Account for Observed Carbon Isotope Fractionation Effects in N. maritimus 58
b. Carbamate Chemistry is Similar to the Chemical Mechanism & Evolution of Carbonic Anhydrase 60
c. Further Investigations Should Focus on Amines as Base Catalysts in CO_2 Hydration and Redox Coupling at the Electron Transport Chain as Alternative Mechanisms 62

3. Broader Implications for Autocatalysis & the Origins of Life 65

Conclusion 67

References 69

Appendix I: Supplementary Data 73

NMR Spectra 73

Appendix II: Glossary 81

Appendix III: Alternative Thesis Titles 83

List of Figures

Figure 1. Scanning electron micrograph of *N. maritimus*..... 4
Figure 2. The 3-HP/4-HB cycle 4
Figure 3. Schematic of amine-mediate CO_2 hydration in *N. maritimus* 9
Figure 4. Reaction VI: tertiary amine base catalysis mechanism. 12
Figure 5. Methods flowchart. 18
Figure 6. Vacuum line setup for NMR tube $^{13}CO_2$ pressurization 23
Figure 7. Control 1 ^{13}C NMR spectrum f 30
Figure 8. Control 1 stacked spectral timeseries 30
Figure 9. Control 1 concentration timeseries. 31
Figure 10. Ethanolamine-glycine mixture ^{13}C NMR spectrum. 34
Figure 11. Ethanolamine-glycine mixture stacked spectral timeseries. 34
Figure 12. Ethanolamine-carbamate and glycine-carbamate reaction mechanisms 35
Figure 13. Ethanolamine ^{13}C NMR spectrum 37
Figure 14. Ethanolamine stacked spectral timeseries. 37
Figure 15. Piperidine ^{13}C NMR spectrum 38
Figure 16. Piperidine stacked spectral timeseries 38
Figure 17. Ethanolamine concentration timeseries 40
Figure 18. Ethanolamine reaction rate curve 41
Figure 19. Ethanolamine-mediated CO_2 hydration mechanism. 41
Figure 20. Piperidine concentration timeseries. 44
Figure 21. Piperidine reaction rate curves. 45
Figure 22. Piperidine-mediated CO_2 hydration mechanism 45
Figure 23. *N. maritimus* chemical kinetic model schematic. 46

Table 1: Amines tested in this study & their properties. 27
Table 2. Amine reactivity. 29
Table 3. *N. maritimus* chemical kinetic model parameters. 48
Table 4. Measured and Modeled Rate Constants and Fluxes. 57

Acknowledgements

Science is a team sport! I'm nobody without my teammates, who have helped me through one of the most challenging years of my life, who have lifted me up and supported me and pushed me to grow throughout these four incredible years of college, and who I know will continue to have my back every step I take into the future. I am so, so grateful. Not even the COVID-19 pandemic can keep us down!

First and foremost, I thank my brilliant coach, Ann Pearson, who inspired me to study EPS the second I walked into her class during my first year, who welcomed me into her lab and under her wing, and who has always had faith in me, even when I did not. You are the best mentor I could have asked for—thank you for teaching me how to be a scientist.

Thank you to Susie Carter, for supplying me with infinite support, laboratory skills, and enough liquid nitrogen and dry ice to freeze all of Hoffman Labs. This thesis would not be possible without you, and the entire fabulous Pearson Lab team—it's been an awesome four years!

Thank you to Jenan Kharbush, who (miraculously and graciously) took a chance on me as a research assistant in the Pearson Lab my first year of college even though I had never held a pipette before. I am forever grateful for your mentorship, support, and trust (and forgiveness…sorry about contaminating all those diatoms!).

Thank you to Esther James and Annika Quick for your endless patience and support in this virtual thesis experience, and of course, thank you to my co-thesis writers, Maddie Goldberg and Ethan Manninen, who are literally geniuses that I could not admire and adore more. Thank you also to Lorenzo Manuali and Jess Moore, for your infinite support and commiseration and deep understanding of the very silly verb "thesising." WE DID IT!!!

Thank you to the rest of my EPS family, with whom I've experienced the unimaginable and done the impossible, from getting towed out of an Icelandic river in a gigantic pastel green bus to writing an original jukebox musical based on this wacky and wonderful department: Sophie Webster, Noah Epstein, Joseph Winters, and Caleb Fried. And of course, thank you to the man, the myth, the legend, Jerry Mitrovica, the best non-geologist geology professor this side of the San Andreas Fault.

Thank you to the single most important figure in my Harvard education, Chenoweth Moffatt, who encouraged me to study EPS that fateful day I first stepped into her office, which was always like walking into sunshine on a cloudy Cambridge day. It was the best decision I have ever made.

I have been outrageously lucky in my life to have had the most dedicated, kind, and gifted teachers in the world. Thank you to my Chem 20 & 30 TFs for teaching me orgo (and dealing with me as you taught me orgo, which is almost the harder task): Min Bae, Petra Vojackova, Porter Ladley, and Corin Wagen. Thank you to Josh Cox and Jessica Liu for being incredible chemistry/biochemistry TFs and for answering my crazy questions, even years after I took your classes. Finally, to the folks who made me want to be scientist in the first place, Ms. Lynch, my

7th grade biology teacher, and Dr. Wahi, my high school chemistry teacher: I am so grateful to have been your student, and I hope I've done you proud!

Thank you to the incredible LPIC staff in CCB, Dongtao Cui and Tony Lowe, without whose generous mentorship on all things NMR this research would not have been possible.

Thank you to my amazing Women in STEM mentor, Hannah Smith, for TOT time and laughter.

Thank you to Izzy Baker, for your selfless mentorship and endless encouragement.

Thank you to my Harvard Forest mentor, Tim Whitby, for letting me frolic in the woods in the name of science during the best summer of my life.

Thank you to Sqad*100*, my teammates since '13: Lindsay, Chloe, Abby, Keila, Emilie, Maya, and Zoe. Lil nerd wrote a thesis!

And, of course, thank you to the best team of all time, the Dewolfepack: Isabelle Blair, Haig Cholakian, Lorenzo Manuali, Matt Gilbert, Carlos Robles, Robby Blank, Isaac Ortega, Shaik Abiden, and especially Harry Hager, who is a chemistry god and who I could not have even conceived of writing this thesis without. Special thanks also to Isabelle Blair, for joint custody of our brain cell—she's worked so hard, and yet we're still fools. Ferda. I love you all with my whole heart. *AWOOOOOOO!!!!!!!!!!*

Finally, thank you to my family: Mom, Dad, Lucy, Greg, Tata, Dedo, Nana, Tatik, Papik, and Griesh. You are my coaches, my teammates, and my #1 fans. Thank you for your love, your sacrifice, your support, your hard work, and your hope. You are my whole world, and I am so proud to be your daughter, your granddaughter, your niece, your sister. Եէս ձէզ աշխարհի չափ սիրում էմ եւ հարքում էմ: Շնորհակալություն:

Introduction and Background

1. *Introduction*

Out in the open ocean there floats a tiny creature that may hold a clue to the origins of life. One thousandth the width of a human hair, *Nitrosopumilus maritimus* is a single-celled species of marine archaea that makes its living in the most dilute waters of the ocean. *N. maritimus* is an ammonia-oxidizing chemoautotroph, meaning it transforms inorganic carbon from its environment into organic carbon using the electron-donating nitrogenous compound ammonia as an energy source (as opposed to plants, which are photoautotrophs that use solar energy, and humans, which are heterotrophs that consume other organisms to survive); it utilizes bicarbonate (HCO_3^-), the ocean's most abundant form of carbon, as its inorganic carbon source. However, two obstacles stand between this microbe and the acquisition of bicarbonate. The first is its cell membrane. Archaeal cell membranes are composed of lipid monolayers that are nearly impermeable to ions, so the cell must transform aqueous carbon dioxide (CO_2) that freely diffuses across the membrane into HCO_3^-. For most organisms, this process is swift and simple due to the nearly ubiquitous enzyme carbonic anhydrase (CA). CA hydrates carbon dioxide to H_2CO_3, which then spontaneously and rapidly dissociates to $HCO_3^- + H^+$. Here lies the second obstacle: *N. maritimus* lacks this key enzyme and any other intracellular enzymatic machinery known to carry out this hydration reaction (Könneke et al., 2014; Pearson et al., 2019). Thus, an existential metabolic problem emerges: how does this archaeon transform carbon dioxide to bicarbonate at a rate fast enough to support its central carbon metabolism?

Without an enzyme to lower the activation energy required for the reaction to proceed, a simple chemical process may substitute as a non-enzymatic alternative. *N. maritimus* is especially energetically short-changed, since it inhabits oligotrophic, or nutrient-poor, zones of the ocean.

All known *Nitrosopumilus* (and the close relative, *Nitrosopelagicus*) isolates grow very slowly, with estimated generation times *in situ* of 2-5 days (Könneke et al., 2005; Santoro & Casciotti, 2011) reflecting their very slow rates of ammonia oxidation (Martens-Habbena et al., 2009) and carbon fixation (Könneke et al., 2014). Thus, an autocatalytic reaction mechanism, in which the product of the reaction re-forms one or more of the reactants in a sort of chemical "recycling," would be a viable enzyme alternative, if it uses reactants that easily complex with carbon dioxide and are widely available within the cell.

One reaction that fits these criteria is the reaction of carbon dioxide with aqueous amines to form a carbon dioxide-amine adduct called carbamate. Amines are chemical functional groups consisting of a reduced nitrogen bonded to carbon (e.g., RNH_2) and are ubiquitous in biological compounds like amino acids, peptides, and proteins. Carbamate can dissociate under slightly basic (pH > 7) conditions to yield HCO_3^- and the original amine, thus completing an autocatalytic cycle and producing the coveted bicarbonate. But how can this theoretical process be tested to find out if it can sustain the metabolism of *N. maritimus*? If the rate of bicarbonate formation from the reaction of carbon dioxide with a solution of aqueous amines under biological conditions can be measured, then it can be compared to the rate of carbon fixation of *N. maritimus*, which is known, and thus it can be determined whether carbamate-bicarbonate dissociation is a viable substitute for carbonic anhydrase. The stakes of solving this metabolic puzzle aren't limited only to understanding the viability of marine ammonia-oxidizing archaea: if this type of enzyme-free, autocatalytic carbon cycling can power the metabolic cycle of a modern organism, it could also serve as a looking glass to the history of autotrophic carbon fixation, the evolution of ancient lineages of archaea, and perhaps even the origins of life itself. In this way, we can answer big

questions about the origins of life and autotrophic carbon fixation by studying theoretical chemistry at the molecular level.

2. *Marine Thaumarchaeota Play an Important Role in the Evolution of Ancient Archaeal Autotrophy*

N. maritimus is a member of the group 1.1a marine Thaumarchaeota, which includes several archaeal ammonia-oxidizers that make up the predominant group of nitrifiers in the global nitrogen cycle (Fig. 1, Berg et al., 2010; Brochier-Armanet et al., 2012; Könneke et al., 2005, 2014). Thaumarchaeota utilize the enzyme acetyl-CoA/propionyl-CoA carboxylase to fix HCO_3^- via the 3-hydroxyproprionate/4-hydroxybutyrate (3-HP/4-HB) pathway of autotrophic carbon fixation (Fig. 2). The 3-HP/4-HB pathway is one of six known autotrophic carbon fixation pathways, which include the Calvin cycle, the reductive citric acid cycle (rTCA), the reductive acetyl-CoA pathway, the 3-hydroxyproprionate (3-HP) cycle, and the dicarboxylate/4-hydroxybutyrate pathway (Berg et al., 2010). The reductive acetyl-CoA, or Wood-Ljungdahl, pathway, anaerobically fixes CO_2 to form the central metabolic two-carbon precursor molecule, acetyl-CoA, and has been suggested to be the closest to ancestral autotrophic carbon fixation for several reasons: it uses carbon monoxide (CO), a common volcanic gas with a strong reduction potential, as an intermediate; it can co-assimilate many simple one-carbon units at various oxidation levels; it has minimal energy requirements; it is present in methanogenic archaea as well as anoxic bacteria; it is reversible because it operates near thermodynamic equilibrium, whereas other autotrophic pathways (save rTCA) are unidirectional; and it extensively uses coenzymes, metal cofactors, and environmental minerals that could have catalyzed a primordial inorganic carbon fixation pathway on early Earth (Berg et al., 2010; Fuchs, 2011; Preiner et al., 2019, 2020).

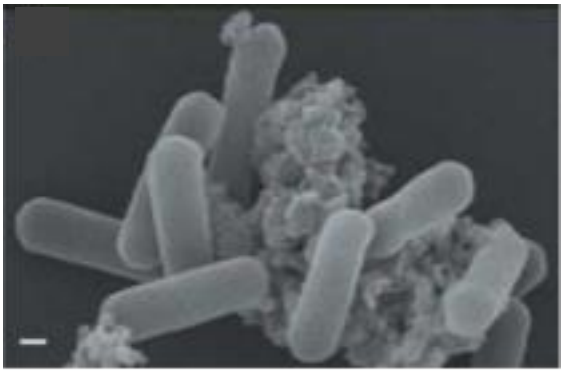

Figure 1. Scanning electron micrograph of Au/Pd-sputtered *N. maritimus* cells, from Könneke et al. (2005). Scale bar represents 0.1µm.

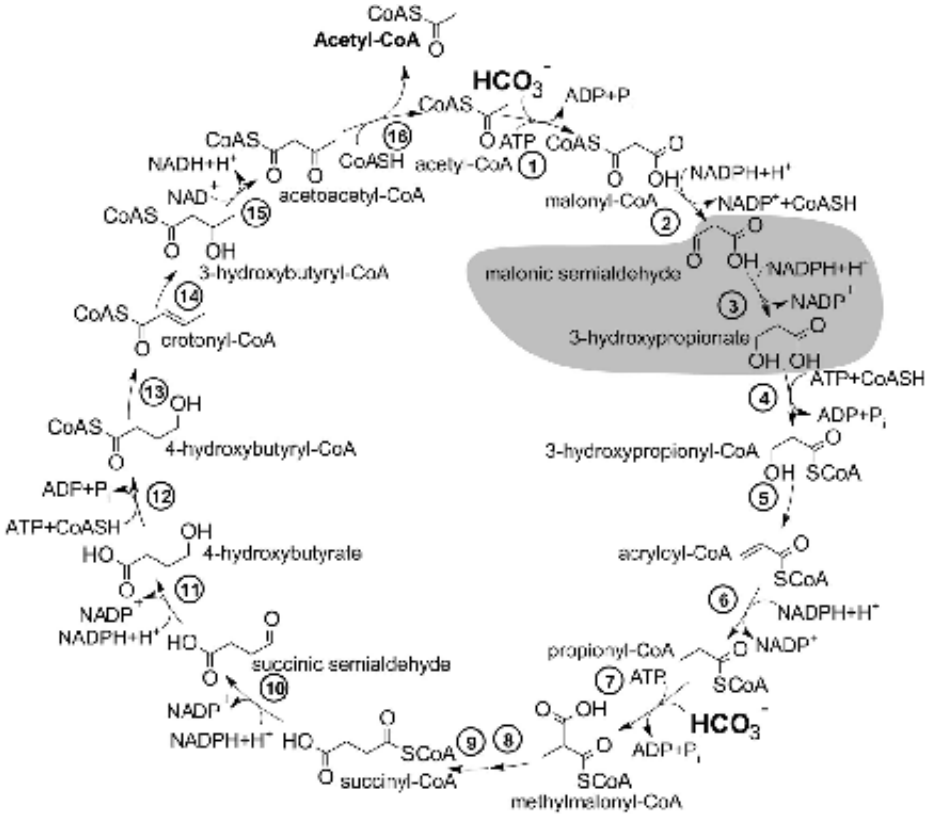

Figure 2. The 3-HP/4-HB cycle for autotrophic carbon fixation in *N. maritimus* (Otte et al., 2015). The numbered enzymes 1 and 7 represent the promiscuous acetyl-CoA/propionyl-CoA carboxylase, using bicarbonate as its carbon substrate to first convert acetyl-CoA to malonyl-CoA, then later propionyl-CoA to methylmalonyl-CoA.

While the reductive acetyl-CoA pathway utilizes CO_2 as its carbon source, autotrophs may profit from using HCO_3^- instead of CO_2, since the slightly alkaline pH of seawater allows for more freely available bicarbonate than dissolved CO_2. Enzymes like the promiscuous acetyl-

CoA/propionyl-CoA carboxylase of the aerobic 3-HP/4-HB pathway, which takes either acetyl-CoA or propionyl-CoA as substrate, have relatively low bicarbonate affinities and would benefit from the higher bicarbonate concentration in seawater (Fuchs, 2011); however, such reasoning has often neglected the complicating factor of ion transport across membranes. Alternatively, ions like HCO_3^- that have low permeability across biological membranes may have promoted the development of more specific, efficient, and easily regulated enzymes and related intracellular cycles (Davis, 1958). Following this reasoning, carbon-fixing enzymes utilizing bicarbonate may have had an evolutionary advantage over enzymes utilizing CO_2. The development of the 3-HP/4-HB pathway could mark an important evolutionary branching point between early anaerobic cycles like reductive acetyl-CoA and the aerobic cycles presently used in many archaea (Fuchs, 2011). Moreover, the potential presence of an enzyme-free, autocatalytic mechanism to hydrate carbon dioxide in the absence of carbonic anhydrase could serve as further evidence of the evolutionary potential to trap ions essential to the development of ancient metabolisms.

3. *Amine-Mediated CO_2 Hydration Has Potential to Act as an Autocatalytic Carbonic Anhydrase Alternative or Antecedent*

Chronic energy stress is believed to be the primary selective pressure governing the evolution of archaea (Valentine, 2007). Protein biosynthesis is one of the most energetically costly cellular processes, so non-enzymatic reactions are low-energy solutions for achieving efficient metabolic chemistry at high selective pressure (Keller et al., 2015). In particular, enzymes in the central metabolism are subject to stronger selective pressure to increase their rates, since high-efficiency enzymes minimize the cost of production (Bar-Even et al., 2011). *N. maritimus* and other marine Thaumarchaeota use the promiscuous acetyl-CoA/propionyl-CoA carboxylase (ACC/PCC) as their primary enzyme (i.e., performing two distinct C-fixation steps with a single enzyme); a dual-function decreases the need for biosynthesis of separate enzymes to deal with different metabolites and allows the cell to scavenge carbon from a larger pool of intermediary sources (Hügler et al., 2003; Könneke et al., 2014). However, enzymes with larger numbers of substrates have lower affinities for each substrate (Bar-Even et al., 2011), so promiscuous enzymes like ACC/PCC are under even greater selective pressure to increase efficiency for multiple substrates. This means that ACC/PCC is simultaneously under pressure to be low-affinity/high-efficiency. Thus, enzymes like carbonic anhydrase, which are ubiquitous among other prokaryotic autotrophs yet biosynthetically costly, are out of the evolutionary reach of *N. maritimus,* which has evolved an extremely streamlined metabolism in order to minimize energy expenditures (the 3-HP/4-HB cycle is more efficient than any other aerobic carbon fixation pathway, using one third less energy than the Calvin cycle of photosynthetic organisms; Könneke et al., 2014). Not only does *N. maritimus* lack carbonic anhydrase, but it also apparently does not engage in bicarbonate import from its surroundings. While the *N. maritimus* genome includes a putative sodium-dependent bicarbonate transporter (Nmar_0485 in Qin et al., 2018; NCBI reference sequence

WP_012214868.1), which could shuttle HCO_3^- across the membrane into the cell via active transport, this gene is minimally expressed; thus, the organism wastes no energy in acquiring HCO_3^- from its surroundings (Offre et al., 2014; Pearson et al., 2019; Qin et al., 2018).

These observations yield critical clues into the development of a biologically robust autocatalytic network as a potential enzyme antecedent for cellular carbon capture, perhaps preceding and eventually leading to the evolution of carbon fixation. Autocatalytic networks are theoretical frameworks for the genetics and metabolism of prebiotic evolution; in these networks, a set of metabolites interacts to generate self-sustaining metabolic systems that promote the synthesis of constituent elements from input molecules (Preiner et al., 2019). Thus, in an energy-stressed archaeon, an autocatalytic cycle that takes advantage of existing intracellular metabolites to hydrate CO_2 to supply its anabolic requirement may have evolved as an enzyme alternative. While for *N. maritimus* this may represent a case of convergent evolution, the critical implication is that a spontaneous bicarbonate-generating mechanism may be inherently the minimum-energy solution to the problem of accessible carbon substrates, and thus a candidate for the most probable pre-biotic generator of intracellular inorganic carbon.

One of the most plausible pathways to build up molecules autocatalytically in aqueous medium is the addition of a carbonyl group to a nucleophile (Ruiz-Mirazo et al., 2014).[1] While there are many such chemical pathways that could facilitate the hydration machinery in *N. maritimus*, one particularly robust process was first proposed by Smith and Ferry (2000): the formation and dissociation of carbamates from CO_2 and free intracellular amines. Amines, in the form of the N-termini of proteins or bound to other metabolic intermediates, can attack incoming CO_2 to from a carbamate adduct, and then release HCO_3^- after base-catalyzed dissociation. If the

[1] Please note that there is a glossary of commonly used chemistry terminology in Appendix II for the reader's reference!

formation and subsequent dissociation of carbamates mediated by free cellular proteins yielded an intracellular flux of HCO_3^- faster than the spontaneous abiotic equilibration of CO_2 and HCO_3^- (0.04 s^{-1}; Zeebe & Wolf-Gladrow, 2001), it could produce sufficient HCO_3^- to fuel ACC/PCC and the 3-HP/4-HB pathway.

The proposed pathway can be modeled through the following chemical equations:

I. $CO_{2e} \rightleftarrows CO_{2i}$
II. $CO_{2i} + R\text{-}NH_2 \rightleftarrows R\text{-}N^+H_2COO^-$
III. $R\text{-}NHCOOH + OH^- \rightleftarrows R\text{-}NHCOOH_2O^-$
IV. $R\text{-}NHCOOH_2O^- \rightarrow R\text{-}NH_2 + HCO_3^-$
V. $HCO_3^- \rightarrow$ ACC/PCC

Here, CO_{2e} and CO_{2i} are the extracellular and intracellular concentrations of carbon dioxide, respectively; $R\text{-}NH_2$ represents a free intracellular amine; $R\text{-}N^+H_2COO^-$ represents the carbamate zwitterion; R-NHCOOH represents the neutral carbamate species; OH^- is hydroxide; $R\text{-}NHCOOH_2O^-$ represents the hydrated carbamate tetrahedral intermediate species; and ACC/PCC is the carbon-fixing enzyme acetyl-CoA/propionyl-CoA carboxylase. Reaction **I** represents the diffusion of aqueous carbon dioxide from seawater across the cell membrane into the cell. Reaction **II** describes the nucleophilic addition of an amine into the carbonyl of carbon dioxide, forming the carbamate zwitterion, which undergoes proton transfer to form the neutral species depicted in Reaction **III**. The carbonyl of this carbamate species can undergo nucleophilic attack by hydroxide (under basic conditions, shown here), or water, to form a tetrahedral intermediate, as shown in Reaction **III**. This intermediate can collapse in a spontaneous decarboxylation step to yield the original amine and bicarbonate, as shown in Reaction **IV**. In Reaction **V**, the bicarbonate product enters the 3-HP/4-HB carbon fixation cycle via the enzyme ACC/PCC, thus completing the proposed autocatalytic CO_2 hydration cycle. These equilibrium reactions are governed by the following rate constants, depicted in Fig. 3: r_1, the diffusion of CO_2

into the cell; r_{-1}, the diffusion of CO_2 out of the cell; r_2, formation of the carbamate zwitterion; r_{-2}, dissociation of the carbamate zwitterion; r_3, formation of the tetrahedral intermediate; r_{-3}, collapse of the tetrahedral intermediate to re-form carbamate and hydroxide; r_4, collapse of the tetrahedral intermediate resulting in decarboxylation to form bicarbonate and the original amine; r_5, bicarbonate uptake by ACC/PCC.

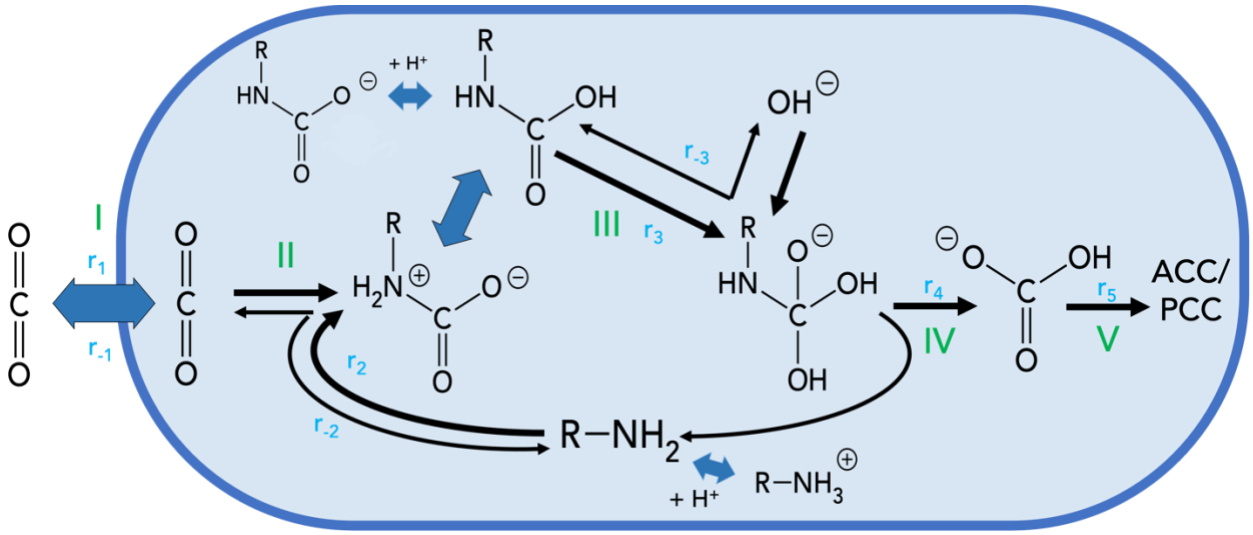

Figure 3. A simplified cell schematic displaying the proposed autocatalytic, amine-mediated carbon dioxide hydration pathway, represented by reactions I-V with equilibria governed by rate constants r_1-r_5**.** Unlabeled proton transfer reactions in the carbamate species and the amine species are depicted with blue arrows.

This process is highly pH-dependent, as is the activity of carbonic anhydrase (CA). The rate of CA-catalyzed CO_2 hydration is maximal at pH 8 and decreases as pH drops (Berg et al., 2002). The midpoint of the rate decrease is near pH 7, suggesting that a deprotonated form of a group with a pKa of 7 plays an important role in carbonic anhydrase activity (Berg et al., 2002). The group responsible is a water molecule, which binds to the zinc contained within the CA enzyme, thus decreasing the pKa of the water molecule to 7 and allowing the generation of OH^- ions at neutral pH via buffer-aided deprotonation (Berg et al., 2002). The resulting Zn-OH^- nucleophile complex attacks CO_2, forming a HCO_3^- ion that is released from the active site upon

the binding of another water molecule, which regenerates the catalytic site (Berg et al., 2002). Thus, in the proposed non-enzymatic, amine-mediated pathway, the pKa of the participating amine group must also be near 7 for this reaction to proceed in a carbonic anhydrase-like fashion.

Inorganic carbon retention by a simple, low-resource non-enzyme strategy may be more prevalent than is currently understood. The facility of carbamate formation as an exothermic and reversible process, the ubiquity of CO_2, and the few well-known examples of carbamate-mediated metabolic chemistry (in the Calvin cycle of plants via the enzyme Rubisco, and in the regulation of hemoglobin) indicate that carbamate chemistry in biological systems may be considerably widespread (Lorimer, 1983). The inorganic chemistry of carbamate formation from amine-containing compounds and CO_2 has been studied widely for climate engineering applications due to the ability of aqueous amines to act as solvents for CO_2 capture (Vaidya & Kenig, 2007); by contrast, its potential activity in biological systems has not been as thoroughly characterized. To test the Smith and Ferry (2000) hypothesis that carbamate chemistry is a viable alternative to prokaryotic carbonic anhydrase, the kinetics and mechanisms of carbamate formation and dissociation under various conditions (abiotic and biological) must be better understood.

4. *Amine-Mediated CO_2 Hydration: Mechanisms & Kinetics*

The first seminal study of carbamate reaction kinetics and mechanisms (Caplow, 1968) investigated kinetics for various primary and secondary amines under uncatalyzed and base-catalyzed conditions. For weakly basic amines, Caplow suggested the rate-limiting step of bicarbonate formation was C-N bond cleavage (Reaction **IV**, Fig. 3); for strongly basic amines, the rate-limiting step was suggested to be proton transfer to the amine nitrogen (product of **RII**, Fig. 3). These hypotheses were later confirmed by Johnson and Morrison (1972), who determined decarboxylation rates of various substituted N-arylcarbamates as a function of pH and buffer

concentration and found that for weakly basic amines, C-N bond cleavage is rate-limiting for decarboxylation, but for strongly basic amines, the rate-limiting mechanism is proton transfer to the N atom to form a short-lived zwitterionic carbamate species, as in Reaction **II**, before decarboxylation to form HCO_3^-. Carbamate chemistry has since been studied extensively in the CO_2 capture literature to determine the kinetics of carbon dioxide absorption by aqueous amine solvents (Barzagli et al., 2018; Couchaux et al., 2014; Holmes et al., 1998; Kortunov et al., 2015; Mani et al., 2006; Perinu et al., 2013, 2014a; Pesci et al., 2017; Stowe et al., 2015; Vaidya & Kenig, 2007; Yu et al., 1985). The mechanism of amine-mediated carbamate and bicarbonate formation from carbon dioxide varies depending on the type of amine participating in the reaction. Primary, secondary, and sterically hindered amines react via the zwitterion mechanism originally proposed by Caplow (1968), while tertiary amines act as base catalysts that generate hydroxide donors from water to induce hydroxylation of CO_2, similar to the mechanism of CA (Reaction **VI**, see Fig. 4; Caplow, 1968; Couchaux et al., 2014; Vaidya & Kenig, 2007). In the zwitterion mechanism, nucleophilic addition of nitrogen in a primary or secondary amine to carbon dioxide results in the formation of a carbamate zwitterion that can decompose in the presence of aqueous or basic conditions to produce the original amine and HCO_3^- (Reactions **II-V**, Caplow, 1968; Couchaux et al., 2014; Pesci et al., 2017; Vaidya & Kenig, 2007). In contrast, tertiary amines have an indirect catalytic effect and follow Reaction **VI**, in which the amine is instantaneously protonated to allow direct hydroxylation of carbon dioxide. In this pathway, no carbamate is formed but bicarbonate can still be produced (see Fig. 4; Couchaux et al., 2014; Yu et al., 1985). More recent mechanistic computational investigations in the carbon capture literature have shown strong agreement with both hypothesized theoretical reaction mechanisms.

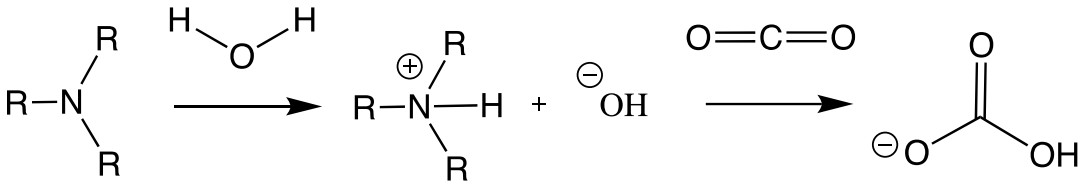

Figure 4. Reaction **VI**. The tertiary amine termolecular mechanism, in which a tertiary or sterically hindered amine acts as a base catalyst by abstracting aqueous protons to free up OH^- to attack CO_2 and form bicarbonate with no carbamate intermediate.

a. Experimental Techniques in Quantifying Carbamate Kinetics

Carbamate formation has been studied experimentally via reverse phase-high performance liquid chromatography (Wlasichuk et al., 2015) and electrospray ionization and mass spectrometry (Terrier & Douglas, 2010). Amine-mediated conversion of carbon dioxide into bicarbonate has been measured via Fourier-transform infrared spectroscopy by Pesci *et al.* (2017), in a study of the thermodynamic and kinetic biocatalytic carboxylation of catechol by 2,3-dihydroxybenzoic acid decarboxylase, which uses bicarbonate as its substrate. It was found that amine mediation improved carboxylation rates, and the extent and nature of amine substitution were the prime determinants of reactivity and carbon dioxide absorption capacity, with highest reactivity observed for highly substituted primary and secondary alkylamines (Pesci et al., 2017). Echoing previous carbamate literature, the authors proposed that these amines react via the two-step zwitterionic mechanism that yields carbamate (Reactions **II**-**V**), while tertiary amines react as base catalysts (Reaction **VI**; Pesci et al., 2017). In an archaeal metabolism lacking carbonic anhydrase, a potential carbamate-based carbon dioxide hydration pathway could be comparable to the decarboxylase studied by Pesci *et al.* (2017) and thus be a viable enzyme alternative.

Another common technique to evaluate the distribution of species in amine/CO_2 aqueous solutions in the carbon capture literature is carbon-13 nuclear magnetic resonance spectroscopy, or ^{13}C NMR spectroscopy (Bartoschek et al., 2000; Barzagli et al., 2018; Holmes et al., 1998; Kortunov et al., 2015; Mani et al., 2006; Perinu et al., 2013, 2014a). An *in-situ* real-time ^{13}C NMR

experiment by Kortunov *et al.* (2015) describes an experimental setup that allowed measurement of the kinetics of amine-CO_2 reactions and the production of time-evolved spectra that was used as a model for the methods of this study. Another study using this technique by Perinu et al. (2014a) measured carbamate formation and decomposition (Reactions **II**, **III**, and **IV**) in aqueous solutions of various linear primary alkanolamines, yielding equilibrium constants for carbamate decomposition in the range of 1.76 to 2.03 x 10^{-2}.

b. Carbamate Chemistry in Biology: What Is Known Thus Far

While the carbon capture literature is thorough and extensive in its characterization of the kinetics of abiotic carbamate formation mechanisms, the relevance of this chemistry in a biological metabolic system has not been determined, especially in an intracellular environment where better electrophiles than CO_2 are abundant and may hinder selective reactions with free amines. Carbamate formation rates in biological systems were first investigated by Chipperfield (1966), in which reaction rates for a variety of amino acids under biological conditions were measured and found to generally increase with increasing pKa (strength of the conjugate acid) of the amine group. The fastest reaction rate observed was with glycine (pKa 9.6) at 25 C, at 9050 M^{-1} s^{-1} (Chipperfield, 1966). Carbamate equilibria in biological systems were later revisited by Gros *et al.*, (1976), in which a stopped flow rapid reaction pH apparatus was used to investigate carbamate formation in solutions of glycylglycine, the simplest peptide that can be metabolized, and in three biological tissues (human plasma, sheep muscle, and sheep brain). The amine ionization constant, carbamate equilibrium constant, and velocity constant for carbamate formation were calculated at different pH and pCO_2, and pH curves were observed to have a "fast phase" representing carbamate formation and a "slow phase" representing its hydroxylation to form HCO_3^-, which was uncatalyzed due to the addition of carbonic anhydrase inhibitors into the biological solutions (Gros

et al., 1976). This is consistent with later literature that indicates the formation of HCO_3^- from carbamate dissociation is slower than carbamate formation and varies depending on the type of amine. Gros *et al.* (1976) measured the rate of carbamate formation from CO_2 and glycylglycine at 37 °C and pH 7-8 to be 2500 M^{-1} s^{-1}, slower than the rate of glycine (Chipperfield, 1966). Notably, glycine is a primary amine with one amine group per molecule, while glycylglycine has two amines per molecule, one primary and one secondary. It is possible that these two amine sites compete for the CO_2 substrate, potentially slowing the rate of carbamate formation. A further comparison of kinetic values collected by Vaidya and Kenig (2007) and Gros *et al.* (1976) shows that the rates of carbamate formation are highly variable based on reaction conditions. In Gros *et al.* (1976), carbamate formation between CO_2 and glycylglycine occurs at a rate 1.5-2x slower than the rates recorded under abiotic conditions for secondary amines and slightly faster than those recorded for sterically hindered amines in Vaidya and Kenig (2007). Whether this difference is due to conformational differences in the amines tested or to the reaction conditions (pH, temperature, etc.) is not immediately clear. Therefore, factors affecting carbamate formation rates are central experimental questions in this work, since the distribution of free amines in an intracellular environment like that of *N. maritimus* (within small peptides, as N-termini of large proteins[2], as free amino acids, etc.) is a key determinant of how any potential carbamate chemistry could proceed.

[2] Recently, O'Neill and Robbins (2017) developed a quantitative mechanistic model of the role of carbamate formation in carbon dioxide transport in blood by exploring the activity of the N-termini of globin chains in hemoglobin during carbon dioxide acquisition and transport, showing that computational quantification of carbamate chemistry at protein N-termini is a robust method of testing these theoretical processes.

c. Carbamate-Driven Methanogenesis in *M. barkeri* is the Closest Biological Analogue for the Comparative Study of *N. maritimus*

Perhaps more immediately relevant to understanding carbamate chemistry in the context of archaeal metabolism is the work of Bartoschek *et al.,* (2000), in which ^{13}C NMR spectroscopy was used to measure the reaction between methanofuran, an amine, and CO_2 to form the carbamate *N*-carboxymethanofuran, an important intermediate reaction in the reduction of CO_2 to methane in methanogenic archaea (Bartoschek et al., 2000). The purpose of their study was to determine whether spontaneous carbamate formation is fast enough to support the observed rate of methanogenesis in *M. barkeri*, or if it instead must be enzymatically catalyzed. While *M. barkeri* utilizes high-CO_2 growth conditions and enzymes that depend on CO_2 rather than bicarbonate, its use of a carbamate-forming intermediate in its central metabolism is relevant to understanding a potential carbamate-mediated pathway in *N. maritimus*. Bartoschek *et al.* (2000) determined that the 2nd-order rate constant for carbamate formation from methanofuran and CO_2 at pH 7 and 27 ºC is 7 M^{-1} s^{-1}. Using this rate constant and approximations for *in situ* concentrations of methanofuran and CO_2, the overall reaction rate for carbamate formation was determined to be between 0.02 – 2 mM s^{-1}. This was found to be of the same order as both the maximal rate of methane formation and the rate of spontaneous CO_2 formation from HCO_3^- (i.e., abiotic HCO_3^- dehydration, which is faster in *M. barkeri* than in *N. maritimus* due to much higher intracellular CO_2/HCO_3^- concentrations). This suggests that the methanogenic pathway does not require an enzyme to catalyze carbamate formation and it can operate on its own; this finding was confirmed by the observation that *M. barkeri* cell lysates did not enhance the carbamate formation rate (Bartoschek et al., 2000). This result suggests not only that carbamate formation is an essential intermediate process in an archaeal autotrophic pathway, but also that because it may have evolved

independently of an enzyme in this pathway, it could have evolved similarly in another marine archaeal phylum – i.e., Thaumarchaeota.

Additionally, Bartoschek et al. (2000) reported that cell extracts of *M. barkeri* do not exhibit carbonic anhydrase activity when grown under 80% H_2/20% CO_2 conditions. This indicates that the rate of spontaneous abiotic CO_2-HCO_3^- equilibrium and the rate of carbamate formation are sufficiently high as to not become rate-limiting for carbon fixation in *M. barkeri*. However, several open reading frames of the *M. barkeri* genome have been found to encode CA, and these could be activated under low-CO_2 conditions—thus, it is possible that carbamate formation could also be activated by an enzyme under suboptimal growth conditions that have yet to be studied (Bartoschek et al., 2000). This has interesting implications for the study of *N. maritimus*, which is chronically energy stressed and grows under limiting conditions, since it suggests that other archaea are able to take advantage of carbamate chemistry under optimal growth conditions but struggle to do so without the aid of enzymes under suboptimal conditions (the CO_2 concentration used by Bartoschek *et al.* to model typical conditions for *M. barkeri* is 60 mM, while the predicted intracellular concentration in *N. maritimus* is modeled to be 0.04 mM—see Table 3 in Results Section 3 for more details about modeled intracellular conditions in *N. maritimus*). Overall, these results support a growing body of evidence for the utility of carbamate chemistry in metabolic systems in the absence of enzymes at rates comparable to those observed in abiotic systems.

5. *Goals & Objectives*

The main goal of this study was to determine the viability of the amine-mediated CO_2 hydration pathway as a potential CA alternative or antecedent in *N. maritimus*. Given the significant knowledge gap in the assessment of the reactivity of amine-containing compounds under "biological conditions," this study aimed to measure, analyze, and model reaction kinetics

of amine-mediated CO_2 hydration for various types of aqueous amines buffered to neutral pH in order to compare the rate of this reaction with that of carbon fixation in *N. maritimus*. In the laboratory, 12 different amine-containing compounds were measured in CO_2 equilibration experiments via ^{13}C NMR spectroscopy to characterize the kinetics of their reaction with CO_2. In addition, a kinetic model of the potential intracellular chemistry of *N. maritimus* was developed in order to analyze and predict reaction rate constants and fluxes. Together, the experimental and modeled results indicate that amine-mediated CO_2 hydration is generally too slow a process to be a plausible CA alternative and act as the primary HCO_3^- source for carbon fixation in *N. maritimus*, although more work needs to be done to further characterize and quantify the specificity and speed of these reactions *in situ*.

Methods

This study focused on measurement of the kinetics of amine-mediated CO_2 equilibration reactions under biological conditions chosen to mimic the context of their potential catalytic activity within a cell. While there are many methods to determine reaction kinetics of amine-CO_2 solutions (outlined in Introduction & Background Section 4a), in my thesis, I chose to use ^{13}C NMR spectroscopy, a common analytical chemistry technique that was easily accessible in Harvard laboratories and produced quantitative timeseries measurements of the specific carbon-containing species relevant to this study. The following section outlines the experimental procedure in the laboratory, including the choice of amine-containing compounds to test, amine-CO_2 reaction mixture preparation, and NMR spectroscopy, as well as methods of data analysis used to extract kinetic parameters and model this chemistry in *N. maritimus*. The entire procedure is outlined in Fig. 5.

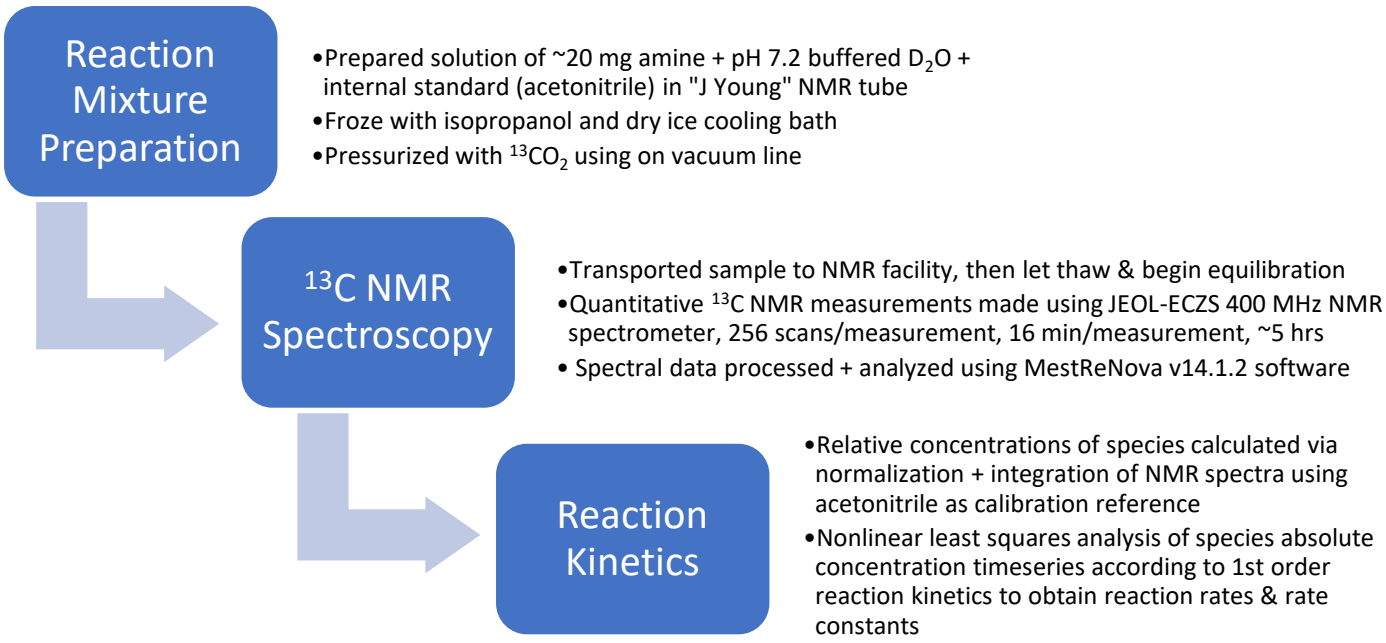

Figure 5. A flowchart detailing the experimental and analytic procedures in this study.

1. *Experimental Procedure for the Use of ^{13}C NMR Spectroscopy to Measure Reaction Kinetics of Amine-Mediated CO_2 Equilibration in Aqueous Solution*

a. Experimental Amines

As described in Table 1, the following amine-containing compounds were tested for their ability to mediate CO_2 equilibration and produce carbamate and bicarbonate: 2-amino-2-methyl-1-propanol, cytochrome C, diethanolamine, ethanolamine, glutathione, glycine, lysine, piperidine, proline, and proline methyl ester. These compounds represent a range of easily acquirable, inexpensive "biological" and "abiotic" amines of various structure and basicity, including common laboratory carbon solvents, amino acids, peptides, and a protein.

b. Sample Preparation

Deuterated Solvent

The "deuterium lock" system in an NMR spectrometer measures the resonance position of deuterium to stabilize the magnetic field and prevent drift. Thus, the use of a deuterated solvent, D_2O, was necessary for field locking and shimming in these NMR spectroscopy experiments.

Buffer

The intracellular pH of *N. maritimus* is estimated to be between 7.2 and 7.6 (Pearson et al., 2019), so in order to emulate intracellular conditions, all samples were made in D_2O solutions of 60 mM phosphate buffer of pH ~7.2. The choice of a buffer containing no carbon was made to avoid signal disturbance during ^{13}C NMR spectroscopy. Buffer was prepared by grinding together 1.07 g Na_2HPO_4 $7H_2O$ and 0.28 g $NaPO_4$ H_2O until thoroughly combined, then dissolving 0.135 g of the combined solid in 10 mL D_2O to make a 60 mM solution of pH 7.2.

Internal Standard

An internal standard is a known amount of reference compound dissolved in a known volume of sample, from which quantitative analyses can be performed by relating the area integral of the species peaks to that of the standard signal (Perinu et al., 2013). Acetonitrile was used as an easily acquired internal standard, with non-overlapping chemical shifts (1.47 and 119.68 ppm) compared to those of the amine and carbamate compounds (Perinu et al., 2014b); 20 µL was added to each sample.

Sample Prep

1 mL samples of amine in buffered D_2O and acetonitrile internal standard were prepared in 2mL vials according to the desired concentrations of each amine (see Table 1 at the end of this section for molarities), calculated based on the minimum amount necessary for good NMR detection, which is about 20 mg.[3] Then, 0.7 mL of prepared sample was transferred into a 5 mm, 7" 400 MHz low pressure/vacuum "J-Young" NMR tube and immediately placed in a -77 °C cooling bath of dry ice and isopropyl alcohol to freeze. The gas-tight "J-Young" style NMR tube allows convenient internal pressurization up to 100 psi (Wilmad-LabGlass). Samples were frozen in a cooling bath in order to overcome a logistical hurdle in which the laboratory where samples were prepared and the NMR spectroscopy laboratory were not located in the same facility, so the physical act of transporting samples between facilities caused a significant delay in kinetic data acquisition. Freezing the sample prevented spontaneous gas exchange between the $^{13}CO_2$ headspace and the amine solution, thus allowing the sample to be transported quickly without *en route* equilibration and allowing NMR spectroscopy to capture as much of the reaction between the aqueous amine solution and the CO_2 as possible.

[3] Ideally, the concentration of amine would reflect the in-situ concentration of free protein groups in an *N. maritimus* cell, but this tiny amount is virtually undetectable via low-sensitivity ^{13}C NMR spectroscopy.

Pressurization with $^{13}CO_2$

The frozen NMR tube containing the sample was pressurized with 99% $^{13}CO_2$ gas from a 0.5 L cylinder (Sigma-Aldrich) using a vacuum line, and internal pressure was measured using a digital pressure gauge (full vacuum line setup and pressurization sequence is shown in Fig. 6). Excess $^{13}CO_2$ was re-collected by cooling the gas cylinder with liquid nitrogen until pressure in the vacuum line dropped below 15 torr, indicating that sufficient $^{13}CO_2$ had been evacuated from the vacuum line and trapped back in the cylinder, thus reducing the risk of leakage. Only the ^{13}C isotope of carbon is detectable by ^{13}C NMR spectroscopy (^{13}C has a magnetically active spin quantum number of ½, while ^{12}C has a spin number of 0 and shows no magnetic activity), but the natural abundance of ^{13}C is 1.1% (Kortunov et al., 2015), thus making it difficult to quantitatively measure reaction kinetics of carbon species due to long signal acquisition times. Thus, $^{13}CO_2$ gas was used instead of unlabeled CO_2 gas to decrease signal acquisition times and improve the signal to noise ratio of spectra, thus improving the ability to quantitatively analyze reaction kinetics.

c. ^{13}C NMR Spectroscopy

The pressurized sample containing frozen amine solution and $^{13}CO_2$ was quickly transported from Hoffman Laboratory in the Department of Earth and Planetary Sciences to the Laukien-Purcell Instrumentation Center in the Department of Chemistry and Chemical Biology at Harvard University, then allowed to thaw. Once thawed, the sample was mixed by regulated rotation and tapping to facilitate equilibration between the gaseous headspace and the amine, then placed in the NMR spectrometer. Quantitative ^{13}C NMR measurements were made on a JEOL-ECZS 400 MHz NMR spectrometer with 256 scans per measurement at about 16 minutes per measurement for a series of twenty consecutive measurements over the course of about five hours. Spectral data were processed and analyzed using MestReNova v14.1.2 software.

NMR spectroscopy is a powerful tool in analytical chemistry that allows the elucidation of chemical composition, structure, and kinetics in a given sample. Nuclei that possess magnetic spin moments, like ^{1}H and ^{13}C, precess under the strong magnetic field imparted by an NMR spectrometer. The nuclei resonate at specific precession frequencies when bombarded by broad spectrum radio waves, which are measured and converted into an NMR spectrum that includes information on the number of specific resonating nuclei (peak intensity) and the relationships between nuclei in relation to one another (chemical shift). Thus, in quantitative NMR, absolute concentrations of compounds can be determined by integrating NMR peaks. While quantitative peak integration is generally not possible in ^{13}C NMR spectroscopy, it was possible to make quantitative measurements in this study of amine-mediated CO_2 equilibration because of the specific carbon species being studied (carbamate and bicarbonate/carbonate ion species). The relative amounts of carbamate and fast exchanging bicarbonate/carbonate ion in aqueous amine/CO_2 solution can be quantified by integrating the carbon resonances produced in the range 165-158 ppm because the ^{13}C atoms present in the ions have low-intensity resonances due to a lack of attached hydrogens and longer relaxation times compared to -CH_2- groups (Barzagli et al., 2018). Further evaluation of the relative amount of bicarbonate and carbonate ion in solution can be done via a procedure described in Mani *et al.,* (2006) and Holmes *et al.,* (1998) in which chemical shifts of calibration references and percent bicarbonate on a molar basis for bicarbonate/carbonate ion resonances are used to correlate the measured chemical shift to the ratio of the two species.

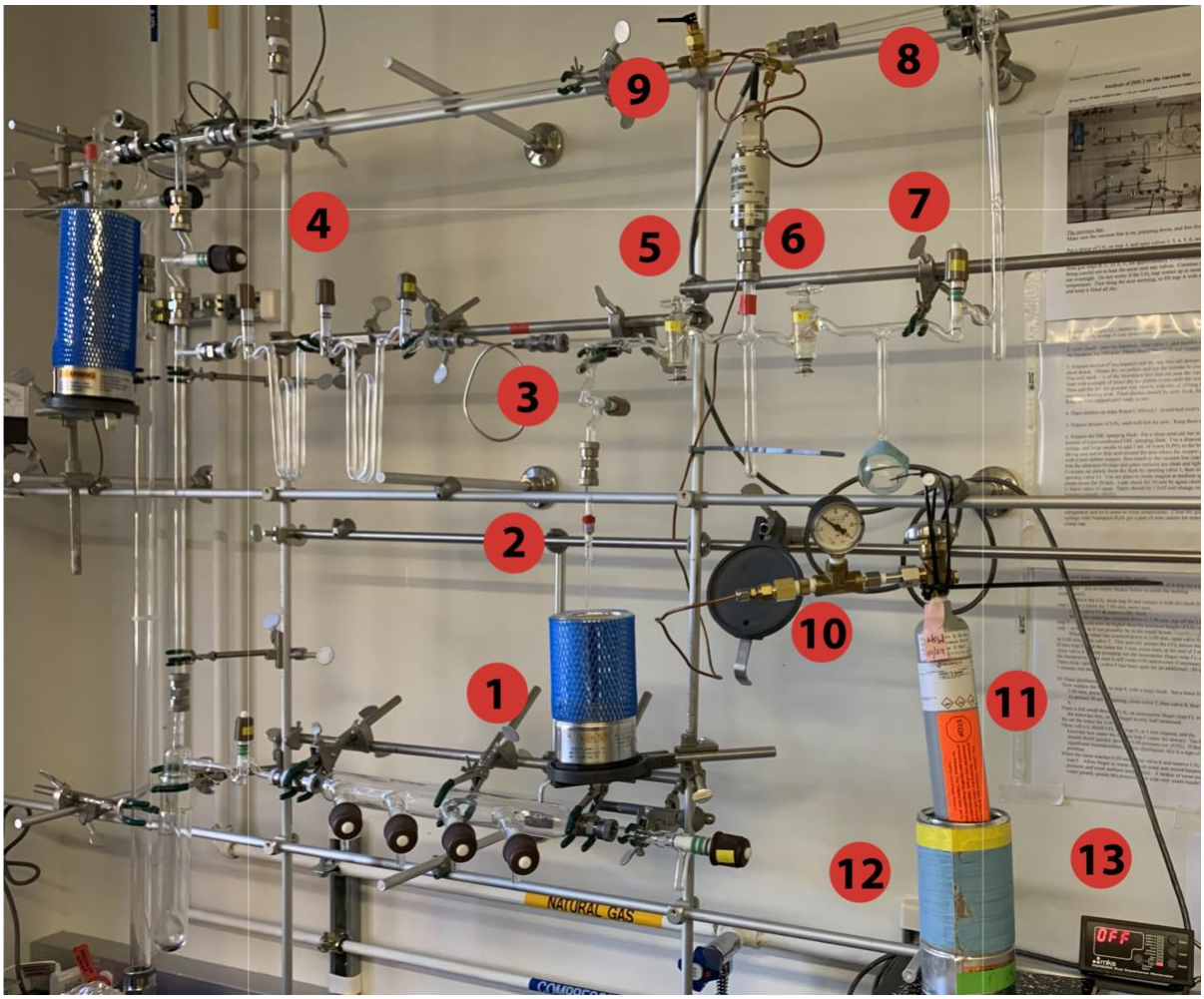

Figure 6. The NMR tube containing aqueous amine sample was pressurized with $^{13}CO_2$ via the following procedure, according to the labeled figure above: A dewar containing the cooling bath (1) and the NMR tube (2) was placed on a stand such that the NMR tube could be affixed to the vacuum line via an ultra-torr fitting. The NMR tube was opened, then valve 3 (3) was opened, allowing equilibration between the contents of the vacuum line and the NMR tube. The three leftmost valves (4) and valve 9 (9) were then opened, introducing the system to a vacuum. One minute after pulling a vacuum, valves 4 and 9 were closed, then valves 5, 6, 7, and 8 were opened in preparation of CO_2 flow into the right-hand side of the vacuum line system. The CO_2 tank (11) was opened, allowing CO_2 to flow though valves 8, 7, 6, 5, 3, and into the NMR tube. Pressure was recorded using a pressure gauge affixed to the tank (10), and if the pressure was too high (over about 15 psi), then the right-most valves from valve group 4 were opened to allow additional volume. The system was allowed to equilibrate for two minutes, after which the NMR tube was closed, followed by valve 3, 5, and 8, trapping the CO_2 between valves 5 and 8 in the right-hand side of the vacuum line. In order to conserve CO_2, the excess gas was trapped back in the tank by submerging the tank in a dewar of liquid nitrogen (12) until the digital pressure gauge that monitored the pressure between valves 8 and 9 (13) read below 10 torr, indicating a sufficient amount of CO_2 had frozen back into its container and that the tank could be closed. After the tank was closed, the freshly pressurized, frozen NMR tube was removed from the vacuum line and transported to the NMR spectroscopy lab for measurement.

2. *Kinetic Analyses & Modeling*

a. Extracting Kinetic Parameters from NMR Spectra

After the NMR spectra for each experiment were analyzed in MestReNova, the signals corresponding to the calibration compound, acetonitrile, were integrated and normalized according to the number of nuclei giving rise to the signal (1 nucleus each is responsible for producing both acetonitrile chemicals shifts at 1.47 and 119.68 ppm; the former was used as a reference signal due to its greater relative strength). The peak integrals of the compounds of interest, including dissolved inorganic carbon (DIC, including bicarbonate and carbonate ion species) and carbamate, as well as the carbon nuclei of the reagent species, were normalized relative to the internal reference standard, acetonitrile (each 0.7 mL sample contained 20 µL of acetonitrile, corresponding to a concentration of 0.547 M). Once normalized relative concentrations of each species of interest were obtained, the timeseries data could be analyzed to understand the reaction kinetics of carbamate and bicarbonate formation and equilibrium, including determining the order of reaction for each of these chemical reactions as well as their rate constants.

Zero, First, and Second Order Reaction Kinetics

A reaction is considered zero order if the rate of the reaction depends only upon the rate constant, first order if the rate is proportional to one concentration of a reactant or product species, second order if the rate is proportional to two concentrations of reactants or products multiplied together, and pseudo-first order if the reaction depends upon two reactants but one serves as a catalyst and its concentration remains relatively constant or is present in excess (Perrin, 2017). Based on the chemical equations developed to model intracellular amine-mediated CO_2 hydration introduced in the Background section, carbamate formation (Reaction II) and bicarbonate formation (Reaction IV) should be second order and first order, respectively; however, Reaction

II can be treated as pseudo-first order with respect to CO_2 because it was present in excess of the amine concentrations in each experiment. Thus, both reactions can be modeled according to the following equations from Perrin (2017):

$$Eq.I \quad [A] = [A_0]e^{-kt}$$

where $[A]$ is the concentration of reactant, $[A_0]$ is the initial reactant concentration, k is the rate constant, and t is time;

$$Eq.II \quad [B] = [A_0](1 - e^{-kt})$$

where $[B]$ is the concentration of product. In order to evaluate the timeseries data derived from the NMR experiments, which are in terms of product concentrations, it is also necessary to consider that these equilibrium reactions do not go to completion; thus, there is reactant leftover when the reaction reaches equilibrium, and this can be modeled by the following equation from Perrin (2017):

$$Eq.III \quad [B] = B_\infty - (B_\infty - B_0)e^{-kt}$$

where B_∞ is the nonzero baseline value that the product concentration approaches over time (horizontal asymptote) and B_0 is the initial concentration of product. Eq. III was the equation used to model kinetics for carbamate and bicarbonate formation as first order reactions.

Nonlinear Least Squares Analyses

The familiar method for extracting rate constants from concentration versus time data for first order reactions is linear least square analysis. However, the heteroskedasticity, or unequal reliability, of kinetic data make this type of analysis defective, especially in this case, in which the measurement of product concentrations requires knowledge of B_0 for proper linearization (Eq. III can be linearized by solving for B_0- B, the logarithm of which is linear with respect to time; thus, small errors in B_0 cause increasing error in the logarithm of of B_0- B; Perrin, 2017). Thus,

nonlinear least squares fitting is more effective (Perrin, 2017). This was achieved using a self-starting three-parameter asymptotic exponential model in R, SSasymp, of the form $y = a - be^{-cx}$ (Crawley, 2007), fit to experimental concentration versus time data for both carbamate and bicarbonate formation. In this way, the rates and rate constants for the bicarbonate-forming and carbamate-forming reactions could be easily extracted from the exponential model and compared to the modeled rate of bicarbonate fixation in *N. maritimus* to understand whether these reaction sequences could feasibly supply the cell with its anabolic requirement.

Compound	Amine groups	Structure	Type	pKa*	Molecular weight (g/mol)	Density (g/mL)***	Sample Molarity (M)	$^{13}CO_2$ Headspace Pressure (atm)****
control	0	-	no amine	-	-	-	-	1.407, 1.68
glutathione	3	primary, secondary	peptide	-	307.32	-	2.79×10^{-1}	1.776
cytochrome C	-	-	protein	-	12×10^{3}	-	2.38×10^{-3}	1.741
diethanolamine	1	secondary	abiotic solvent	8.96	105.14	1.09	2.72×10^{-1}	1.789
lysine	2	primary, 2 amines	amino acid	8.95, 10.53**	146.19	-	1.95×10^{-1}	1.796
lysine methyl ester	2	primary, 2 amines	amino acid	8.95, 10.53**	233.14	-	2.45×10^{-1}	1.646
ethanolamine	1	primary	abiotic solvent	9.5	61.08	1.01	4.68×10^{-1}	1.169
glycine	1	primary	amino acid	9.6	75.07	-	3.81×10^{-1}	1.878, 2.057
2-amino-2-methyl-1-propanol	1	primary, sterically hindered	abiotic solvent	9.7	89.14	0.934	3.21×10^{-1}	1.748
proline	1	secondary	amino acid	10.6	115.13	1.32	2.48×10^{-1}	1.857
proline methyl ester	1	secondary (protected)	amino acid	10.6	165.62	1.32	1.73×10^{-1}	1.776
piperidine	1	secondary	abiotic solvent	11.28	85.15	0.862	3.36×10^{-1}	1.748, 1.878
glycine + ethanolamine mixture	2	primary	amino acid + abiotic solvent	-	*see individual masses*	*see individual densities*	5×10^{-1}	1.707

Table 1: List of amine-containing compounds tested in 13C NMR experiments and their properties. *Refers to the pKa of the amine group. **The former value is the pKa of the alpha-amino group; the latter value is the pKa of the amine side chain of lysine. ***Densities are only listed for compounds used in their liquid forms.****If the amine-containing compound was tested more than once, the headspace pressures are listed chronologically.

Results

1. *Amine Reactivity*

Fifteen NMR spectroscopy experiments were carried out to measure the rate of CO_2 equilibration in aqueous media mediated by the following different amine-containing molecules or mixtures: glycine (two experiments), lysine, proline, proline methyl ester (three experiments), lysine methyl ester, ethanolamine, diethanolamine, piperidine (two experiments), a glycine-ethanolamine equimolar mixture, 2-amino-2-methyl-1-propanol, glutathione, and cytochrome C. NMR spectra of each experiment were compared to two blank control experiments: the first containing D_2O buffered to pH 7.2, acetonitrile, and 1.407 atm $^{13}CO_2$; and the second containing buffered D_2O and 1.68 atm $^{13}CO_2$ and no acetonitrile (to ensure its lack of reactivity in solution with CO_2). In each control experiment, dissolved bicarbonate/carbonate species (δ 160.71, 160.29 ppm in Control 1 and Control 2 respectively) and aqueous carbon dioxide (δ 125.15, 124.69 ppm Control 1 and Control 2 respectively) concentrations remained stable over time (see Figs. 7-9 for Control 1). A complete table of amine reactivity can be found in Table 2.

Compound	Structure at pH 7	Amine Type	pKa	Carbamate	Bicarbonate
Lysine methyl ester	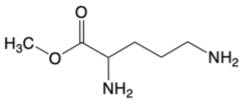	primary	8.95, 10.53	N	N
Lysine	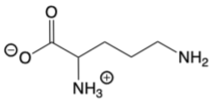	primary	8.95, 10.53	N	N
Diethanolamine	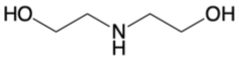	secondary	8.96	N	N
Ethanolamine	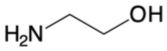	primary	9.5	Y	N
Glycine	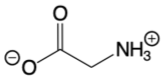	primary	9.6	N	N
2-amino-2-methyl-1-propanol	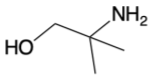	primary, sterically hindered	9.7	Y	N
Proline methyl ester	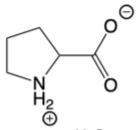	secondary	10.6	N	N
Proline	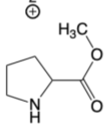	secondary	10.6	N	N
Piperidine		secondary	11.28	Y	Y
Ethanolamine + Glycine Equimolar Mixture	NA	primary	NA	Y	N

Table 2. Table of reactivity showing each experimental amine, its structure at experimental pH (~7), its structural type, pKa (in the case of the lysine derivatives, the two listed pKa values are in order of amino group and side chain amine), and yes/no (Y/N) classification of carbamate and bicarbonate production upon equilibration with CO_2.

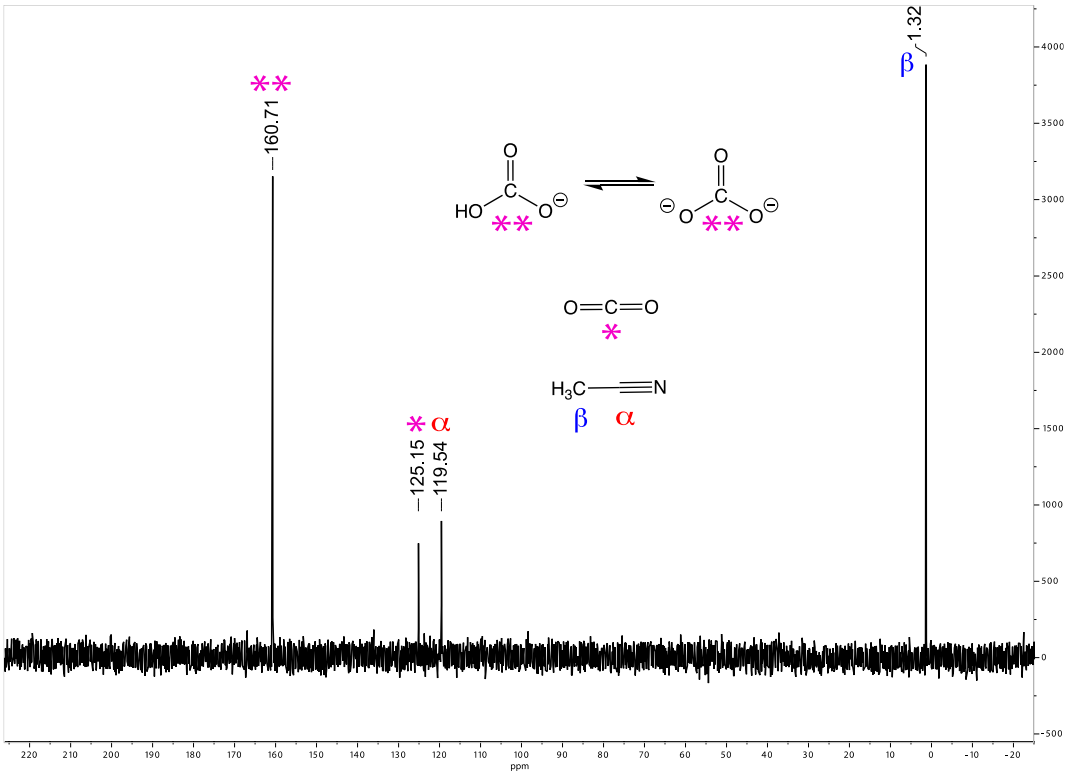

Figure 7. A sample ^{13}C NMR spectrum from the Control 1 experiment. Labeled peak assignments are as follows: dissolved bicarbonate/carbonate ion species (160.70 pm), aqueous carbon dioxide (125.14 ppm), the acetonitrile alpha carbon (119.54 ppm), and the acetonitrile beta carbon (1.32 ppm). Each peak is labeled with a symbol representing the location of that carbon nucleus in the molecule.

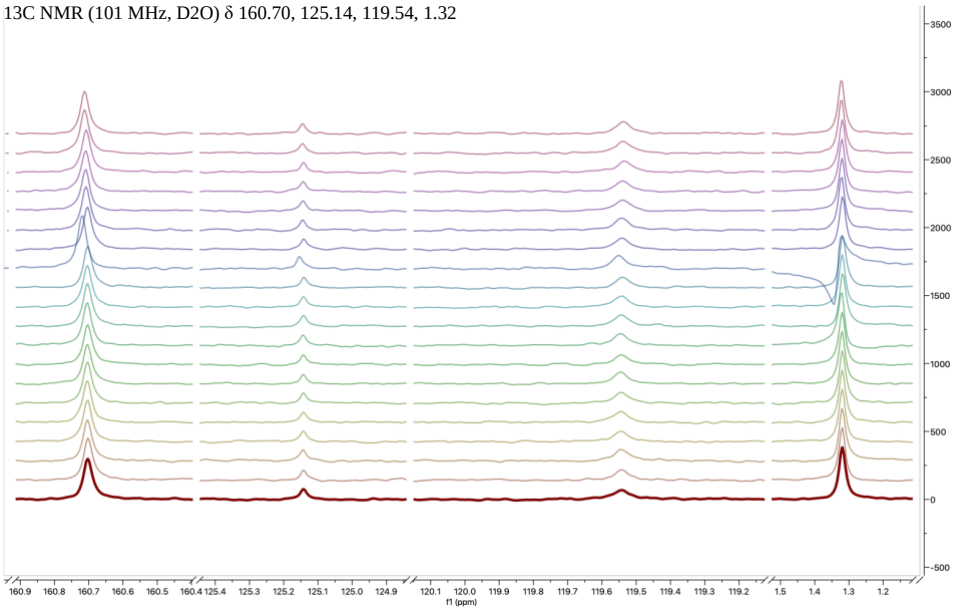

Figure 8. Control 1 experiment: Stacked spectral timeseries, depicting spectra at sixteen-minute intervals for 320 total minutes of measurement. The bottom-most spectrum is the first measurement, going forward in time to the final measurement, the top-most spectrum.

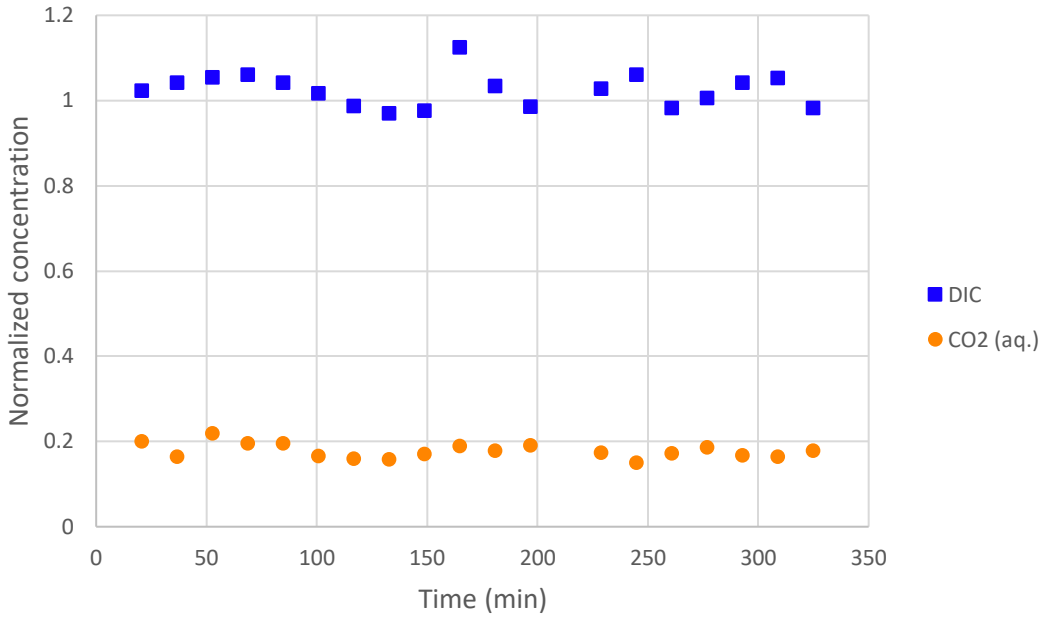

Figure 9. Normalized concentration of aqueous CO_2 and dissolved bicarbonate + carbonate ion (DIC) relative to the acetonitrile reference standard in Control 1 over time.

In general, amino acids and amino acid methyl esters were unreactive, carbamate was produced by abiotic solvents with high pKa values and the equimolar ethanolamine-glycine mixture, and only piperidine, a strong base, produced both carbamate and bicarbonate. Glycine, proline, and lysine, amino acids that are zwitterionic at neutral pH did not produce carbamate or bicarbonate. Finally, protecting the carboxylate groups of proline and lysine with methyl esters did not improve reactivity. However, protecting an amino acid, glycine, with a primary amine-containing abiotic solvent, ethanolamine, in an equimolar mixture led to the production of the carbamate adducts of both compounds. Diethanolamine, a secondary amine-containing abiotic solvent, did not react, but ethanolamine, a primary amine-containing abiotic solvent with a higher pKa, did react with carbon dioxide to produce ethanolamine-carbamate. 2-amino-2-methyl-1-propanol (AMP), a primary, sterically hindered amine-containing abiotic solvent, also produced carbamate. The only species that produced both carbamate and bicarbonate was piperidine, a strongly basic heterocyclic amine. Detailed analyses of each experiment are carried out below.

a. Amino Acids

Glycine

Glycine-mediated aqueous CO_2 equilibrium was measured in two experiments, Glycine 1 and Glycine 2. The former was pressurized with 1.878 atm $^{13}CO_2$, the latter with 2.057 atm; both had 0.381 M concentrations of glycine dissolved in D_2O buffered to pH 7.2. Qualitative analysis of the Glycine 1 spectrum indicates steady concentrations of bicarbonate/carbonate ion species (δ 160.72 ppm) and glycine (δ 172.91, 41.83 ppm for alpha and beta carbons respectively) over time, as well as ethanol contamination (δ 57.85, 17.23 ppm). The Glycine 2 spectrum shows steady concentrations of bicarbonate/carbonate ion species (δ 160.70 ppm), aqueous carbon dioxide (δ 125.11 ppm), and glycine (δ 172.91, 41.83 ppm), consistent with the control experiment. Carbamate was not detected in either experiment. All amino acid NMR spectra can be found in the Supplementary Data (see Figs. S1 and S2 for glycine).

Lysine

0.195 M lysine pressurized with 1.796 atm $^{13}CO_2$ showed steady concentrations of bicarbonate/carbonate ion species (δ 160.69 ppm) and lysine (δ 175.13, 54.85, 39.43, 30.28, 26.80, 21.82 ppm) over time, with no carbamate detection (Figs. S3 and S4).

Proline

0.248 M proline pressurized with 1.857 atm $^{13}CO_2$ showed steady concentrations of bicarbonate/carbonate ion species (δ 160.71 ppm) and proline (δ 175.19, 61.61, 46.48, 29.43, 24.19 ppm) over time, with no carbamate detection (Figs. S5 and S6).

b. Protected Amino Acids & Mixtures

Proline Methyl Ester

0.173 proline methyl ester pressurized with 1.707 atm $^{13}CO_2$ showed steady concentrations of bicarbonate/carbonate ion species (δ 160.71 ppm), aqueous carbon dioxide (δ 125.13 ppm), and proline (δ 61.63, 46.49, 29.43, 24.19) over time; however, the alpha carbon and methyl carbon of proline were not detected. Carbamate was not detected (see Figs. S7 and S8). This experiment was repeated three times with similar results.

Lysine Methyl Ester

0.245 M lysine methyl ester pressurized with 1.646 atm $^{13}CO_2$ showed no reactivity and poor spectral acquisition, with only lysine methyl ester carbons (δ 170.97, 53.53, 52.61, 48.89, 39.00, 29.40, 26.26, 21.46 ppm) detected and no acetonitrile or other carbon species detected (see Figs. S9 and S10). Absence of acetonitrile peaks and poor overall spectral quality indicate there may have been an NMR instrument problem with this experiment.

Glycine-Ethanolamine Mixtures

An equimolar mixture of 0.5 M glycine and 0.5 M ethanolamine pressurized with 1.776 atm $^{13}CO_2$ showed formation of glycine-carbamate (δ 164.77, 45.84 ppm; the carboxylic acid carbon was not detected) and ethanolamine-carbamate (δ 165.16, 61.74, 43.59 ppm), alongside glycine (δ 176.31, 43.01 ppm), ethanolamine (δ 59.81, 41.96 ppm), and bicarbonate/carbonate ion species (around 160 ppm), as shown in Figs. 10 and 11. In addition to the production of ethanolamine-carbamate (which is favored on its own, see next section), nucleophilic attack of the amine in ethanolamine into the carboxylate end of glycine served to "protect" the otherwise zwitterionic amino acid and allowed the glycine-ethanolamine complex to react with CO_2 to form glycine-carbamate (Fig. 12).

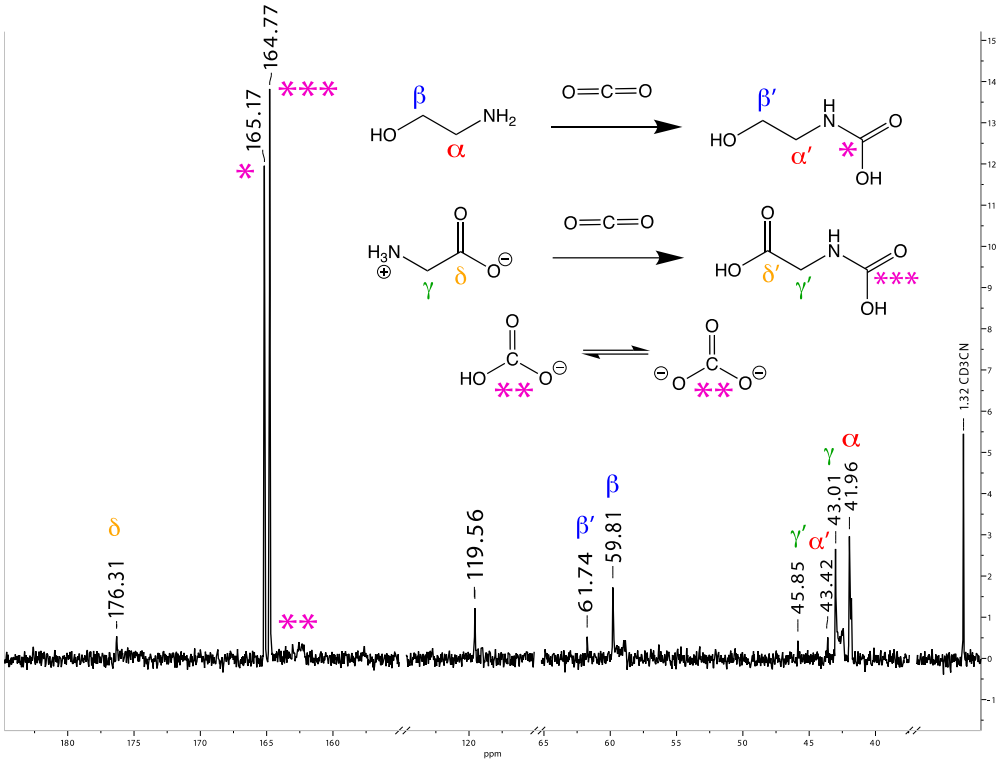

Figure 10. A sample ^{13}C NMR spectrum from the equimolar ethanolamine-glycine experiment. Labeled peak assignments are as follows: dissolved bicarbonate/carbonate ion species (~ 165 ppm), ethanolamine-carbamate (165.17, 61.74, 43.42 ppm), ethanolamine (59.81, 41.96 ppm), glycine-carbamate (164.77, 45.85 ppm – the carboxylate carbon was not detected), glycine (176.31, 43.01 ppm), and acetonitrile carbons (119.56, 1.32 ppm).

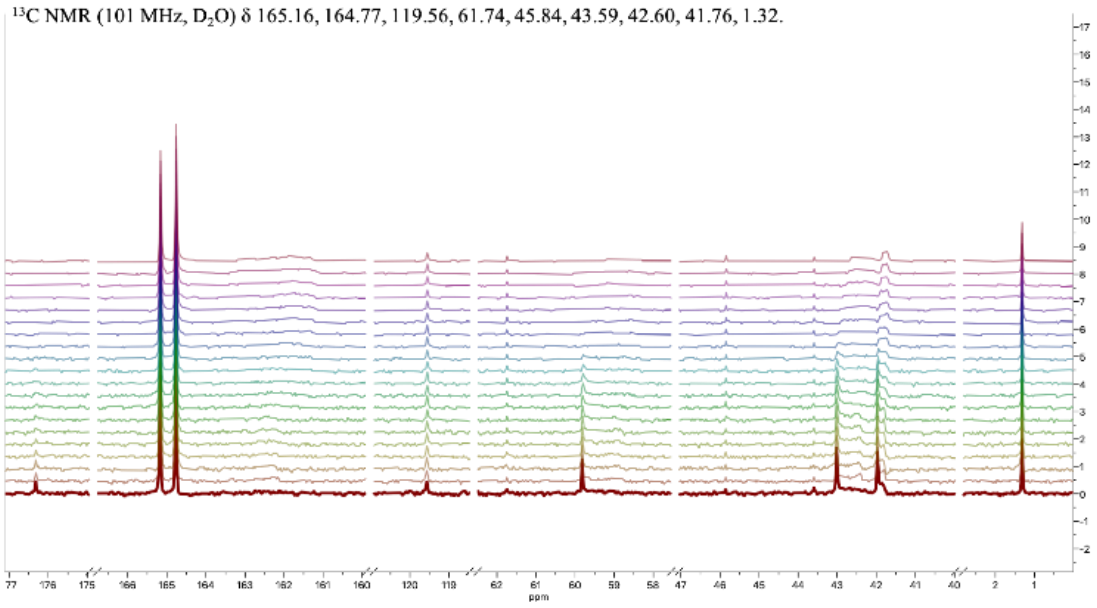

Figure 11. Ethanolamine-glycine mixture experiment stacked spectral timeseries, depicting spectra at sixteen-minute intervals for 320 total minutes of measurement. The bottom-most spectrum is the first measurement, going forward in time to the final measurement, the top-most spectrum. Note the decrease in the ethanolamine and glycine carbon nuclei relative concentrations over time.

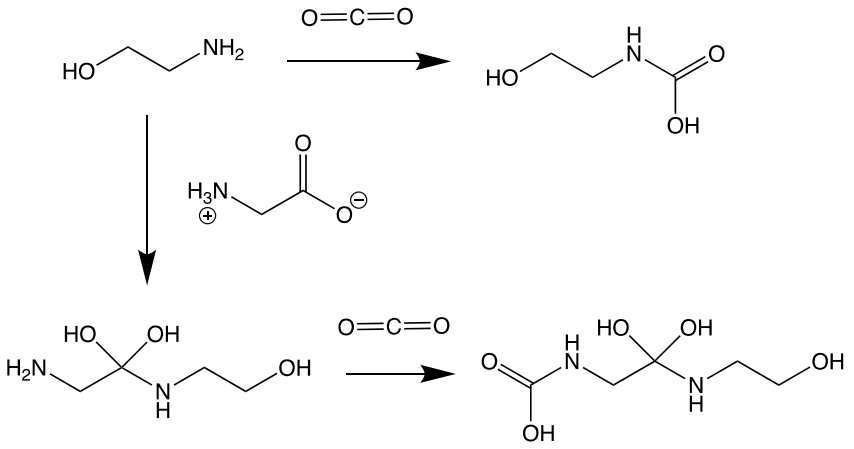

Figure 12. The reaction mechanism for ethanolamine-carbamate and glycine-carbamate production in the equimolar ethanolamine-glycine mixture experiment. Ethanolamine can combine with CO_2 to produce ethanolamine-carbamate, or combine with glycine to form an adduct that frees the glycine amine group to combine with CO_2 to produce glycine-ethanolamine carbamate. Compounds are shown in their protonated forms in this figure, but note that these exist in equilibrium with deprotonated forms at pH 7.

c. Abiotic Solvents

Ethanolamine

0.468 M ethanolamine pressurized with 1.169 atm $^{13}CO_2$ showed production of ethanolamine-carbamate (δ 165.70, 61.81, 43.63 ppm) and bicarbonate/carbonate ion species (δ 163.73 ppm) alongside ethanolamine (δ 42.18; beta carbon not resolved) as well as ethanol contamination (δ 57.85, 17.25 ppm), shown in Figs. 13 and 14.

Diethanolamine

0.272 M diethanolamine pressurized with 1.789 atm $^{13}CO_2$ showed only constant diethanolamine (δ 58.74, 49.78 ppm) over time, with no detected carbamate or carbonate species, likely due to a poor signal:noise ratio (see Figs. S11 and S12).

Piperidine

Piperidine-mediated aqueous CO_2 equilibrium was measured in two experiments, Piperidine 1 and Piperidine 2. The former was pressurized with 1.748 atm $^{13}CO_2$, the latter with 1.878 atm; both had 0.336 M concentrations of piperidine. The Piperidine 1 experiment is not

included in this analysis due to an instrument malfunction during spectral collection that resulted in an incomplete dataset; however, it did produce both carbamate and HCO_3^-. The Piperidine 2 experiment was complete and provided the only continuous timeseries for carbamate and HCO_3^- production via amine-CO_2 equilibration. Fig. 15 shows a sample NMR spectrum from the experiment, including the following species: dissolved bicarbonate/carbonate ion species (168.26 ppm), piperidine-carbamate (163.84, 45.85, 26.05, 24.85 ppm), and piperidine (45.29, 23.85, 22.85 ppm). The stacked spectra in Fig. 16 shows the relative concentrations of bicarbonate and piperidine-carbamate increase over time.

2-amino-2-methyl-1-propanol

0.321 M 2-amino-2-methyl-1-propanol pressurized with 1.748 atm $^{13}CO_2$ showed carbamate (δ 165.78 ppm; no other carbon peaks resolved) alongside 2-amino-2-methyl-1-propanol (δ 67.90, 52.38, 24 ppm), both of which had stable concentrations over time (see Figs. S13 and S14). The quantitative power of the carbamate concentration measurements is limited due to the non-Lorentzian shape of the NMR spectral peaks (see Fig. S14), most likely due to a shimming error within the spectrometer itself.

d. Peptides and Proteins: Glutathione and Cytochrome C

0.279 M glutathione pressurized with 1.776 atm $^{13}CO_2$ showed steady concentrations of glutathione (δ 175.29, 174.54, 174.17, 172.69, 56.01, 54.25, 42.27, 31.59, 26.42, 25.81 ppm) and aqueous carbon dioxide (δ 125.08 ppm) over time. No carbamate or carbonate species were detected (see Fig. S15). 2.38×10^{-3} M cytochrome C pressurized with 1.741 $^{13}CO_2$ behaved similarly to Control 2, with no detection of anything other than steady concentrations of bicarbonate/carbonate ion species (δ 160.72 ppm) and aqueous carbon dioxide (δ 125.15 ppm) over time (see Fig. S16).

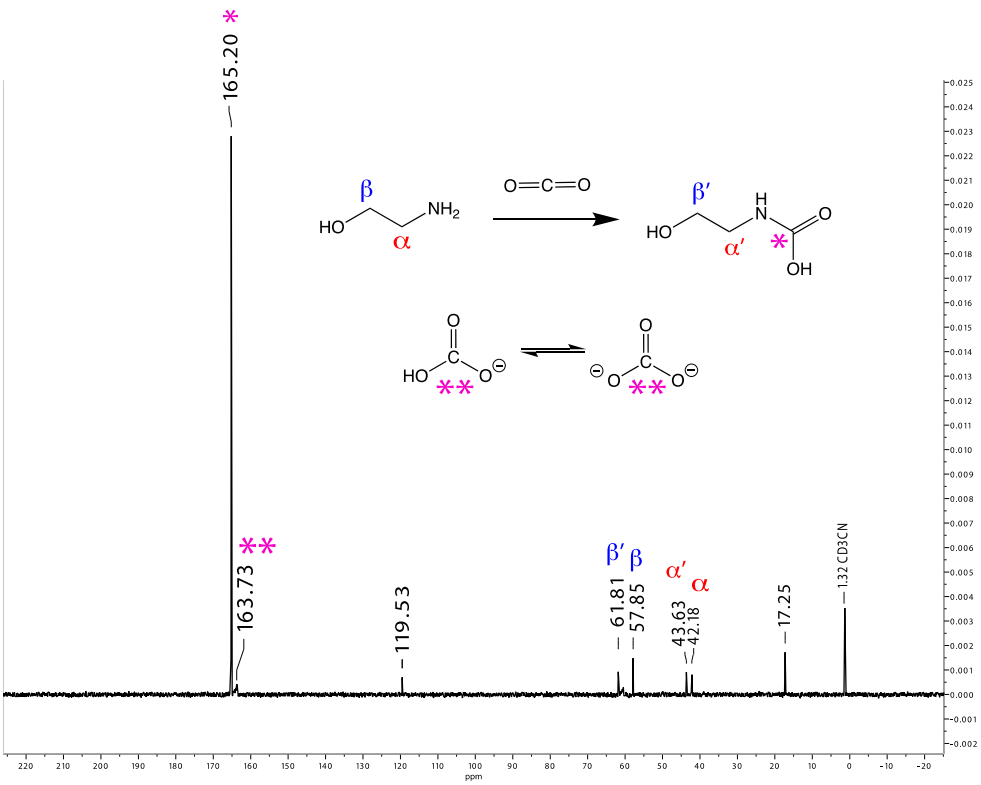

Figure 13. A sample ^{13}C NMR spectrum from the ethanolamine experiment. Labeled peak assignments are as follows: dissolved bicarbonate/carbonate ion species (163.73 ppm), ethanolamine-carbamate (165.20, 61.81, 43.63 ppm), ethanolamine (~60, 42.18 ppm) and acetonitrile carbons (119.56, 1.32 ppm). The peaks at 57.85 and 17.25 correspond to ethanol contamination in the sample.

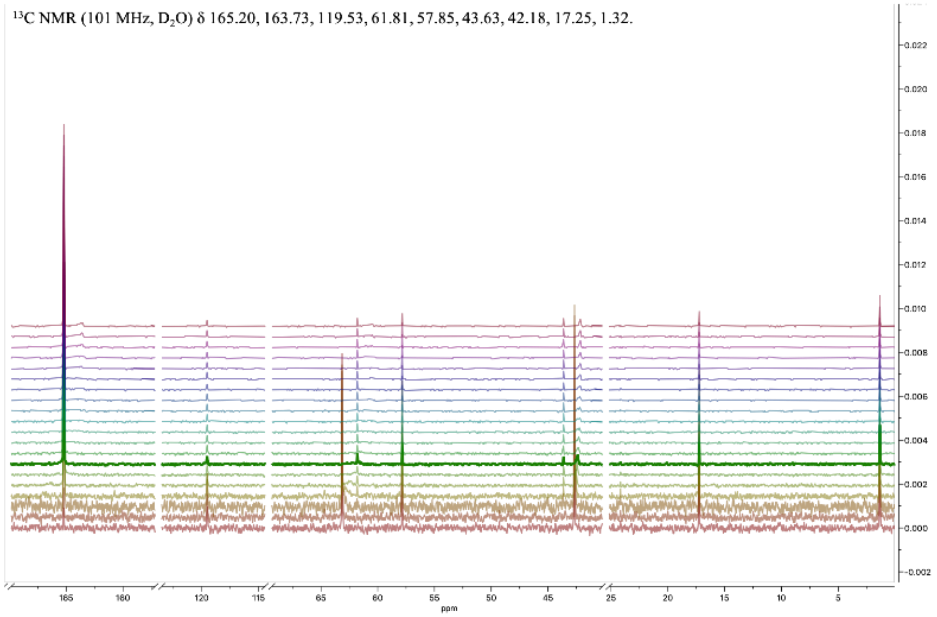

Figure 14. Ethanolamine experiment stacked spectral timeseries, depicting spectra at sixteen-minute intervals for 320 total minutes of measurement. The bottom-most spectrum is the first measurement, going forward in time to the final measurement, the top-most spectrum. Note the decrease in the ethanolamine carbon nuclei relative concentrations to the ethanolamine-carbamate nuclei over time.

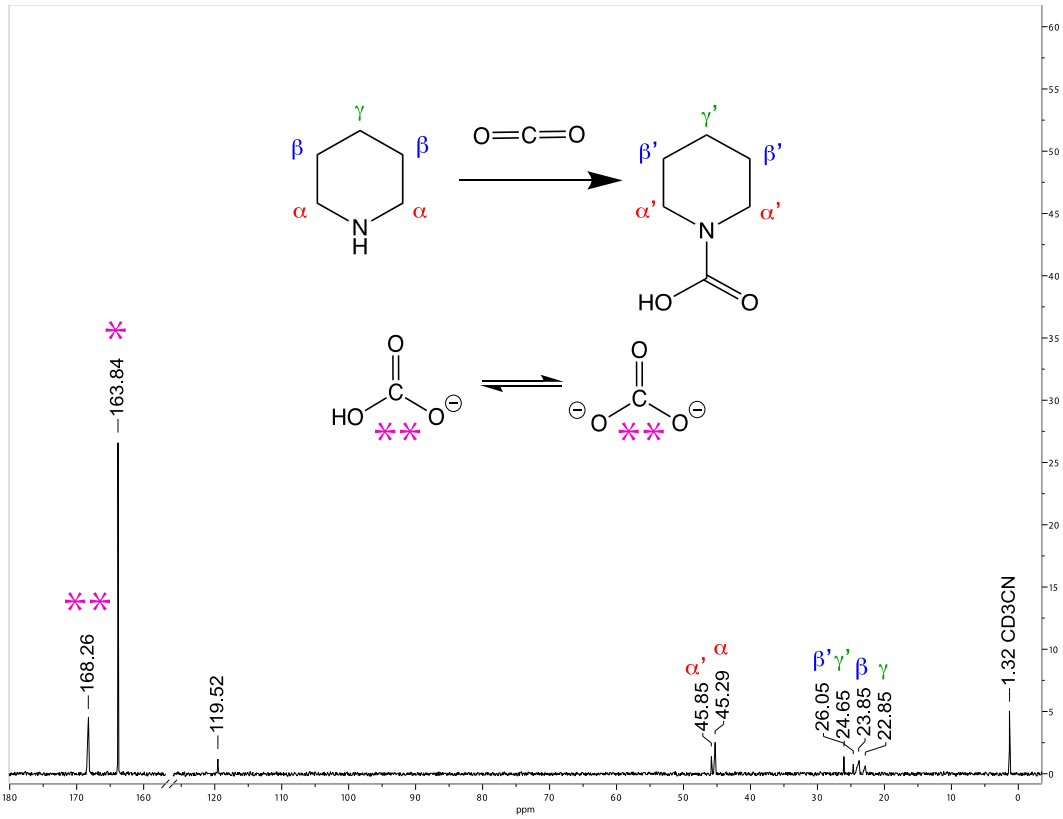

Figure 15. A sample ^{13}C NMR spectrum from the Piperidine 2 experiment. Labeled peak assignments are as follows: dissolved bicarbonate/carbonate ion species (168.26 ppm), piperidine-carbamate (163.84, 45.85, 26.05, 24.85 ppm), piperidine (45.29, 23.85, 22.85 ppm) and acetonitrile carbons (119.56, 1.32 ppm).

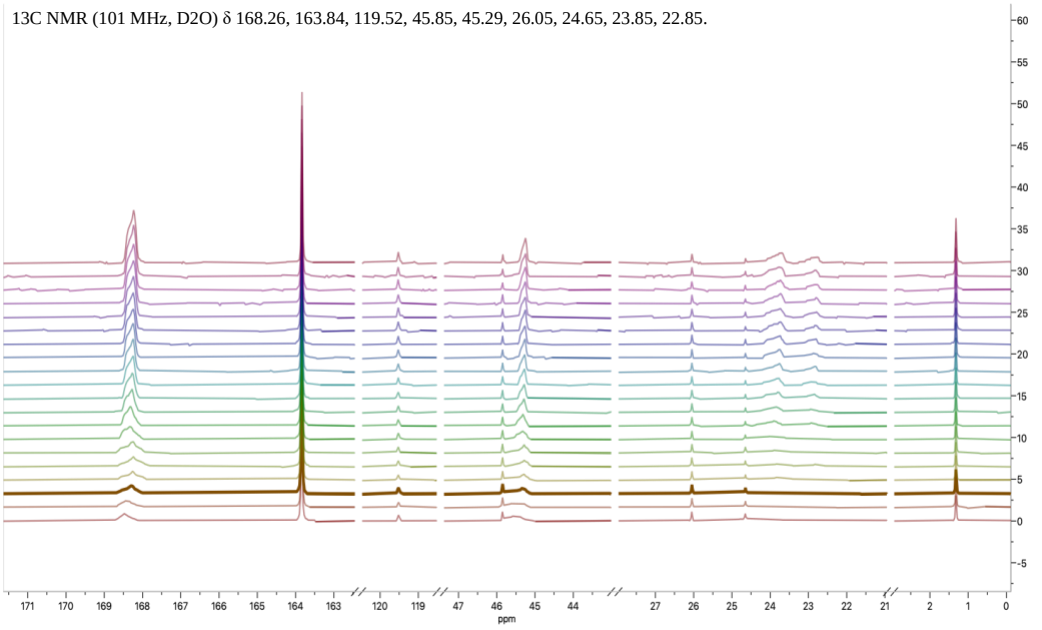

Figure 16. Piperidine 2 experiment stacked spectral timeseries, depicting spectra at sixteen-minute intervals for 320 total minutes of measurement. The bottom-most spectrum is the first measurement, going forward in time to the final measurement, the top-most spectrum. Note the gradual appearance of up-field piperidine-carbamate carbon nuclei as well as the increase in bicarbonate at 168.26 ppm.

2. *Kinetic Analyses of Carbamate- and Bicarbonate-Producing Reactions*

Of the reactive, carbamate-producing amines, only ethanolamine showed clear pseudo-1st order reaction kinetics with respect to carbamate, and only piperidine produced both carbamate and bicarbonate. Thus, only these two species can be reliably assessed for their kinetics, and the following section outlines modeled reaction rates and rate constants for carbamate and bicarbonate formation mediated by aqueous ethanolamine and piperidine.

a. Ethanolamine

The normalized relative concentration of carbamate produced by the ethanolamine-CO_2 experiment over the course of the 320 minute measurement period is shown in Fig. 17. The relative concentration of carbamate was determined based on integration and normalization of the 165.20 ppm chemical shift of the carbamate carbonyl nucleus (see Methods Section 1b); while the absolute concentration cannot be determined with quantitative accuracy, the reaction rate and rate constant can still be determined from fitting the acquired relative concentration data to a 1st order reaction model via nonlinear least squares analysis (see Methods Section 2a). The concentration data and the reaction rate model are depicted in Fig. 18, governed by the following equation:

$$Eq.IV \quad [C_2H_2NOHCO_2] = [C_2H_2NOHCO_2]_\infty + ([C_2H_2NOHCO_2]_\infty - [C_2H_2NOHCO_2]_0)e^{-k_{carb}t}$$

where $[C_2H_2NOHCO_2]$ is the concentration of ethanolamine-carbamate and the rate constant, k_{carb}, is 1.1 x 10^{-2} s^{-1}. The values of $[C_2H_2NOHCO_2]_\infty$, the equilibrium concentration of carbamate (horizontal asymptote), and $[C_2H_2NOHCO_2]_0$, the initial carbamate concentration (see Eq. III in Methods Section 2a), are 11.49 and -3.389 respectively. These are meaningless relative solution values, but the rate constant depends on relative change per time and is therefore accurate. Given a 1.169 atm headspace of CO_2 during the experiment, corresponding to an aqueous equilibrium concentration of 0.0403 M in solution (assuming gas-aqueous equilibrium was achieved), and an

excess ethanolamine concentration of 0.468 M, the rate of the carbamate formation reaction, r_{carb}, can be modeled as first-order with respect to CO_2 (since CO_2 was in excess of ethanolamine; see Methods Section 2a):

$$Eq.V \quad r_{carb} = [CO_2]k_{carb}$$

Thus, the production rate of carbamate in solution was 4.43 x 10^{-4} M s^{-1}. The inferred 2nd-order rate constant can be determined from the following equation:

$$Eq.VI \quad r_{carb,2} = [NH_2][CO_2]k_{carb,2}$$

where $[NH_2]k_{carb,2}$ is equal to k_{carb}, 1.1 x 10^{-2} s^{-1}. Solving for $k_{carb,2}$ yields 2.35 x 10^{-2} M^{-1} s^{-1}.

The proposed reaction mechanism is shown in Fig. 19, in which nucleophilic attack of CO_2 by the amine group in ethanolamine forms a carbamate zwitterion, detectable in its protonated form.

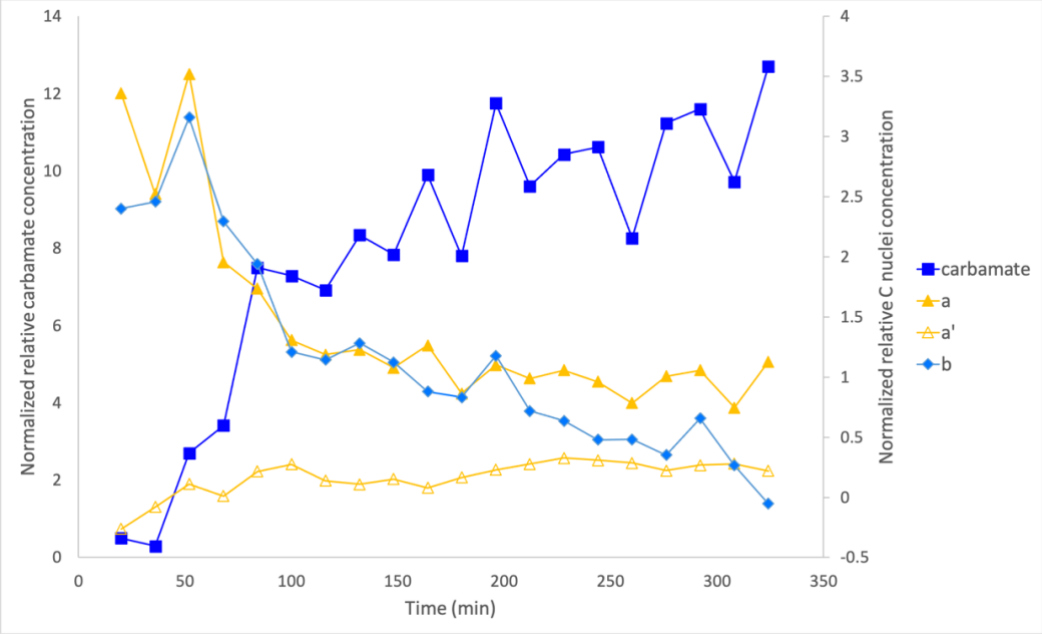

Figure 17. A timeseries plot of the carbon nuclei species in the ethanolamine experiment, as measured by NMR spectroscopy. The normalized relative ethanolamine-carbamate concentration, based on the 165.20 ppm chemical shift of the carbamate carbonyl nucleus, is plotted on the left y-axis and the normalized relative concentrations of the ethanolamine and ethanolamine-carbamate carbon nuclei are plotted on the right y-axis. Note that the b' carbon nucleus was not sufficiently detected by NMR spectroscopy and thus is not included in this plot. The locations of the a, a', b, and b' carbons in ethanolamine are pictured in Fig. 19.

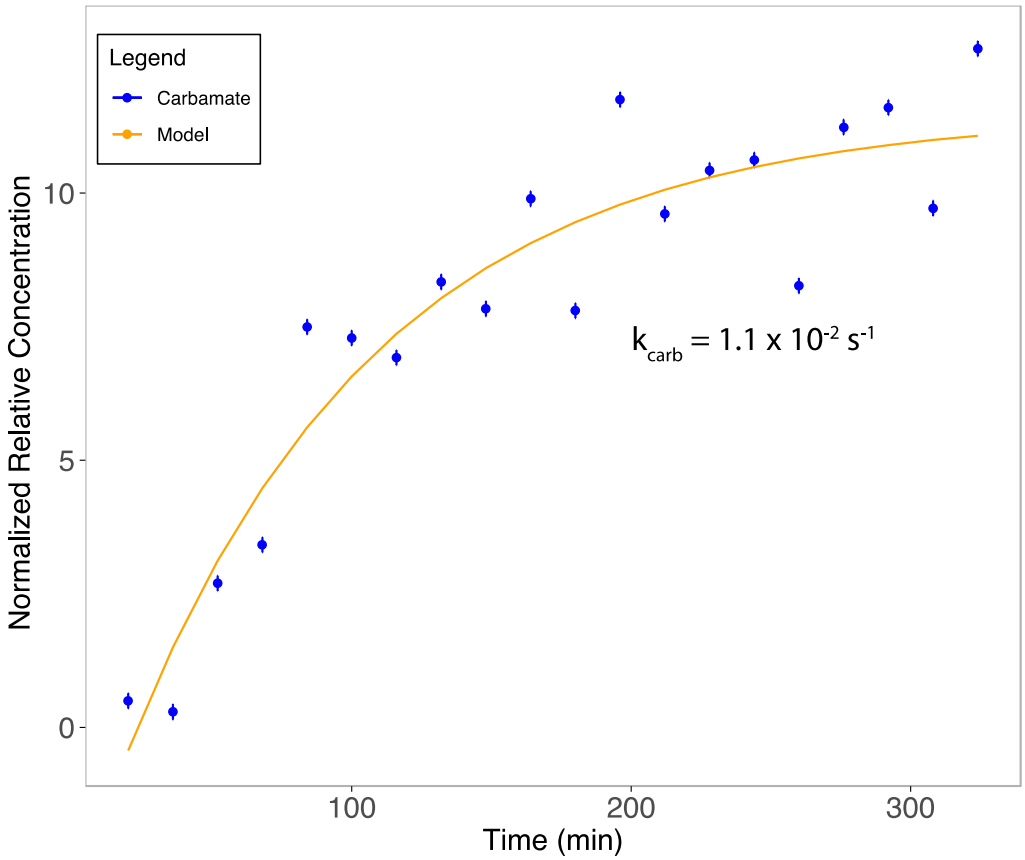

Figure 18. A timeseries plot of the normalized relative concentration of ethanolamine-carbamate as measured by the 165.20 ppm chemical shift of the carbamate carbonyl nucleus (blue points, blue bars represent standard error) and the modeled pseudo-1st order reaction rate, k_{carb} = 1.1 x 10^{-2} s^{-1}.

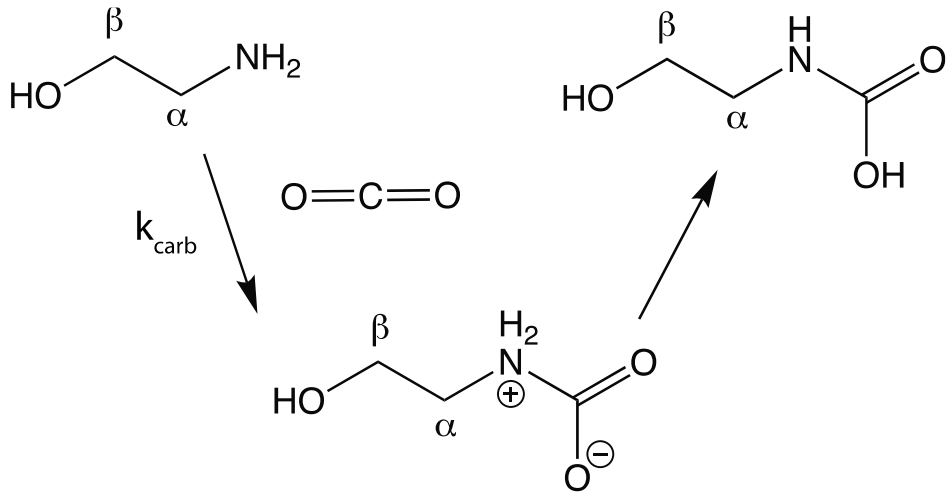

Figure 19. The general reaction mechanism for amine-mediated ethanolamine-carbamate formation. Nucleophilic attack of CO_2 by ethanolamine, governed by the rate constant k_{carb}, forms an ethanolamine-carbamate zwitterion in equilibrium with the protonated species at neutral pH.

b. Piperidine

The normalized relative concentrations of bicarbonate and carbamate produced by the piperidine-CO_2 experiment over the course of the 320-minute measurement period is shown in Fig. 20. The relative concentrations of carbamate and bicarbonate were determined based on integration and normalization of the 163.84 ppm chemical shift of the carbamate carbonyl nucleus and the 168.26 ppm chemical shit of the bicarbonate carbonyl nucleus (see Methods Section 1b). The modeled 1st order reaction rate constants of bicarbonate formation and carbamate dissociation were determined to be 4.87 x 10^{-3} s^{-1} and 4.893 x 10^{-3} s^{-1} respectively. The concentration data and kinetic models are depicted in Fig. 21, governed by the following equations (as in Eq. III in the Methods Section 2a):

$$Eq.VII \quad [carbamate] = ([carbamate]_0 - [carbamate]_\infty) * e^{-k_{dcarb}*t} + [carbamate]_\infty$$

where $[carbamate]$ is the concentration of carbamate and the 1st order rate constant of carbamate consumption, k_{dcarb}, is 4.893 x 10^{-4} s^{-1}. The initial concentration of the piperidine-carbamate tetrahedral intermediate, $[carbamate]_0$, and the equilibrium concentration, are modeled by the values 11.16 and 2.83 respectively. As in the ethanolamine experiment, these values are not quantitative reflections of the true composition of the solution.

The bicarbonate formation reaction is governed by the following equation (as in Eq. III in the Methods Section 2a):

$$Eq.VIII \quad [DIC] = [DIC]_\infty + ([DIC]_0 - [DIC]_\infty)e^{-k_{DIC}t}$$

where $[DIC]$ is the concentration of bicarbonate and the 1st order rate constant, k_{DIC}, is 4.87 x 10^{-3} s^{-1}. The values of the equilibrium concentration of the piperidine-carbamate intermediate ($[DIC]_\infty$, the horizontal asymptote), and the initial piperidine-carbamate carbamate intermediate concentration ($[DIC]_0$) are 10.58 and 1.53 respectively.

The flux of the carbamate dissociation and bicarbonate formation reaction, r_{hyd}, can be modeled according to the following equation:

$$Eq.VIX \quad r_{hyd} = [C_6NO_3H_{12}^{-}]k_{hyd}$$

where $[C_6NO_3H_{12}^{-}]$ represents the intracellular concentrations of piperidine-carbamate tetrahedral intermediate after hydroxide addition and k_{hyd} is the associated rate constant, which can be taken as the average of the rate constants for carbamate dissociation, k_{dcarb}, and bicarbonate formation, k_{DIC}. Thus, k_{hyd} is 4.88 x 10^{-3} s^{-1}, which is approximately 8 times slower than the abiotic CO_2 hydration rate, 0.04 s^{-1} (Zeebe & Wolf-Gladrow, 2001). The proposed reaction mechanism is shown in Fig. 22, in which nucleophilic attack of CO_2 by the amine group in piperidine forms a carbamate zwitterion. The protonated carbamate then undergoes addition of a hydroxide ion in aqueous solution to form a tetrahedral intermediate, which produces piperidine and bicarbonate upon spontaneous decarboxylation. The rate of this final reaction step is modeled by r_{hyd}, which depends upon the concentration of carbamate intermediate that is available to react.

In summary, the carbamate formation pseudo-1st order rate constant, k_{carb}, in the ethanolamine experiment was 1.1 x 10^{-2} s^{-1}, and the carbamate dissociation/bicarbonate formation 1st order rate constant, k_{hyd}, in the piperidine experiment was 4.88 x 10^{-3} s^{-1}. If we assume that the rates of carbamate formation and dissociation in ethanolamine and piperidine are similar (at least the same order of magnitude), then the ratio between the rate constants of carbamate formation and dissociation, k_{carb}/k_{hyd}, is 2.05, implying that carbamate is produced twice as quickly as it dissociates into bicarbonate.

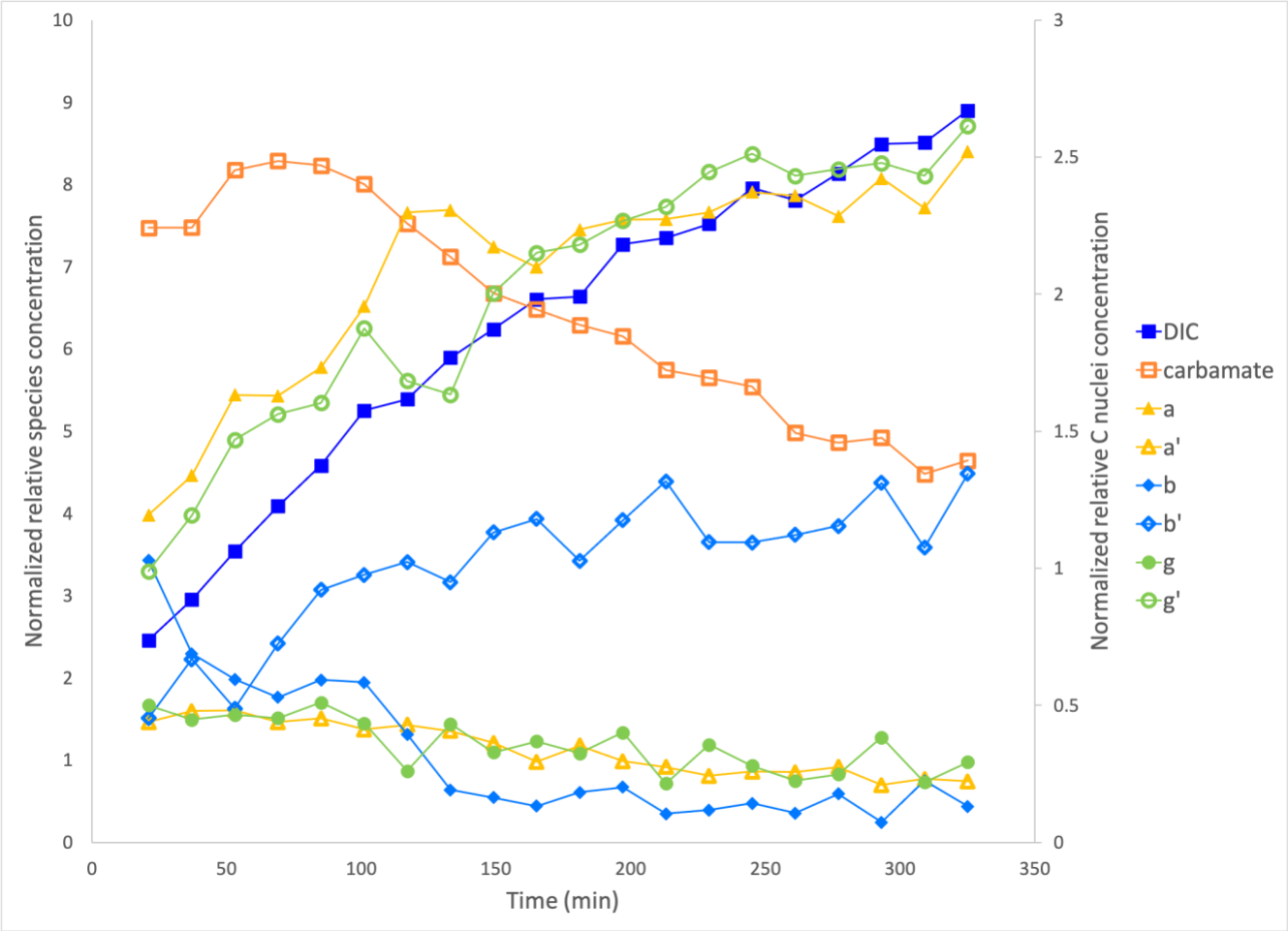

Figure 20. A timeseries plot of the carbon nuclei species in the Piperidine 2 experiment, as measured by NMR spectroscopy. The normalized relative bicarbonate (DIC, blue filled squares) and piperidine-carbamate (orange squares) concentrations, based on the 168.26 and 163.84 ppm chemical shifts of the carbamate and bicarbonate carbonyl nuclei respectively, are plotted on the left y-axis and the normalized relative concentrations of the piperidine and remaining piperidine-carbamate carbon nuclei are plotted on the right y-axis. The a (yellow filled triangles) and g'(green circles) carbons closely track the general increasing trend of the bicarbonate species, the b' carbon (blue diamonds) increases steadily over time, and the a' (yellow triangles), b (blue triangles), and g (green filled circles) decrease slightly over time. The piperidine-carbamate species dominates initially before steadily decreasing beginning at around 75 minutes while the bicarbonate species increases and takes over as the dominant species in solution as the reaction trends towards equilibrium.

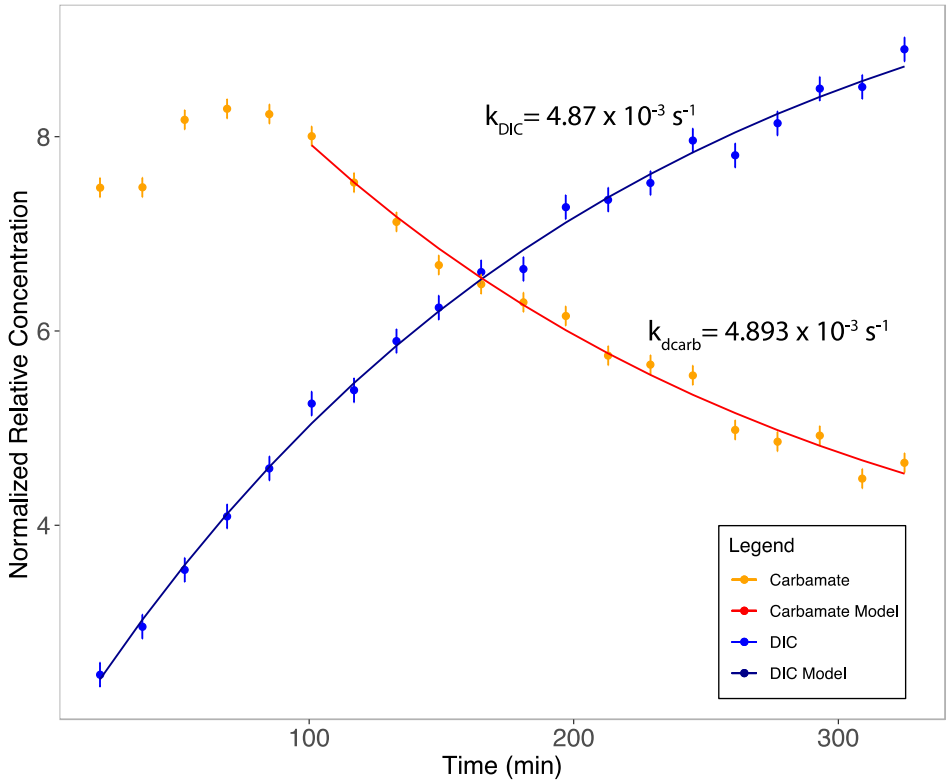

Figure 21. A timeseries plot of the normalized relative concentrations of bicarbonate as measured by the 168.26 ppm chemical shift of the bicarbonate carbonyl nucleus (blue points, blue bars represent standard error) and carbamate as measured by the 163.84 ppm chemical shift of the carbamate carbonyl nucleus (orange points, orange bars represent standard error). The modeled 1st order reaction rate constants of bicarbonate formation (blue line) and carbamate consumption (red line) are k_{DIC} = 4.87 x 10^{-3} s^{-1} and k_{dcarb} = 4.893 x 10^{-3} M^{-1} s^{-1} respectively (see Fig. 22 for reaction mechanism).

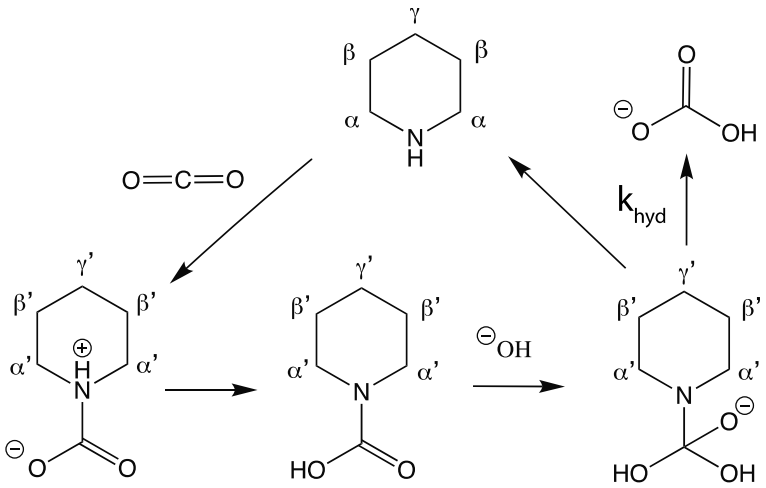

Figure 22. The general reaction mechanism of piperidine-mediated CO_2 hydration in the Piperidine 2 experiment. Piperidine nucleophilically adds into CO_2 to form the zwitterionic piperidine-carbamate species, which can be attacked by free hydroxide ions in aqueous solution in its protonated form to form a carbamate-hydroxide tetrahedral intermediate. This intermediate undergoes spontaneous decarboxylation to produce piperidine and bicarbonate. Reaction arrows are labeled with corresponding rate constants.

3. *Modeling Amine-Mediated CO_2 Hydration Chemistry in N. maritimus*

To determine what the potential carbamate formation and dissociation rates would be in the intracellular environment of *N. maritimus*, a simple four-box model was developed based on a prescribed carbon fixation rate (previously determined in Pearson et al., 2019) and coupled chemical kinetic and flux equations. A schematic of the model is pictured Fig. 23, depicting the four carbon inventories (C_e, extracellular CO_2; C_i, intracellular CO_2; carbamate, intracellular carbamate produced via amine-CO_2 adduct formation; HCO_3^-, intracellular bicarbonate; and C_{fix}, the bicarbonate that is fixed by acetyl-CoA/propionyl-CoA carboxylase) and the eight relevant fluxes (f_1, diffusion of CO_2 into the cell; f_{-1}, diffusion of CO_2 out of the cell; f_2, formation of carbamate via nucleophilic addition of an amine into CO_2; f_{-2}, dissociation of carbamate back into free amine and CO_2; f_4, dissociation of carbamate tetrahedral intermediate into bicarbonate upon addition of hydroxide; f_{hyd}, abiotic hydration of CO_2 to form bicarbonate; f_{dhyd}, abiotic dissociation of bicarbonate back into CO_2; f_5, bicarbonate fixation by acetyl-CoA/propionyl-CoA carboxylase; numbered based on Reactions I-V in Fig. 3). All the model parameters are listed in Table 3.

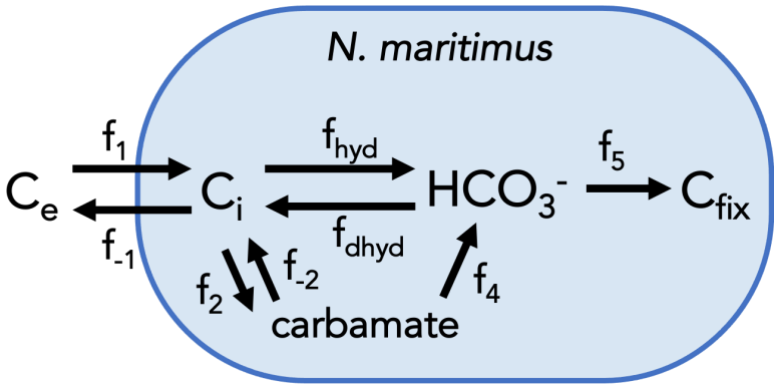

Figure 23. A schematic of the intracellular chemical kinetic model for amine-mediated CO_2 hydration in N. maritimus. The numbering scheme is consistent with that of Reactions I-V in Fig. 3, but simplified to exclude Reaction III, and with the addition of abiotic bicarbonate fluxes (f_{hyd} and f_{dhyd}).Fluxes defined in main text and in Table 3.

Two main scenarios were modeled: the first ascribed a fixed intracellular pH of 7.2 (Pearson et al. 2019) and the second modeled the effects of slightly more basic pH, varying this

parameter from pH = 7 to pH = 8 in intervals of 0.1. In both scenarios, the rate of abiotic HCO_3^- production, assumed to be 1.7 x 10^{-3} s^{-1} (see Table 3), is 10^2 times too small to support C_{fix}. This implies that the bicarbonate flux from carbamate dissociation, f_4, is 0.2153 mM s^{-1}. If we assume a 2nd-order carbamate formation rate constant of 4 mM^{-1} s^{-1}, which is a typical literature value in early studies of basic solutions of amino acids and in carbon capture studies (Chipperfield, 1966; Gros et al., 1976; Vaidya & Kenig, 2007), the carbamate flux, f_2, is 0.5067 mM s^{-1}, and the carbamate backflow, f_{-2} is 0.291 mM s^{-1}. These values have almost no dependence on pH and can thus be treated as constants. This leads to a modeled outcome for the ratio between carbamate formation and dissociation, f_2/f_4, that is approximately 2.35. This indicates that carbamate formation is just over twice as fast as bicarbonate formation. The carbamate backflow, f_{-2}, is 57% of the carbamate flux. The modeled f_2/f_4 ratio is generally in agreement with the experimental ratio that can be derived from the carbamate formation rate constant measured in the ethanolamine-CO_2 experiment (1.1 x 10^{-2} s^{-1}) and the carbamate dissociation rate constant measured in the piperidine-CO_2 experiment (4.88 x 10^{-3} s^{-1}), if it is assumed that these rates, derived from different amines, are comparable within an order of magnitude. The experimental f_2/f_4 ratio is approximately 2, implying a carbamate backflow of 50%, which is just under the modeled backflow of 57%. Note that while the model input for the carbamate formation rate constant (4 mM^{-1} s^{-1}, derived from carbon capture literature, 2nd order) is three orders of magnitude greater than the experimental rate constant derived from the ethanolamine experiment (1.1 x 10^{-2} s^{-1}, pseudo-1st order), carbamate dissociation fluxes calculated from both the model input rate constant and the experiment rate constant agree in orders of magnitude. Thus, while the experimental rates from NMR spectroscopy may not be entirely quantitative, they offer useful comparisons to model this process on a first-order level.

Table 3. *N. maritimus* intracellular CO_2 hydration model parameters. Note that OH^-, the internal concentration of hydroxide, is determined by the pH. All numerical input values were adopted from Wilkes and Pearson, 2019, and Pearson et al., 2019. *The parameters listed in this table assume a constant pH of 7.2; parameter values under varying pH are discussed in the text.

Parameter	Value	Units	Definition
N	6333.33	amol	total cell N inventory assuming 1N:6C
Am	3.17	mM	hypothetical free amine inventory, 0.05% N
k	4	$mM^{-1}\ s^{-1}$	typical carbamate formation rate
k_{carb}	12.67	s^{-1}	pseudo-1st order carbamate formation rate, k*Am
m_1	0.04	mM	extracellular CO_2
m_2	0.04	mM	intracellular CO_2
m_3	0.01*Am - 0.1*Am	mM	carbamate concentrations, 1-100% of amine inventory
m_4	0.0019	mM	intracellular HCO_3^-
T	298.15	K	temperature
S	35		salinity
pH	7.2; 7-8*		
k_{hyd}	0.0017	s^{-1}	abiotic CO_2 hydration rate constant
k_{dhyd}	0.0375	s^{-1}	abiotic CO_2 dehydration rate constant
D	400	s^{-1}	diffusive transport of CO_2 across the cell
V_{mx}	3.64	$mM\ s^{-1}$	ACC/PCC
K_m	0.03	mM	ACC/PCC
C_{fix}	0.2168	$mM\ s^{-1}$	ACC/PCC, $V_{mx}*m_4/(Km+m_4)$
f_1	$D*m_1$	$mM\ s^{-1}$	flux of CO_2 into the cell
f_{-1}	$f_1-f_{hyd}+f_{dhyd}-f_2+f_{-2}$	$mM\ s^{-1}$	flux of CO_2 out of the cell
f_2	$k_{carb}*m_2$	$mM\ s^{-1}$	flux of carbamate in cell
f_{-2}	f_2-f_3	$mM\ s^{-1}$	flux of $CO_{2,i}$, carbamate dissociation
f_3	$f_{dhyd}+f_5-f_{hyd}$	$mM\ s^{-1}$	flux of $HCO_3^-{}_i$, carbamate-OH^- dissociation
f_{hyd}	$k_{hyd}*m_2$	$mM\ s^{-1}$	flux of $HCO_3^-{}_i$, abiotic hydration
f_{dhyd}	$k_{dhyd}*m_4$	$mM\ s^{-1}$	flux of CO_2, abiotic HCO_3^- dehydration
f_5	C_{fix}	$mM\ s^{-1}$	carbon fixation by ACC/PCC
k_{dcarb}	$f_3/(OH*m_3)$	$mM^{-1}\ s^{-1}$	carbamate dissociation, 2nd order
$k_{dcarbOH}$	$k_{dcarb}*OH$	s^{-1}	carbamate dissociation, pseudo-1st order

Discussion

1. *Amine-CO_2 Reactivity is Determined by Amine pKa and Structure*

In general, the two primary determinants of molecular reactivity in aqueous amine-CO_2 systems are the pKa and structure of the amine (Kortunov et al., 2015; Stowe et al., 2015). The pKa of an amine group determines the degree of protonation of that amine at a given pH, and the degree of protonation of the nitrogen atom determines its nucleophilicity. For example, a protonated and positively charged amine group with sp^3 bond character would have no free lone pairs with which to attack into an electrophilic orbital such as that of CO_2. In this case, it cannot act as a Lewis base with surrounding water molecules either, and pKa can be used to gauge approximate basicity or nucleophilicity with respect to local protons. In addition, the structure of the amine can strain its ability to act as a strong nucleophile due to physical steric effects from bulky side groups (such as in the case of tertiary amines or sterically hindered secondary amines). In the following section, I will use these general guiding principles to understand and explain the observed reactivity of the various tested amine-containing molecules with CO_2 in aqueous solution.

a. Amino Acids, Protecting Groups, and Mixtures

The amino acids glycine, proline, and lysine did not react with aqueous CO_2 to form stable carbamate and bicarbonate species because of their zwitterionic nature at neutral pH. At pH ~7, amino acids contain a positively charged ammonia group and a negatively charged carboxylate group; thus, the nitrogen lacks sufficient electron density to act as a potent nucleophile. The addition of a methyl ester protecting group to neutralize the carboxylate of an amino acid was hypothesized to improve reactivity by increasing the nucleophilicity of the amine group; however, reactions with CO_2 were not observed for proline methyl ester or lysine methyl ester. One potential

explanation for the failure of the methyl ester groups to sufficiently protect the carboxylate termini of the amino acids could be unforeseen ester hydrolysis. At neutral pH, it was assumed that ester groups would be relatively stable given that a strong acid catalyst is generally necessary to hydrolyze an ester, but both proline methyl ester and lysine methyl ester were used in their hydrochloride salt form. In aqueous solution, the additional HCl might not have been sufficiently neutralized by the phosphate buffer, leading to ester protonation and hydrolysis, potentially driving the equilibria towards the formation carboxylate termini and free methanol. However, no methanol was observed in the NMR spectra for lysine methyl ester or proline methyl ester, meaning that this species was under the detection limit or, more likely, that this alternative side reaction did not happen at all, since the buffer concentration was more than sufficient. An alternative possibility is that protection of the carboxylate groups with a methyl ester may have allowed the amino acid methyl esters to react with themselves to form stable amides, in which the esters would outnumber and perhaps outcompete CO_2 as electrophiles. This suggests that the presence of carbonyls within amine compounds hinder the nucleophilicity of the amines, which is consistent with the ability of amines to neutralize amino acids as protecting groups (discussed below).

Amine-neutralized amino acids have also been used to improve amino acid reactivity with CO_2 in aqueous amine solvents (Ciftja et al., 2014). In this study, an equimolar mixture of ethanolamine and glycine successfully produced carbamate (see Fig. 10 in Results Section 1b), indicating that amino acid protection with an amine is more effective than the use of a methyl ester protecting group. In agreement with the literature, both ethanolamine-carbamate and glycine-carbamate were produced, but no bicarbonate was produced; the latter is most likely due to a low CO_2:amine concentration ratio. In Citfja et al. 2014, no bicarbonate was produced below 0.31 mol CO_2/mol alkalinity; this study, with a headspace CO_2 concentration of 0.0726 M and a 0.5-0.5 M

solution of glycine and ethanolamine, had a ratio of 6.12 x 10^{-2} mol CO_2/mol alkalinity, and did not meet this requirement. This ratio is likely comparable to what might be found in *N. maritimus.* If we assume that the intracellular CO_2 inventory is 0.04 mM and the approximate amount of free amine available to react is 3.17 mM (see Table 3), and that the cell volume of *N. maritimus* is 0.022 μm^3 (Pearson et al., 2019), the intracellular ratio would be about 1.39 x 10^{-2} mol CO_2/mol alkalinity. This estimate is about 10 times smaller than the bicarbonate production limit found in Citfja et al. 2014, suggesting that the limited flux of intracellular CO_2 would disfavor carbamate production via this mechanism in *N. maritimus.*

The same study found that the use of 2-amino-2-methyl-1-propanol as an amino acid neutralizer in equimolar mixture with glycine produced almost exclusively glycine-carbamate, and attributed this difference to steric hindrances afforded by the methyl groups in 2-amino-2-methyl-1-propanol that decrease the stability of its carbamate species. Based on these findings, the ideal amino acid protecting group must be comparable in basicity to the amino acid but sterically accommodating.

b. Ethanolamine

Ethanolamine has been studied extensively as a carbon capture solvent, in which capacity it is a powerful absorbent in very basic solution. A primary amine with a pKa of 9.5, ethanolamine is a sterically unhindered base, and previous studies such as one by Kortunov *et al.* (2015) have characterized trends in its reactivity with CO_2 to be similar to those of piperidine, a secondary cyclic amine and a much stronger base (with a pKa of 11.28). However, the results of the aqueous ethanolamine-CO_2 experiment carried out in this study do not completely agree with the findings of Kortunov et al. (2015). Their study of ethanolamine mirrored their findings on piperidine; that is, initial carbamate production and decline following bicarbonate production after about 20

minutes of CO_2 bubbling. In this study, ethanolamine was found to produce only carbamate, and no bicarbonate species were detected (Results Fig. 11). One potential explanation is that, similarly to the case of the amino acid methyl esters, buffering the solution to a neutral pH stymied amine-base catalysis of both carbamate dissociation and CO_2 hydroxylation, leading the solution to become carbamate-saturated. However, it is also possible that bicarbonate production was simply not captured by NMR spectroscopy due to very low concentrations that were unresolvable at the scanning parameters. Repetition of this experiment would be helpful for determining which of these two scenarios is responsible for the observed reactivity, as well as performing similar experiments at slightly more basic and acidic pH ranges. Indeed, repetition of all the experiments carried out in this study would be helpful, and while more acidic/basic conditions may not accurately model the true intracellular environment, such experiments could provide insight into the dependence of the carbamate dissociation and bicarbonate formation reaction rates on hydroxide concentrations. Additionally, while the goal of this study was to study these reactions as they might occur in a cytosolic environment, it is possible that *N. maritimus* maintains or alters intracellular pH adjacent to the cell membrane to be closer to that of incoming seawater—this idea is discussed in greater detail in Discussion Section 2c.

c. Diethanolamine

Puzzlingly, diethanolamine showed no reactivity in this study, despite its documentation as a carbamate- and bicarbonate-producing carbon capture solvent in the literature (Barzagli et al. 2018). This could also potentially be attributed to the low CO_2:amine ratio in the experimental solution—in Barzagli et al. (2018), an amine:CO_2 ratio of 10:1 produced little carbamate and no bicarbonate, while a ratio of 1:2 produced both species. In this study, the diethanolamine:CO_2 ratio was 4.5:1. With a pKa of 8.96, diethanolamine may not be a strong enough nucleophile in neutral

solution to produce significant quantities of carbamate or bicarbonate product. It is also quite possible that the poor spectral acquisition of the diethanolamine NMR experiment resulted in the loss of spectral information at the higher carbonyl resonance frequencies. Pursuing further experiments with better signal acquisition parameters tuned to the relaxation times of diethanolamine carbamate carbons would improve the current understanding of the reactivity of this molecule at neutral pH.

d. Piperidine

Piperidine, with a pKa of 11.28, was the most strongly basic amine tested in this study, and proved to be the most reactive.[4] The results of the aqueous piperidine-CO_2 experiment agree with a similar ^{13}C NMR spectroscopy study done by Kortunov *et al.* (2015), in which the reaction of aqueous piperidine in solution produced an initial excess of carbamate species that declined after about 20 minutes of continuous CO_2 bubbling, at which point bicarbonate production dominated until the two species reached equilibrium after about two hours (Kortunov et al., 2015). In the Kortunov et al. (2015) study, continuous bubbling of CO_2 allowed faster gas exchange and thus decreased the time it took for the reaction to reach equilibrium compared to the current study, which was much slower due to the limiting rate of gaseous CO_2 dissolution from the NMR tube headspace into the sample. Despite this difference, the clarity of the NMR data for piperidine in this study was remarkable: not only were the carbonyl resonances of both the carbamate and bicarbonate/carbonate ion species detected, but the cyclic piperidine-carbamate carbons also had strong, clear signals. The upfield shift of these carbon signals arises from inductive effects of the addition of the electron-withdrawing carbonyl (there exists a resonance structure in which the nitrogen lone pair can delocalize across the carbon-nitrogen bond into the electronegative carbonyl

[4] Incidentally, piperidine was also the very first compound tested via ^{13}C NMR spectroscopy in this study. First time's the charm!

oxygen, drawing electron density away from the cyclic carbons). Thus, detection of those peaks as well as the downfield carbamate carbonyl are strong indicators of true carbamate production via the two-step zwitterionic mechanism.

The reaction of piperidine and CO_2 appears to occur via two time-dependent regimes: initial carbamate production, then rapid carbamate hydroxylation and decarboxylation followed by preferential accumulation of bicarbonate. Carbamate is more thermally stable than bicarbonate, especially at neutral pH, but the buildup of carbamate leads to rapid hydrolysis in aqueous solution (Kortunov *et al.*, 2015). Thus, over longer time periods, bicarbonate production dominates the system. It has been suggested that secondary amines like piperidine also produce a substantial amount of bicarbonate via the base-catalysis mechanism (Reaction **VI**, Fig. 4) compared to primary amines with similar pKa due to the steric hindrance of the cyclic carbons surrounding the amine nitrogen (Kortunov et al., 2015). Without quantitative data for at least diethanolamine, it is difficult to distinguish between the competing effects of steric hindrance and pKa in the case of these two secondary amines.

e. 2-amino-2-methyl-1-propanol

2-amino-2-methyl-1-propanol (AMP), a sterically hindered primary amine with a pKa of 9.7 (comparable to that of ethanolamine, an unhindered primary amine), showed interesting reactivity, in part at odds with behavior documented in the carbon capture literature. In this study, AMP produced only carbamate, and NMR spectroscopy only detected the presence of the carbonyl carbon of AMP-carbamate, with little to no detection of shifted alkyl AMP-carbamate carbons. However, prior molecular dynamics studies have observed almost exclusive production of bicarbonate over carbamate via the Reaction **VI** mechanism favored by tertiary and sterically hindered amines (see Fig. 4; Stowe et al. 2015). It is argued that the steric hindrance of the two

methyl groups in AMP results in a more planar, sp^2-like character about the carbon-nitrogen bond, which induces a slight dipole that affords the nitrogen a more negative charge, strengthening its interactions with surrounding water molecules and decreasing the accessibility of that binding site to CO_2 (Stowe et al. 2015). While studies comparing the reactivity of AMP and its similarly basic analog, ethanolamine, have shown clear differences in carbamate/bicarbonate production attributed to these structural and steric effects, the current study finds similar behavior between ethanolamine and AMP at neutral pH. It is important to note that while carbamate was detected in the AMP-CO_2 NMR experiment (see Fig S.14), the signal acquisition was poorer than the ethanolamine and the piperidine experiments, and the peaks exhibited non-Lorentzian shapes with asymmetrical broadening. These data acquisition errors are most likely attributable to a shimming error in the NMR spectrometer itself and decrease the resolution and quantitative power of the resulting spectra. It's possible that the lower resolution caused an insensitivity to more complex splitting patterns, especially in the carbonyl range – i.e., making it impossible to detect free bicarbonate/carbonate. This makes ascertaining the reason for the observed reactivity and its difference from the expected outcome challenging; however, these results may be explained by considering the pH dependence of these reactions. Previous studies have used unbuffered aqueous solutions of AMP, allowing the basic amine to contribute to CO_2 dissolution and bicarbonate production via the base catalytic effect. In this study, the high concentration of phosphate buffer locks the pH near 7.2, thus decreasing the ability of AMP to alter solution's pH. If base catalysis is the primary pathway of bicarbonate formation, then at neutral pH, AMP might behave more like its cousin ethanolamine and favor the carbamate-forming two-step zwitterionic mechanism.

f. Peptides and Proteins

The two experiments testing glutathione (an oligopeptide) and cytochrome C (an easily accessible heme protein found in the electron transport chain of mitochondria) yielded results similar to those of the control experiments, suggesting an inability of the experimental methodology to accurately capture chemistry between large protein-type molecules and CO_2. Thus, these experiments will not be discussed in detail. Future work should focus on developing a procedure tailored to detecting carbamate production by free N-termini of small, relevant proteins; or alternatively, focus on other N-functionalized small molecule metabolites. In particular, it would be of great interest to study the potential for this chemistry in the intracellular domains of transmembrane proteins isolated from *N. maritimus* or related organisms; or alternatively, to study known cellular osmolytes such as glycine-betaine or beta-glutamic acid. While out of the temporal scope of this study, a similar experiment could be developed with *N. maritimus* cell lysate to determine if there is net CO_2 capture and tease out responsible N-containing fractions.

2. *Experimental & Model Results Suggest Low Viability of Amine-Mediated CO_2 Hydration in N. maritimus*

Together, the experimental and computational analyses in this study show that the hypothesis that *N. maritimus* uses amine-mediated CO_2 hydration to produce sufficient bicarbonate for its anabolic requirement in the absence of the enzyme carbonic anhydrase is an insufficient explanation of the true hydration pathway, which remains unclear (Table 4). As discussed previously, while the experimental results from ^{13}C NMR spectroscopy are not wholly quantitative, the kinetics derived from those experiments are useful in understanding the order of magnitude and general trends of these reaction rates in comparison to previously measured rates and those modeled in this study. Combining these data with the modeled chemical behavior of this system in an *N. maritimus* cell (see Table 4) makes it possible to determine whether this process

is 1) a viable biological pathway, and 2) fast enough to explain both the carbon fixation rate of acetyl-CoA/propionyl-CoA carboxylase and the measured and modeled carbon isotope excursions of the intracellular carbon pool of *N. maritimus*. In this section, the experimental and model results are compared and analyzed in accordance with a previous study of the intracellular carbon dynamics of *N. maritimus* (Pearson et al. 2019) to attempt to answer these guiding questions, the originally hypothesized reaction pathway is compared to the mechanism of action of carbonic anhydrase itself, and potential alternative mechanisms are proposed and discussed.

Table 4. Comparisons of measured and modeled rate constants and fluxes for carbamate formation (Reaction II), carbamate dissociation/bicarbonate formation (Reaction IV), and carbon fixation by ACC/PCC (Reaction V). Note that reactions are labeled with numbers as per Fig. 3. The experimental pseudo-1st order and 1st-order reaction rate constants for Reactions II and IV come from the ethanolamine and piperidine experiments, respectively. "Experimental Flux" refers to the estimated intracellular carbamate formation and bicarbonate formation rates inferred from experimental rate constant data. The experimental flux estimates were calculated with the assumption that the intracellular CO_2 concentration is 0.04 mM (see Table 3; Pearson et al. 2019) and that the intracellular carbamate ranges from ~0.03-3 mM (see Table 3; Pearson et al. 2019). These assumptions also govern the model flux estimates. *The range of values reflects the potential range of carbamate concentrations that could be present in *N. maritimus* based on the amount of available free amine.

Reaction	Description	Experimental Rate Constant (s^{-1})	Experimental Flux (mM s^{-1})	Model Flux (mM s^{-1})
Rxn. II	Carbamate formation	1.1×10^{-2}	4.4×10^{-4}	5.067×10^{-1}
Rxn. IV	Carbamate dissociation/bicarbonate formation	4.88×10^{-3}	$1.46 \times 10^{-4} – 1.46 \times 10^{-2}$ *	2.153×10^{-1}
Rxn V	Carbon fixation by ACC/PCC	-	-	2.168×10^{-1}

a. Carbamate Dissociation Could Account for Observed Carbon Isotope Fractionation Effects in *N. maritimus*

Overall, kinetic analysis of the buffered amine-CO_2 equilibration experiments at biological pH yielded reaction rates that are too slow to be the sole catalytic producers of bicarbonate in *N. maritimus*. The amine-mediated carbamate dissociation/bicarbonate formation rate constant, 4.88 x 10^{-3} s^{-1}, is too slow by about an order of magnitude compared to the abiotic CO_2 hydration rate constant (0.04 s^{-1}; Zeebe & Wolf-Gladrow, 2001), and the associated HCO_3^- flux from this reaction is too slow by about three orders of magnitude to the modeled bicarbonate fixation rate in acetyl-CoA/propionyl-CoA carboxylase, 0.2168 mM s^{-1} (see Table 4; Pearson et al 2019). Of course, due to the inconclusive nature of the majority of the amine-CO_2 equilibration experiments done in this study, further research is necessary to determine the average reaction rate of these types of amine-containing compounds under biological conditions. However, for the purposes of this study, it seems that the hypothesized pathway is not fast enough at neutral pH to keep up with the modeled rate of carbon fixation in *N. maritimus*.

The intracellular carbon dynamics of *N. maritimus* have been measured and modeled extensively in order to characterize the total biosynthetic isotope effect associated with the 3-HP/4-HB autotrophic pathway, which appears to be sensitive to changes in growth rate and seawater CO_2 concentrations and is thus a promising candidate for pCO_2 paleobarometry, or the use of marine archaeal lipid carbon isotope excursions as proxies for ancient marine and atmospheric CO_2 concentrations (Pearson et al. 2019). To that end, CO_2 hydration rates and associated isotope effects have been modeled in *N. maritimus* and thus can serve as an external check on the proposed hydration pathway: if the proposed mechanism can affect a similar isotope effect as has been modeled to exist in this organism, this could be evidence for its viability as the true hydration

pathway. The isotope effect imparted by the hydration mechanism cannot be greater than the kinetic isotope effect associated with abiotic CO_2 hydration, which is estimated to be 25‰ (Wilkes & Pearson, 2019; Zeebe, 2014). According to a previous study, the biomass of *N. maritimus* is uncharacteristically ^{13}C-depleted for the 3-HP/4-HB pathway, implying the carbon fixation substrate, bicarbonate, is isotopically more negative than the extracellular supply. This necessarily indicates there must be internal $CO_2 \leftrightarrow$ bicarbonate disequilibrium that drives the overall isotope effect of 19.6‰ (Pearson et al., 2019). This process is controlled by the balance between the CO_2 hydration flux and the carbon fixation rate, which together determine the backflow ratio for bicarbonate dehydration (Pearson et al., 2019).

The experimental and modeled rates of carbamate formation and dissociation in this study produced carbamate flux ratios, f_2/f_4, of 2 and 2.35 respectively, implying a 50-57% backflow of carbamate back into CO_2 and amine for every mole of carbamate produced (see Results Section 3). These ratios indicate that this hydration pathway is not wholly unidirectional. If the bicarbonate production pathway is not unidirectional, the carbon isotope excursion imparted by the hydration process would not be conserved across each step of the forward reaction. Thus, if 50-57% of the carbamate production reverts back into the intracellular CO_2 pool, only 50-57% of the maximum kinetic isotope effect associated with abiotic CO_2 hydration, 25‰, would be expressed. This gives a HCO_3^- pool that is at most 14‰ ^{13}C-depleted relative to the intracellular CO_2 pool, which is estimated to have a -9‰ value if in equilibrium with seawater. In total this yields a maximum isotope effect of 14 – (-9) = 23‰, which is at the upper end of the 18-23‰ effect modeled from environmental data (Pearson et al. 2019). Thus, amine-mediated CO_2 hydration via the carbamate-formation pathway could ostensibly account for the observed and modeled carbon isotope dynamics present in *N. maritimus*. The alternative base-catalysis mechanism of amine-mediated

CO_2 hydration (Reaction **VI**, Fig. 4) could also account for the isotope effect—this idea is discussed later in Section 2c.

b. Carbamate Chemistry is Similar to the Chemical Mechanism & Evolution of Carbonic Anhydrase

While the proposed pathway does not completely align with these previous analyses of the inner machinations of *N. maritimus*, it cannot be completely ruled out, given the uncertainties associated with the current kinetic and carbon isotope models of this organism. In order to understand the viability of this pathway in an evolutionary and mechanistic context, it must be compared to the enzyme that it is hypothesized to replace or precede: carbonic anhydrase.

As discussed briefly in the Background section of this paper, carbonic anhydrase is a highly pH-dependent enzyme, operating at an optimal pH of 8 and declining in activity under more acidic conditions. The catalytic site of carbonic anhydrase is its central zinc atom, which binds to water and decreases its pKa to generate hydroxide ions at neutral pH (J. Berg et al., 2002). It is the nucleophilic attack of the resulting hydroxide into CO_2 that forms bicarbonate, which is released from the active site to allow another water molecule to bind to zinc and continue catalysis (J. Berg et al., 2002). The participation of a buffer species is essential to this mechanism: while hydroxide and proton concentrations are limited to 10^{-7} M at neutral pH, buffer concentrations have no such requirement and thus can participate in proton abstraction of the zinc-bound water molecule, allowing the rate of hydroxide formation and thus catalysis to reach speeds of up to 10^6 s^{-1} (J. Berg et al., 2002). Carbonic anhydrases have evolved proton shuttles containing histidine residues that allow the manipulation of protons in the vicinity of the enzyme such that a proton can be transferred from the water in the catalytic site to a buffer acceptor via a histidine imidazole ring (J. Berg et al., 2002). Precise mediation of proton transfer steps in this hydration mechanism is the

driving evolutionary force behind carbonic anhydrase's enzymatic success at regulating acid-base catalysis—thus, an organism lacking this adept machinery might have evolved similar, if simpler, methods of "proton passing" to manage the rate-limiting hydroxide production step.

While no carbonic anhydrase homologs have been found in the genome of *N. maritimus*, several species of soil Thaumarchaeota encode γ-class carbonic anhydrase analogs containing N-terminal signal peptides that indicate extracellular localization, suggesting a role that facilitates the conversion of extracellular bicarbonate into CO_2 to allow diffusion through the cell membrane (Kerou et al., 2016). Similar carbonic anhydrase homologs exist in ammonia oxidizing bacteria whose activity has been found to correlate with CO_2 fixation rates under carbon-limiting conditions (Kerou et al., 2016). The terrestrial cousins of marine Thaumarchaeaota offer evolutionary clues into the independent development of fixation-dependent CO_2 hyration mechanisms in this archaeal lineage: since carbon is not limiting in the ocean, marine Thaumarchaeaota have no need to implement extracellular conversion and capture mechanisms, while the unpredictable carbon flux in a terrestrial envrionment would necessitate these adaptations for soil-bound ammonia oxidizing archaea. Instead, the issue lies in regulating the acid-base equilibria of intracellular CO_2 hydration to trap and concentrate carbon inside the cell to sufficiently feed the central carbon fixation enzyme acetyl-CoA/propionyl-CoA carboxylase, since the uncatalyzed equilibration, although it tends towards bicarbonate at neutral pH, is not fast enough to supply the enzyme at growth rates consistent with current cultures and models.

Of the amine-CO_2 reaction pathways that produce (or hypothetically produce) bicarbonate, the tertiary amine termolecular/base catalysis mechanism is the most similar to the mechanism of carbonic anhydrase in its specific regulation of proton transfer to allow faster hydration of CO_2 by water. The majority of amines tested in this study are thought to react via the two-step zwitterioinic

carbamate formation mechanism, and the intrecellular chemical model also assumed a reaction pathway via this carbamate-forming pathway. Thus, it is necessary to discuss an alternative CO_2 hydration mechanism in *N. maritimus* in which amines fuel bicarbonate production as base catalysts rather than as carbamate precursors.

c. Further Investigations Should Focus on Amines as Base Catalysts in CO_2 Hydration and Redox Coupling at the Electron Transport Chain as Alternative Mechanisms

If we assume carbamate intermediates are not involved, it remains possible that sterically hindered, secondary and tertiary amines are still able to catalyze CO_2 hydration via proton abstraction in a manner similar to the activity of carbonic anhydrase (Pesci et al., 2017, Stow et al., 2015). Analyzing the viability of this alternative pathway then becomes a question of intracellular acid-base chemistry and proton inventory. The generation of hydroxide is the rate-limiting, energetically costly step in nearly all mechanisms of CO_2 hydration, including the amine-mediated bicarbonate formation from carbamate mechanism scrutinized in this study. The generation of hydroxide ions necessary for carbamate decarboxylation or CO_2 hydration *in situ* could occur by raising the pH of the immediate intracellular surroundings coupled to electron transport, a process that has been shown in some strains of cyanobacteria (Li & Canvin, 1998; Smith & Ferry, 2000). This proton regulation would need to occur in the vicinity of the cell membrane to allow quick sequestration of the OH^- left behind by H^+ translocation, and it would need to couple it immediately to reaction with CO_2. This could perhaps occur by coupling transmembrane protein N-termini to some kind of membrane redox potential via a dehydrogenase associated with electron transport. In cyanobacteria, an NADPH dehydrogenase called NDH-1 (NADH ubiquinone oxidoreductase) has been characterized that catalyzes the first step at Complex I of the mitochondrial electron transport chain (Ogawa & Mi, 2007). One NDH-1 complex, NDH-

1S, contains four subunits, two of which, CupA and CupB, are presumed to have a carbonic anhydrase-like activity and play a role in the conversion of CO_2 to HCO_3^- (Ogawa & Mi, 2007). In *N. maritimus,* the ammonia oxidation respiration pathway runs through an electron transport chain containing an NDH-1 complex as well as various copper-containing oxidoreductases (Walker et al., 2010); it is possible that coupling amine-mediated CO_2 hydration to oxidoreductase activity at the cell membrane could drive sufficient proton abstraction to increase hydroxide attack into CO_2.

In addition to its similarity to the carbonic anhydrase mechanism of hydration, the base catalysis mechanism, as an acid-base reaction, would ostensibly occur with faster rate constants than carbamate formation and dissociation (on the order of 10^{-1} s^{-1}, according to measurements of tertiary amines in Littel et al., 1990), and if these equilibria were product-favoring at the local pH then this pathway would represent a unidirectional CO_2 hydration mechanism with little backflow. Thus, both the base-catalysis and carbamate-forming mechanisms could account for the perceived kinetic isotope effect of CO_2 hydration in *N. maritimus*.

It is also possible that the NDH-1 complex in *N. maritimus* may be able to directly catalyze carbon dioxide hydration without the need for any type of amine mediation at all, be it primary, secondary, or tertiary. If amine-mediated hydration cannot quantitatively account for bicarbonate production and there are no other plausible indirect pathways, all arrows point to direct hydration of bicarbonate in a carbon concentrating mechanism analogous to the type present in marine cyanobacteria. The genes that encode the NDH-1 complex in cyanobacteria, *chpX* and *chpY*, have no homologies with known carbonic anhydrase families, but conserved amino acid residues (two histidine and one cysteine) have been identified across ten cyanobacteria that could act as zinc coordination sites, like in carbonic anhydrase (Badger & Price, 2003). Assuming that these

residues can in fact coordinate with zinc, the reaction sequence that is thought to drive carbon dioxide hydration in these complexes involves the following two steps: first, electron donation to NDH-1 by a donor molecule, such as NADPH or ferredoxin, which produces a reduced intermediate that can act as a base to abstract protons from the water-bound zinc to produce hydroxide (Badger & Price, 2003). Then, the abstracted proton is translocated across the membrane via a proton shuttle path within a hydrophobic protein channel, causing a net production of bicarbonate (Badger & Price, 2003). In the case of cyanobacteria, this process is thought to occur at the thylakoid membrane in chloroplasts to drive photosynthesis, but the NDH-1 complex in *N. maritimus* associated with ammonia oxidation is located at the cell membrane and thus could simultaneously act as a carbon concentrator.

There are some notable genetic similarities between Thaumarchaeota and marine phytoplankton that may help elucidate the potential for NDH-1 to aid carbon concentration in *N. maritimus*. The *N. maritimus* genome has a similar ratio of energy production, coenzyme transport and metabolism, and translation genes to the cyanobacterial phyla *Prochlorococcus* and *Synechococcus*, and the presence of copper-containing electron carriers in *N. maritimus* also bears resemblance to the eukaryotic marine diatom *Thalassiosira oceanica* (Walker et al., 2010b). *T. oceanica* uses a copper-containing protein, plastocyanin, instead of common iron-containing cytochromes in its electron transport chain in order to reduce the amount of iron necessary for growth, allowing for allocation of iron to other essential functions and giving the cell an energetic advantage (Peers & Price, 2006). These open-ocean organisms have developed needs for specific metal cofactors under nutrient-limiting conditions, particularly in carbon concentrating complexes, and many species of marine phytoplankton can substitute cadmium and cobalt for zinc in carbonic anhydrase (Morel et al., 2020). Perhaps it is possible, then, that *N. maritimus* uses the abundant

copper in its respiratory pathway as a zinc alternative in a carbonic anhydrase-like hydration complex in NDH-1. Additionally, it is possible that proton translocation mechanisms such as the one hypothesized for the NDH-1 complex could have predated the other carbon concentration mechanisms in marine plankton and even carbonic anhydrase. Indeed, if *N. maritimus* has found a way to trap bicarbonate using a prototypical version of modern carbonic anhydrases, then elucidating the mechanism of this pathway could reveal the unknown evolutionary history of autotrophic carbon fixation across all three domains of life.

3. *Broader Implications for Autocatalysis & the Origins of Life*

A primary motivation for this work was to gain a deeper understanding of the chemical and molecular selective pressures that may drive the evolution of complex, efficient, highly conserved enzymes from simple, ubiquitous, and recyclable organic building blocks. Autocatalytic cycles such as the one scrutinized in this study are the quintessential components of the larger building blocks of life: cells. These self-starting, self-perpetuating cycles give rise to the three key fundamental properties of life—metabolism, self-replication, and self-containment via a lipid membrane—and have been theorized as the essential driver of life since Tibor Gánti developed the first computational abstract of a protocell, the chemoton (Marshall, 2020). While direct amine-mediated CO_2 hydration may be too slow to power carbon fixation in the modern 3-HP/4-HB cycle of *N. maritimus*, studying this mechanism can still provide clues as to what an ancient CA antecedent could have looked like and how it may persist in remarkable archaea like *N. maritimus* today. The base-catalysis mechanism of tertiary and sterically hindered amines (Reaction **VI**, Fig. 4) closely mirrors that of modern CA, save the use of a metal ligand to act as a catalytic site. Thus, it is plausible that this mechanism could be an "early version" of the catalytic activity of modern CAs, before the embedding of metals within the amine structures of early proteins led to faster

hydration rates that were selected for in slow-growth ecological regimes. As previously mentioned, the ubiquitous copper-containing oxidoreductases present in redox structures along the cell membrane of *N. maritimus* could potentially serve a dual role as metal-containing catalysts for both proton abstraction and CO_2 hydroxylation, and this type of thrifty, dual-purpose activity would serve as a characteristic oligotrophic adaptation in an organism that already utilizes enzyme promiscuity to its advantage. Similarly energy-stressed organisms in the dilute Archaean ocean of three billion years ago may have taken advantage of this theoretical coupling of the redox activity of metal cations with the autocatalytic tendencies of simple organic compounds. Such interactions may mark the initiation not only of early life, but also of the marine carbon cycle. While further bioinformatic analysis of the genetic history of *N. maritimus* will shed more light on its evolution and the development of its streamlined, efficient, and potentially ancient autotrophic metabolism, this study provides a looking glass with which to view the potential diversity of life-giving chemistry in Earth's oceans.

Conclusion

In my thesis, I sought to answer the question, how do marine Thaumarchaeota like *N. maritimus* produce HCO_3^- to supply their autotrophic carbon fixation cycles without the ubiquitous CO_2 hydration enzyme, carbonic anhydrase? The hypothesized mechanism, involving the reaction of amines with CO_2 to form carbamate and HCO_3^- species autocatalytically, was analyzed experimentally and computationally to determine the specific kinetics of this reaction in conditions similar to the neutral aqueous intracellular environment of *N. maritimus*. ^{13}C NMR spectroscopy experiments of 12 different amines, while insufficiently quantitative for a comprehensive understanding of absolute reaction kinetics, showed that amine reactivity with CO_2 generally increases with increasing amine pKa, but is highly dependent on structure, with more sterically hindered amines (such as secondary and tertiary amines) being more likely to form bicarbonate species than primary amines.

The two main reaction mechanisms for amine-mediated CO_2 hydration observed in this study were formation and decarboxylation of a carbamate zwitterion species and base catalysis via proton abstraction by amines in aqueous solution, the latter being more similar to the catalytic activity of CA. The observed 1st-order reaction rate constants for carbamate formation and dissociation were 1.1×10^{-2} s^{-1} and 4.88×10^{-3} s^{-1} respectively, which would yield intracellular fluxes of carbamate and bicarbonate of 4.4×10^{-4} mM s^{-1} and $1.46 \times 10^{-4} – 1.46 \times 10^{-2}$ mM s^{-1}, respectively. These rates are too slow compared to the modeled fluxes necessary to sustain the carbon fixation rate of the enzyme acetyl-CoA/propionyl-CoA carboxylase (2.168×10^{-1} mM s^{-1}), which are 5.067×10^{-1} mM s^{-1} for carbamate formation and 2.153×10^{-1} mM s^{-1} for carbamate dissociation. While it was not studied experimentally, the base-catalysis mechanism of CO_2 hydration exhibited by tertiary and sterically hindered amines may be a viable alternative

mechanism, since proton abstraction operates on much faster timescales than the rate of carbamate-forming and dissociating nucleophilic reactions. If this process is coupled to redox potentials present in copper-containing oxidoreductase enzymes responsible for electron transfer at the cell membrane, proton pumping could generate sufficient hydroxyl concentrations to quickly and preferentially produce HCO_3^- from diffusing CO_2. Future work should focus on further characterization of this alternative pathway in a biological context, as well as developing more quantitatively robust experimental methods in order to analyze reaction kinetics with more complex, biologically relevant amines, like larger peptides and transmembrane proteins.

While the metabolic mystery of carbon fixation in *N. maritimus* lives on, this study offers insight into the potential for simple organic autocatalytic reactions to catalyze early autotrophic cycles and serve as models for the evolution of carbon hydration enzymes like carbonic anhydrase, one of the most conserved structures across all domains of life on Earth. In this way, we can begin to understand and answer big, fundamental scientific questions about the origins of life by analyzing simple chemistry at the cellular and molecular level. Perhaps even the largest questions in science, on Earth, and in the universe can be answered by the tiniest creatures, living simply and quietly out in the open sea.

References

Bar-Even, A., Noor, E., Savir, Y., Liebermeister, W., Davidi, D., Tawfik, D. S., & Milo, R. (2011). The moderately efficient enzyme: Evolutionary and physicochemical trends shaping enzyme parameters. *Biochemistry*, *50*(21), 4402–4410. https://doi.org/10.1021/bi2002289

Bartoschek, S., Vorholt, J. A., Thauer, R. K., Geierstanger, B. H., & Griesinger, C. (2000). N-Carboxymethanofuran (carbamate) formation from methanofuran and CO 2 in methanogenic archaea Thermodynamics and kinetics of the spontaneous reaction. *European Journal of Biochemistry*, *267*(11), 3130–3138.

Barzagli, F., Giorgi, C., Mani, F., & Peruzzini, M. (2018). Reversible carbon dioxide capture by aqueous and non-aqueous amine-based absorbents: A comparative analysis carried out by 13C NMR spectroscopy. *Applied Energy*, *220*(January), 208–219. https://doi.org/10.1016/j.apenergy.2018.03.076

Berg, I. A., Kockelkorn, D., Ramos-Vera, W. H., Say, R. F., Zarzycki, J., Hügler, M., et al. (2010, June). Autotrophic carbon fixation in archaea. *Nature Reviews Microbiology*. https://doi.org/10.1038/nrmicro2365

Berg, J., Tymoczko, J., & Stryer, L. (2002). *Biochemistry, 5th edition*. *Biochemistry*.

Brochier-Armanet, C., Gribaldo, S., & Forterre, P. (2012). Spotlight on the Thaumarchaeota. *ISME Journal*, *6*(2), 227–230. https://doi.org/10.1038/ismej.2011.145

Caplow, M. (1968). Kinetics of Carbamate Formation and Breakdown. *Journal of the American Chemical Society*, *90*(24), 6795–6803. https://doi.org/10.1021/ja01026a041

Chipperfield, J. R. (1966). The kinetics of combination of carbon dioxide with the anions of glycine, glycyl-glycine, and related amino acids. *Proceedings of the Royal Society of London. Series B, Containing Papers of a Biological Character. Royal Society (Great Britain)*, *164*(996), 401–410. https://doi.org/10.1098/rspb.1966.0040

Ciftja, A. F., Hartono, A., & Svendsen, H. F. (2014). Amine neutralized amino acid as CO2 absorbents: A quantitative 13C-NMR study. *International Journal of Greenhouse Gas Control*, *27*, 169–177. https://doi.org/10.1016/j.ijggc.2014.05.011

Couchaux, G., Barth, D., Jacquin, M., Faraj, A., & Grandjean, J. (2014). Kinetics of Carbon Dioxide with Amines. I. Stopped-Flow Studies in Aqueous Solutions. A Review. *Oil and Gas Science and Technology*, *69*(5), 865–884. https://doi.org/10.2516/ogst/2013150

Crawley, M. J. (2007). Chapter 20 - Non-linear Regression. *The R Book*, 661–684.

Davis, B. D. (1958). On the Importance of Being Ionized. *Archives of Biochemistry and Biophysics*, *78*, 497–509.

Fuchs, G. (2011). *Alternative Pathways of Carbon Dioxide Fixation: Insights into the Early Evolution of Life? Annual Review of Microbiology* (Vol. 65). https://doi.org/10.1146/annurev-micro-090110-102801

Gros, G., Forster, R. E., & Lin, L. (1976). The carbamate reaction of glycylglycine, plasma, and tissue extracts evaluated by a pH stopped flow apparatus. *Journal of Biological Chemistry*, *251*(14), 4398–4407.

Holmes, P. E., Naaz, M., & Poling, B. E. (1998). Ion concentrations in the CO2-NH3-H2O system from13C NMR spectroscopy. *Industrial and Engineering Chemistry Research*, *37*(8), 3281–3287. https://doi.org/10.1021/ie9707782

Hügler, M., Krieger, R. S., Jahn, M., & Fuchs, G. (2003). Characterization of acetyl-CoA/propionyl-CoA carboxylase in Metallosphaera sedula: Carboxylating enzyme in the 3-

hydroxypropionate cycle for autotrophic carbon fixation. *European Journal of Biochemistry*, *270*(4), 736–744. https://doi.org/10.1046/j.1432-1033.2003.03434.x

Johnson, S. L., & Morrison, D. L. (1972). Kinetics and Mechanism of Decarboxylation of N-Arylcarbamates. Evidence for Kinetically Important Zwitterionic Carbamic Acid Species of Short Lifetime. *Journal of the American Chemical Society*, *94*(4), 1323–1334. https://doi.org/10.1021/ja00759a045

Keller, M. A., Piedrafita, G., & Ralser, M. (2015). The widespread role of non-enzymatic reactions in cellular metabolism. *Current Opinion in Biotechnology*, *34*, 153–161. https://doi.org/10.1016/j.copbio.2014.12.020

Kerou, M., Offre, P., Valledor, L., Abby, S. S., Melcher, M., Nagler, M., et al. (2016). Proteomics and comparative genomics of Nitrososphaera viennensis reveal the core genome and adaptations of archaeal ammonia oxidizers. *Proceedings of the National Academy of Sciences of the United States of America*, *113*(49), E7937–E7946. https://doi.org/10.1073/pnas.1601212113

Könneke, M., Bernhard, A. E., De La Torre, J. R., Walker, C. B., Waterbury, J. B., & Stahl, D. A. (2005). Isolation of an autotrophic ammonia-oxidizing marine archaeon. *Nature*, *437*(7058), 543–546. https://doi.org/10.1038/nature03911

Könneke, M., Schubert, D. M., Brown, P. C., Hügler, M., Standfest, S., Schwander, T., et al. (2014). Ammonia-oxidizing archaea use the most energy-efficient aerobic pathway for CO2 fixation. *Proceedings of the National Academy of Sciences of the United States of America*, *111*(22), 8239–8244. https://doi.org/10.1073/pnas.1402028111

Kortunov, P. V., Siskin, M., Baugh, L. S., & Calabro, D. C. (2015). In Situ Nuclear Magnetic Resonance Mechanistic Studies of Carbon Dioxide Reactions with Liquid Amines in Aqueous Systems: New Insights on Carbon Capture Reaction Pathways. *Energy and Fuels*, *29*(9), 5919–5939. https://doi.org/10.1021/acs.energyfuels.5b00850

Li, Q., & Canvin, D. T. (1998). Energy Sources for HCO3- and CO2 Transport in Air-Grown Cells of Synechococcus UTEX 625. *Plant Physiology*, *116*(3), 1125–1132. https://doi.org/10.1104/pp.116.3.1125

Littel, R. J., Van Swaaij, W. P. M., & Versteeg, G. F. (1990). Kinetics of Carbon Dioxide with tertiary Amines in aqueous solution. *AIChE Journal*, *36*(11), 1633–1640. https://doi.org/10.1002/aic.690361103

Lorimer, G. H. (1983). Carbon dioxide and carbamate formation: the makings of a biochemical control system. *Trends in Biochemical Sciences*, *8*(2), 65–68. https://doi.org/10.1016/0968-0004(83)90393-6

Mani, F., Peruzzini, M., & Stoppioni, P. (2006). CO2 absorption by aqueous NH3 solutions: Speciation of ammonium carbamate, bicarbonate and carbonate by a 13C NMR study. *Green Chemistry*, *8*(11), 995–1000. https://doi.org/10.1039/b602051h

Marshall, M. (2020). He may have found the key to the origins of life. So why have so few heard of him? *National Geographic*, Dec. 14th, 2020. Accessed on March 17th, 2021. https://www.nationalgeographic.com/science/article/he-may-have-found-the-key-to-origins-of-life-tibor-ganti-chemoton

Martens-Habbena, W., Berube, P. M., Urakawa, H., De La Torre, J. R., & Stahl, D. A. (2009). Ammonia oxidation kinetics determine niche separation of nitrifying Archaea and Bacteria. *Nature*, *461*(7266), 976–979. https://doi.org/10.1038/nature08465

O'Neill, D. P., & Robbins, P. A. (2017). A mechanistic physicochemical model of carbon dioxide transport in blood. *Journal of Applied Physiology*, *122*(2), 283–295.

https://doi.org/10.1152/japplphysiol.00318.2016
Offre, P., Kerou, M., Spang, A., & Schleper, C. (2014). Variability of the transporter gene complement in ammonia-oxidizing archaea. *Trends in Microbiology*, *22*(12), 665–675. https://doi.org/10.1016/j.tim.2014.07.007
Ogawa, T., & Mi, H. (2007). Cyanobacterial NADPH dehydrogenase complexes. *Photosynthesis Research*, *93*(1–3), 69–77. https://doi.org/10.1007/s11120-006-9128-y
Otte, J., Mall, A., Schubert, D. M., Könneke, M., & Berg, I. A. (2015). Malonic semialdehyde reductase from the archaeon Nitrosopumilus maritimus is involved in the autotrophic 3-hydroxypropionate/4- hydroxybutyrate cycle. *Applied and Environmental Microbiology*, *81*(5), 1700–1707. https://doi.org/10.1128/AEM.03390-14
Pearson, A., Hurley, S. J., Elling, F. J., & Wilkes, E. B. (2019). CO2-dependent carbon isotope fractionation in Archaea, Part I: Modeling the 3HP/4HB pathway. *Geochimica et Cosmochimica Acta*, *261*, 368–382. https://doi.org/10.1016/j.gca.2019.06.042
Perinu, C., Arstad, B., & Jens, K. J. (2013). 13CNMR experiments and methods used to investigate amine-CO 2-H2O systems. *Energy Procedia*, *37*(1876), 7310–7317. https://doi.org/10.1016/j.egypro.2013.06.669
Perinu, C., Arstad, B., Bouzga, A. M., Svendsen, J. A., & Jens, K. J. (2014a). NMR-based carbamate decomposition constants of linear primary alkanolamines for CO2 capture. *Industrial and Engineering Chemistry Research*, *53*(38), 14571–14578. https://doi.org/10.1021/ie5020603
Perinu, C., Arstad, B., Bouzga, A. M., Svendsen, J. A., & Jens, K. J. (2014b). NMR-based carbamate decomposition constants of linear primary alkanolamines for CO2 capture. *Industrial and Engineering Chemistry Research*, *53*(38), 14571–14578. https://doi.org/10.1021/ie5020603
Perrin, C. L. (2017). Linear or Nonlinear Least-Squares Analysis of Kinetic Data? *Journal of Chemical Education*, *94*(6), 669–672. https://doi.org/10.1021/acs.jchemed.6b00629
Pesci, L., Gurikov, P., Liese, A., & Kara, S. (2017). Amine-Mediated Enzymatic Carboxylation of Phenols Using CO2 as Substrate Increases Equilibrium Conversions and Reaction Rates. *Biotechnology Journal*, *12*(12), 1–8. https://doi.org/10.1002/biot.201700332
Preiner, M., Xavier, J. C., Do Nascimento Vieira, A., Kleinermanns, K., Allen, J. F., & Martin, W. F. (2019). Catalysts, autocatalysis and the origin of metabolism. *Interface Focus*, *9*(6), 1–8. https://doi.org/10.1098/rsfs.2019.0072
Preiner, M., Igarashi, K., Muchowska, K. B., Yu, M., Varma, S. J., Kleinermanns, K., et al. (2020). A hydrogen-dependent geochemical analogue of primordial carbon and energy metabolism. *Nature Ecology and Evolution*, *4*(4), 534–542. https://doi.org/10.1038/s41559-020-1125-6
Qin, W., Amin, S. A., Lundeen, R. A., Heal, K. R., Martens-Habbena, W., Turkarslan, S., et al. (2018). Stress response of a marine ammonia-oxidizing archaeon informs physiological status of environmental populations. *ISME Journal*, *12*(2), 508–519. https://doi.org/10.1038/ismej.2017.186
Ruiz-Mirazo, K., Briones, C., & De La Escosura, A. (2014). Prebiotic systems chemistry: New perspectives for the origins of life. *Chemical Reviews*, *114*(1), 285–366. https://doi.org/10.1021/cr2004844
Santoro, A. E., & Casciotti, K. L. (2011). Enrichment and characterization of ammonia-oxidizing archaea from the open ocean: Phylogeny, physiology and stable isotope fractionation. *ISME Journal*, *5*(11), 1796–1808. https://doi.org/10.1038/ismej.2011.58
Smith, K. S., & Ferry, J. G. (2000). Prokaryotic carbonic anhydrases. *FEMS Microbiology*

Reviews, *24*(4), 335–366. https://doi.org/10.1016/S0168-6445(00)00030-9

Stowe, H. M., Vilčiauskas, L., Paek, E., & Hwang, G. S. (2015). On the origin of preferred bicarbonate production from carbon dioxide (CO2) capture in aqueous 2-amino-2-methyl-1-propanol (AMP). *Physical Chemistry Chemical Physics*, *17*(43), 29184–29192. https://doi.org/10.1039/c5cp04876a

Terrier, P., & Douglas, D. J. (2010). Carbamino group formation with peptides and proteins studied by mass spectrometry. *Journal of the American Society for Mass Spectrometry*, *21*(9), 1500–1505. https://doi.org/10.1016/j.jasms.2010.05.008

Vaidya, P. D., & Kenig, E. Y. (2007). CO2-alkanolamine reaction kinetics: A review of recent studies. *Chemical Engineering and Technology*, *30*(11), 1467–1474. https://doi.org/10.1002/ceat.200700268

Valentine, D. L. (2007). Adaptations to energy stress dictate the ecology and evolution of the Archaea. *Nature Reviews Microbiology*, *5*(4), 316–323. https://doi.org/10.1038/nrmicro1619

Walker, C. B., De La Torre, J. R., Klotz, M. G., Urakawa, H., Pinel, N., Arp, D. J., et al. (2010). Nitrosopumilus maritimus genome reveals unique mechanisms for nitrification and autotrophy in globally distributed marine crenarchaea. *Proceedings of the National Academy of Sciences of the United States of America*, *107*(19), 8818–8823. https://doi.org/10.1073/pnas.0913533107

Wilkes, E. B., & Pearson, A. (2019). A general model for carbon isotopes in red-lineage phytoplankton : Interplay between unidirectional processes and fractionation by RubisCO. *Geochimica et Cosmochimica Acta*, *265*, 163–181. https://doi.org/10.1016/j.gca.2019.08.043

Wlasichuk, K. B., Tan, L., Guo, Y., Hildebrandt, D. J., Zhang, H., Karr, D. E., & Schmidt, D. E. (2015). Determination of equilibrium constant of amino carbamate adduct formation in sisomicin by a high pH based high performance liquid chromatography. *Journal of Pharmaceutical and Biomedical Analysis*, *111*, 126–130. https://doi.org/10.1016/j.jpba.2015.03.033

Yu, W. C., Astarita, G., & Savage, D. W. (1985). Kinetics of carbon dioxide absorption in solutions of methyldiethanolamine. *Chemical Engineering Science*, *40*(8), 1585–1590. https://doi.org/10.1016/0009-2509(85)80101-9

Zeebe, R. E. (2014). Kinetic fractionation of carbon and oxygen isotopes during hydration of carbon dioxide. *Geochimica et Cosmochimica Acta*, *139*, 540–552. https://doi.org/10.1016/j.gca.2014.05.005

Zeebe, R. E., & Wolf-Gladrow, D. (2001). *CO2 in Seawater: Equilibrium, Kinetics, Isotopes*. *Elsevier Oceanography Series* (Vol. 65).

Appendix I: Supplementary Data

NMR Spectra

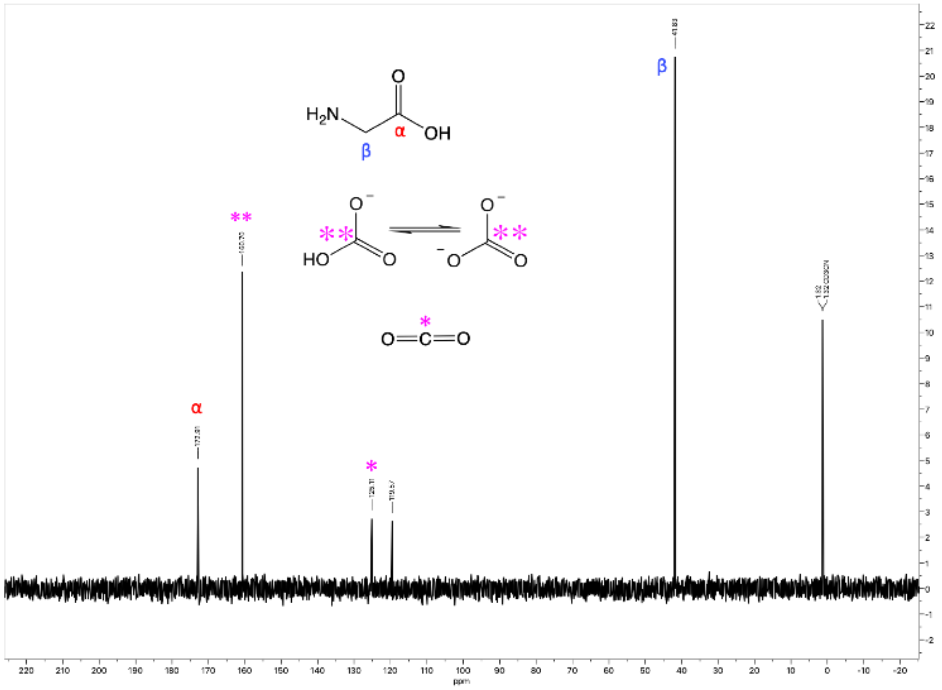

Figure S1. A sample ^{13}C NMR spectrum from the Glycine 2 experiment. Labeled peak assignments are as follows: dissolved bicarbonate/carbonate ion species (160.70 ppm), aqueous carbon dioxide (125.11 ppm), the glycine alpha and beta carbons (172.91, 41.83 ppm), and the acetonitrile carbons (119.54, 1.32 ppm).

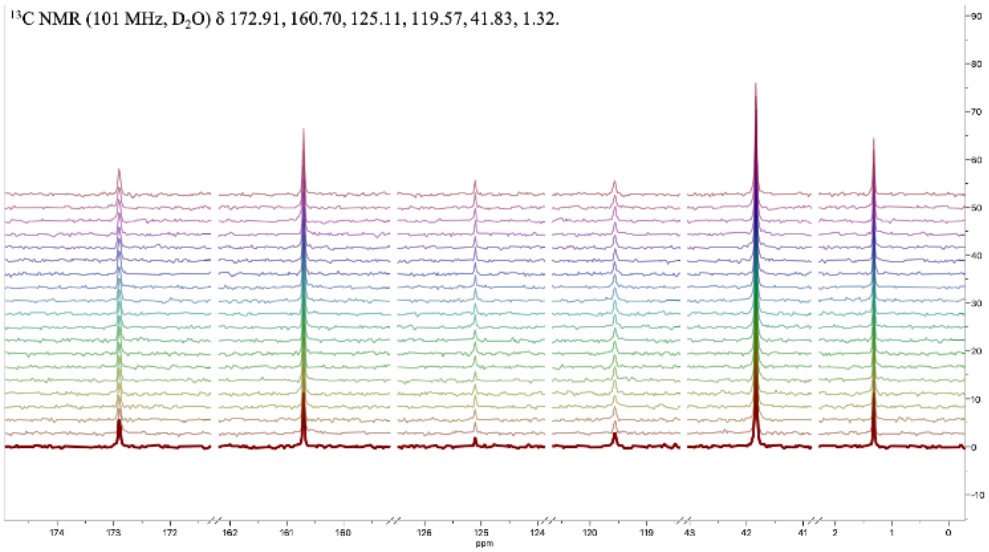

Figure S2. Glycine 2 experiment stacked spectral timeseries, depicting spectra at sixteen minute intervals over the course of 320 minutes of measurement. The bottom-most spectrum is the first measurement, going forward in time to the final measurement, the top-most spectrum.

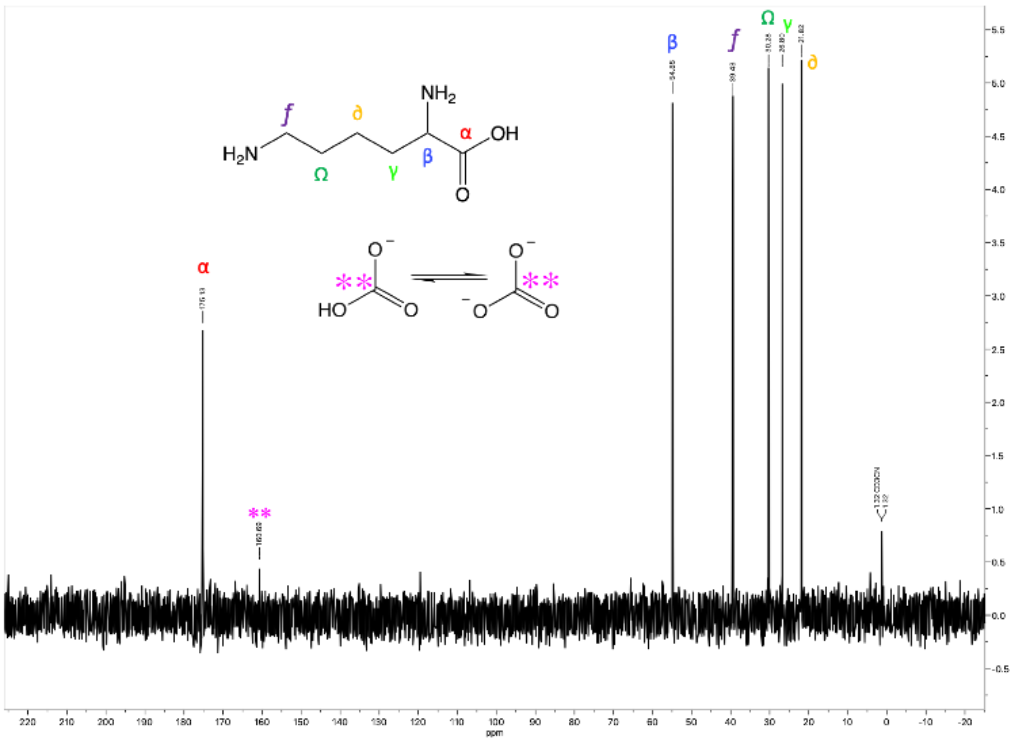

Figure S3. A sample ^{13}C NMR spectrum from the lysine experiment. Labeled peak assignments are as follows: dissolved bicarbonate/carbonate ion species (160.69 ppm), the lysine carbons (175.13, 54.85, 39.43, 30.28, 25.80, 21.82 ppm), and the acetonitrile carbon (1.32 ppm; the chemical shift at 119 was undetected).

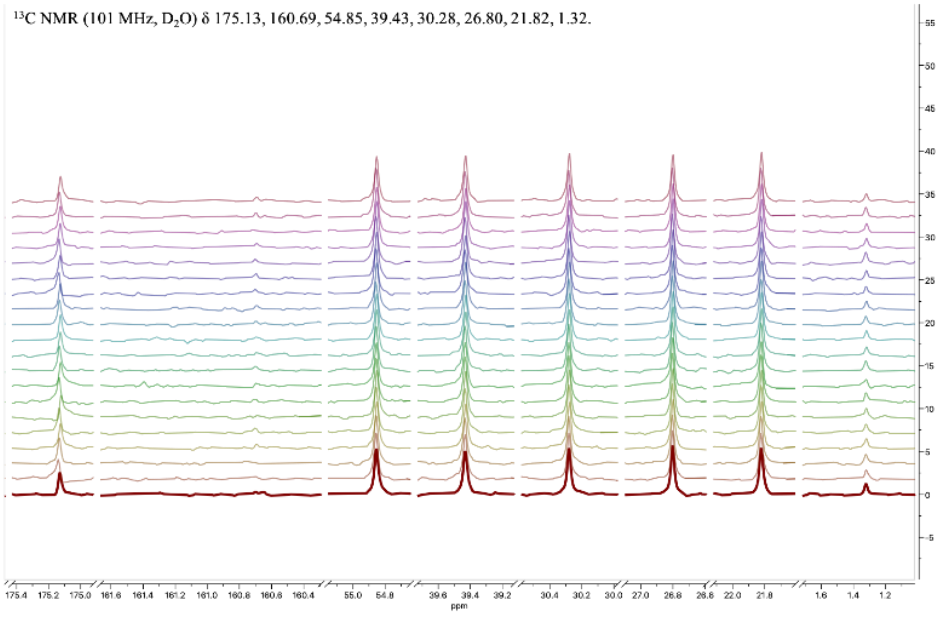

Figure S4. Lysine experiment stacked spectral timeseries, depicting spectra at sixteen minute intervals over the course of 320 minutes of measurement. The bottom-most spectrum is the first measurement, going forward in time to the final measurement, the top-most spectrum.

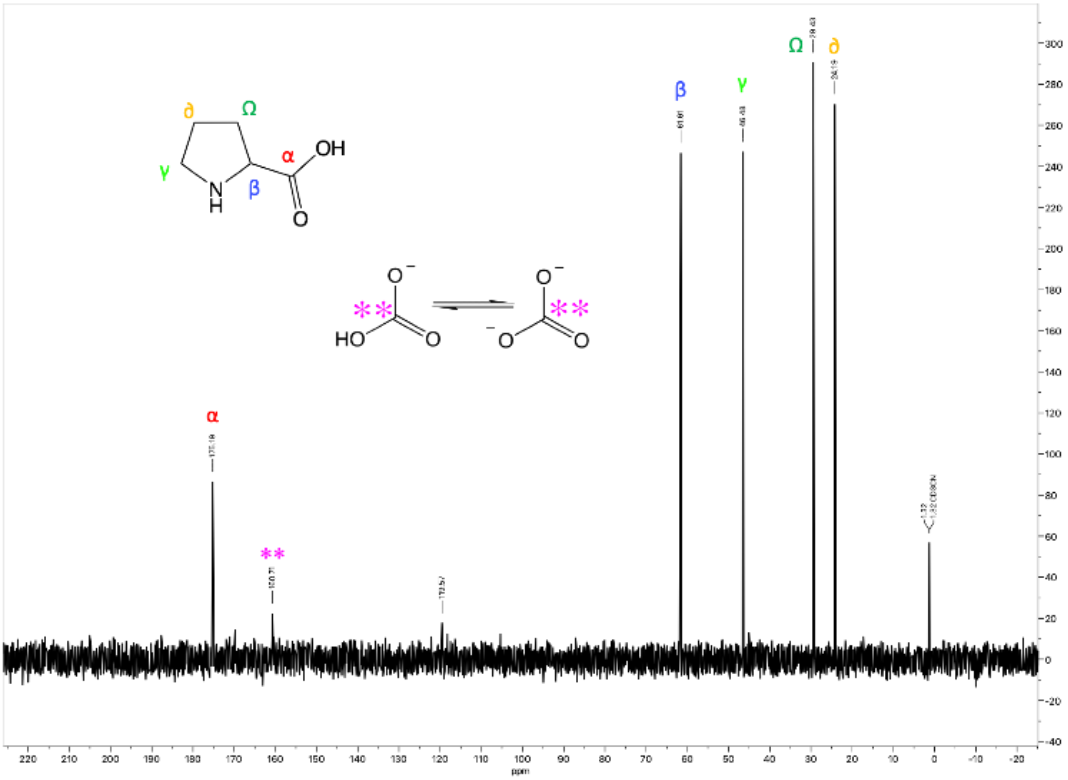

Figure S5. A sample ^{13}C NMR spectrum from the proline experiment. Labeled peak assignments are as follows: dissolved bicarbonate/carbonate ion species (160.71ppm), the proline carbons (175.19, 61.61, 45.48, 29.43, 24.19 ppm), and the acetonitrile carbon (119.57, 1.32 ppm).

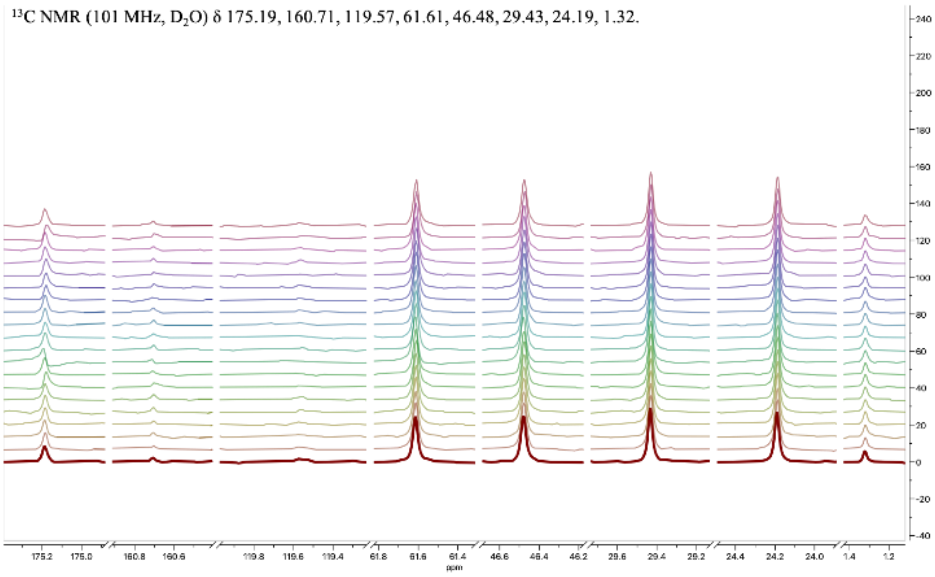

Figure S6. Proline experiment stacked spectral timeseries, depicting spectra at sixteen minute intervals over the course of 320 minutes of measurement. The bottom-most spectrum is the first measurement, going forward in time to the final measurement, the top-most spectrum.

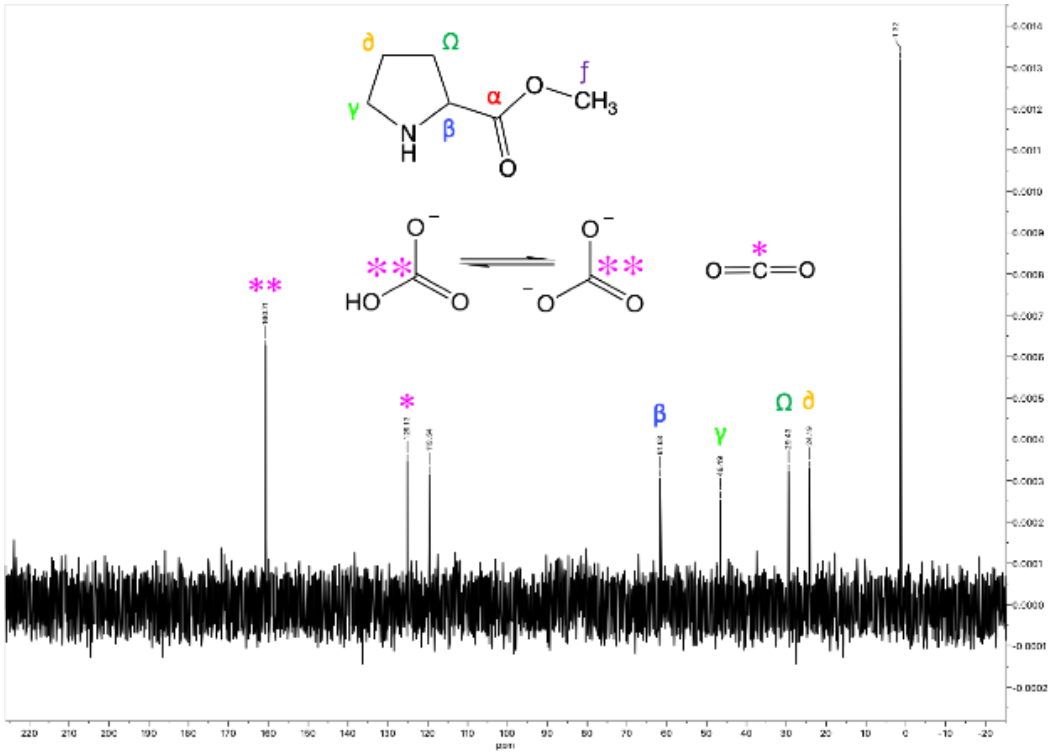

Figure S7. A sample 13C NMR spectrum from the proline methyl ester experiment. Labeled peak assignments are as follows: dissolved bicarbonate/carbonate ion species (160.71ppm), aqueous CO_2 (125.12 ppm), the proline carbons (61.63, 45.49, 29.43, 24.19 ppm), and the acetonitrile carbons (119.57, 1.32 ppm). The carbonyl carbon (alpha) and the methyl carbon (f) were not detected.

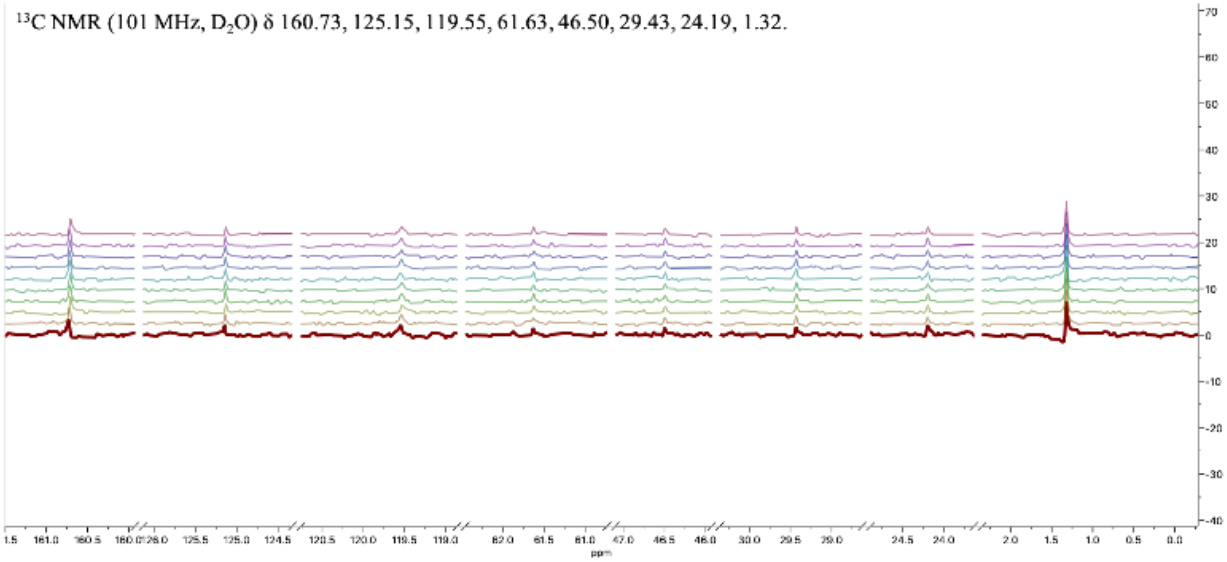

Figure S8. Proline methyl ester experiment stacked spectral timeseries, depicting spectra at sixteen minute intervals over the course of 160 minutes of measurement. The bottom-most spectrum is the first measurement, going forward in time to the final measurement, the top-most spectrum.

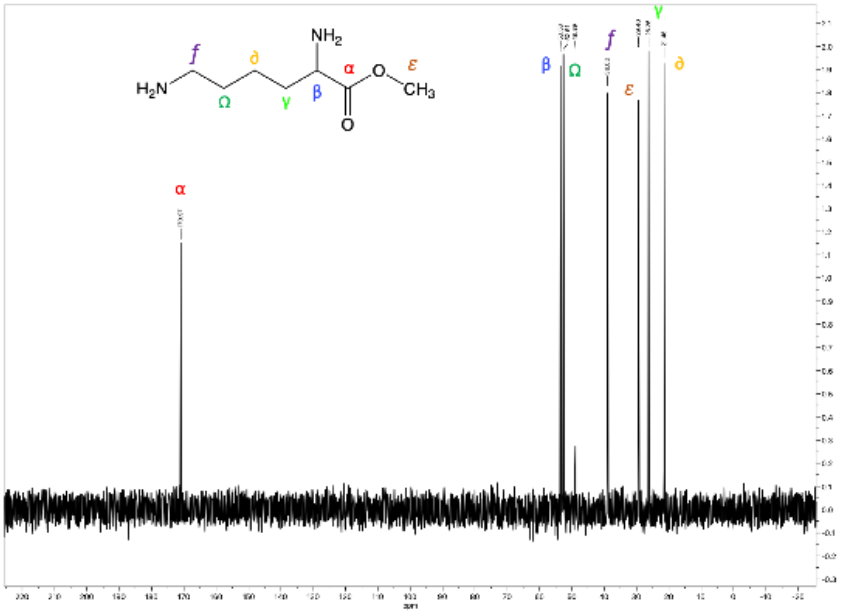

Figure S9. A sample 13C NMR spectrum from the lysine methyl ester experiment. Labeled peak assignments are as follows: lysine methyl ester carbons (170.97, 53.53, 52.61, 39, 29.40, 26.26, 21.46 ppm). No other carbon species were detected, including the internal reference standard, most likely due to a poor signal:noise ratio.

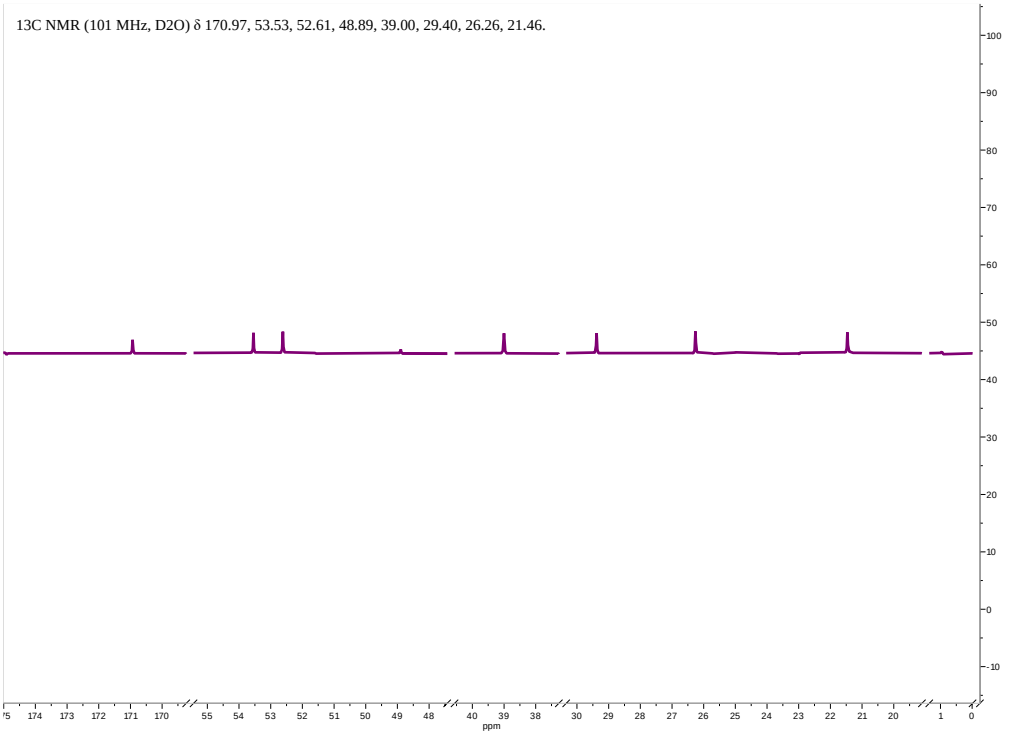

Figure S10. Lysine methyl ester experiment stacked spectral timeseries, depicting spectra at sixteen minute intervals over the course of 160 minutes of measurement. The bottom-most spectrum is the first measurement, going forward in time to the final measurement, the top-most spectrum.

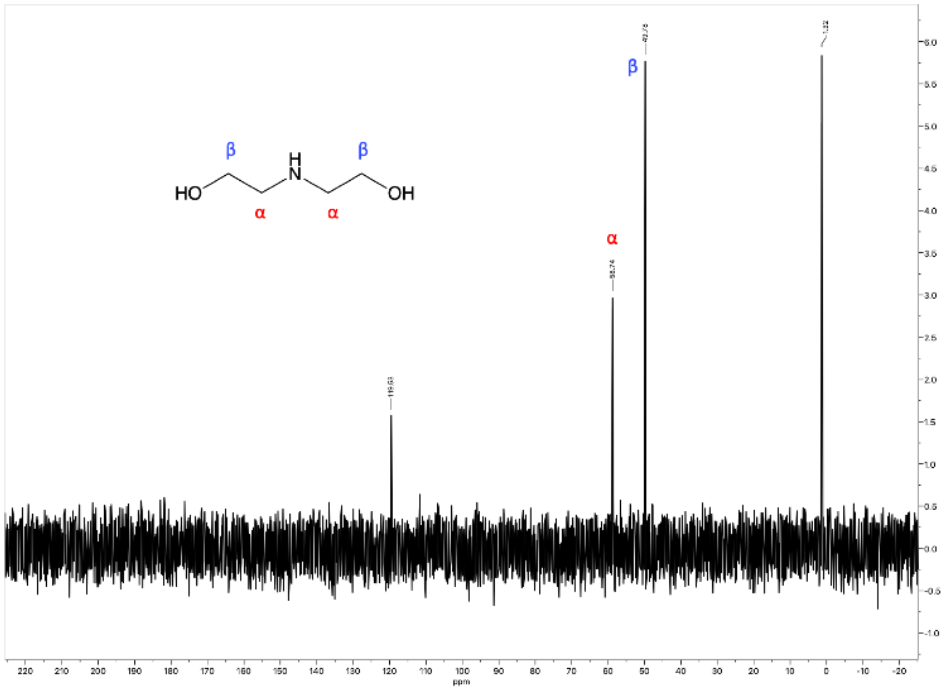

Figure S11. A sample 13C NMR spectrum from the diethanolamine experiment. Labeled peak assignments are as follows: diethanolamine carbons (58.74 and 49.76 ppm) and the acetonitrile carbons (119.57, 1.32 ppm). No other carbon species were detected, most likely due to a low signal:noise ratio.

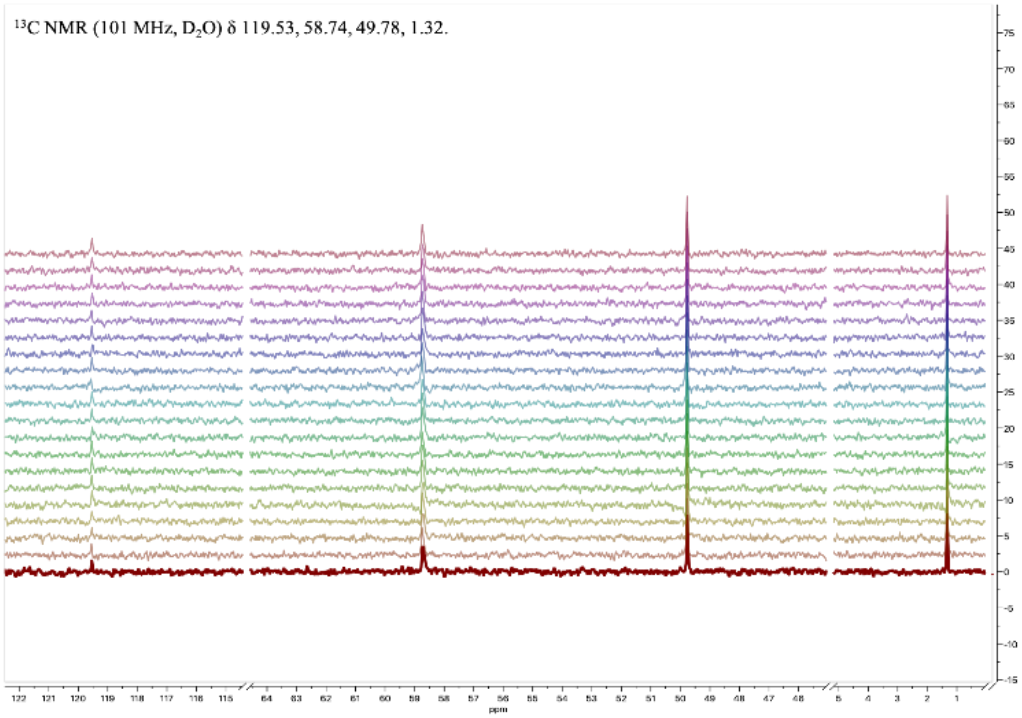

Figure S12. Diethanolamine experiment stacked spectral timeseries, depicting spectra at sixteen minute intervals over the course of 160 minutes of measurement. The bottom-most spectrum is the first measurement, going forward in time to the final measurement, the top-most spectrum.

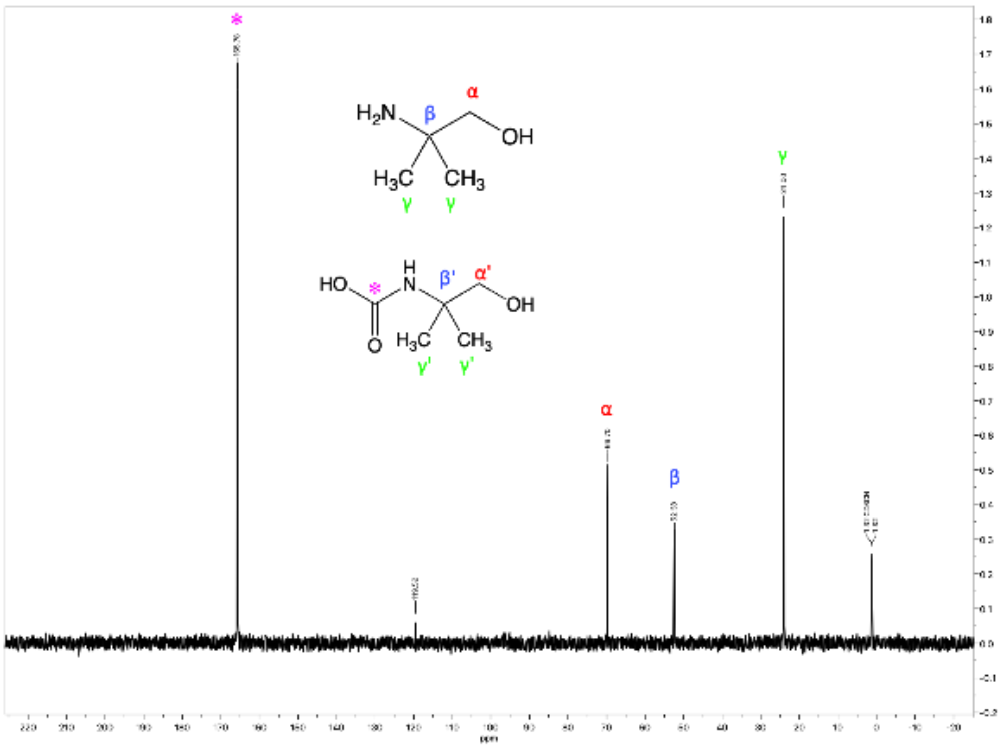

Figure S13. A sample 13C NMR spectrum from the 2-amino-2-methyl-1-propanol (AMP) experiment. Labeled peak assignments are as follows: carbamate (165.78 ppm), AMP carbons (69.70, 52.38, and 24.00 ppm) and the acetonitrile carbons (119.57, 1.32 ppm).

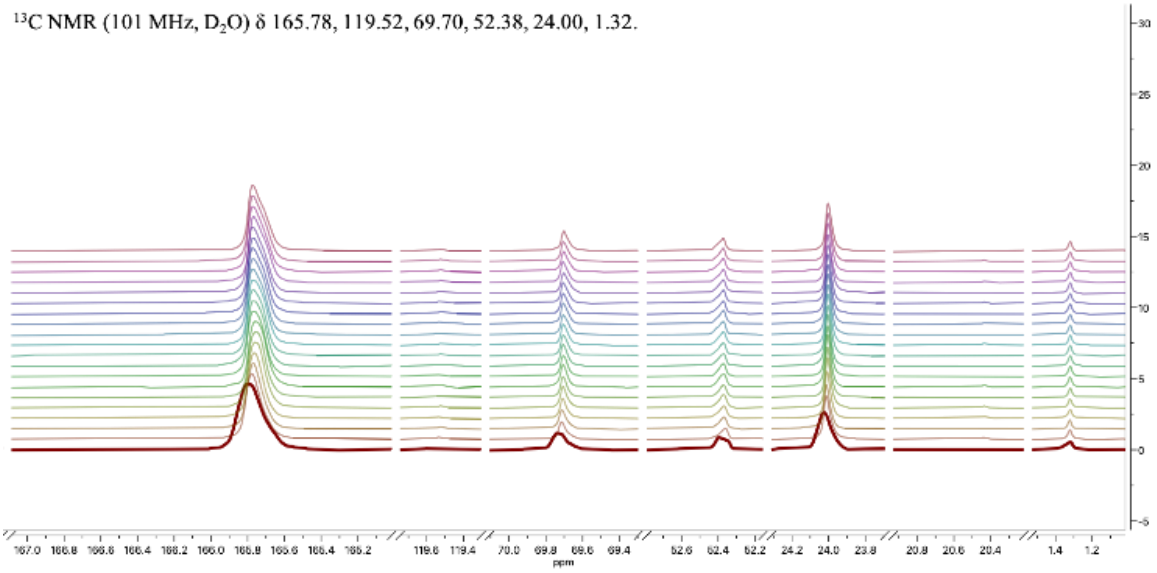

Figure S14. AMP experiment stacked spectral timeseries, depicting spectra at sixteen minute intervals over the course of 160 minutes of measurement. The bottom-most spectrum is the first measurement, going forward in time to the final measurement, the top-most spectrum.

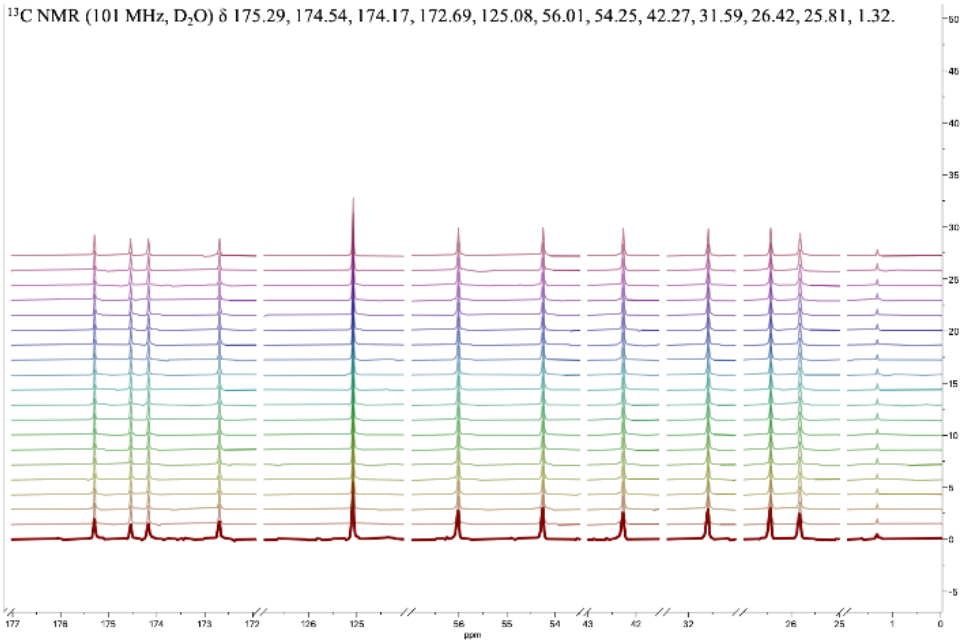

Figure S15. Glutathione experiment stacked spectral timeseries, depicting spectra at sixteen minute intervals over the course of 160 minutes of measurement. The bottom-most spectrum is the first measurement, going forward in time to the final measurement, the top-most spectrum.

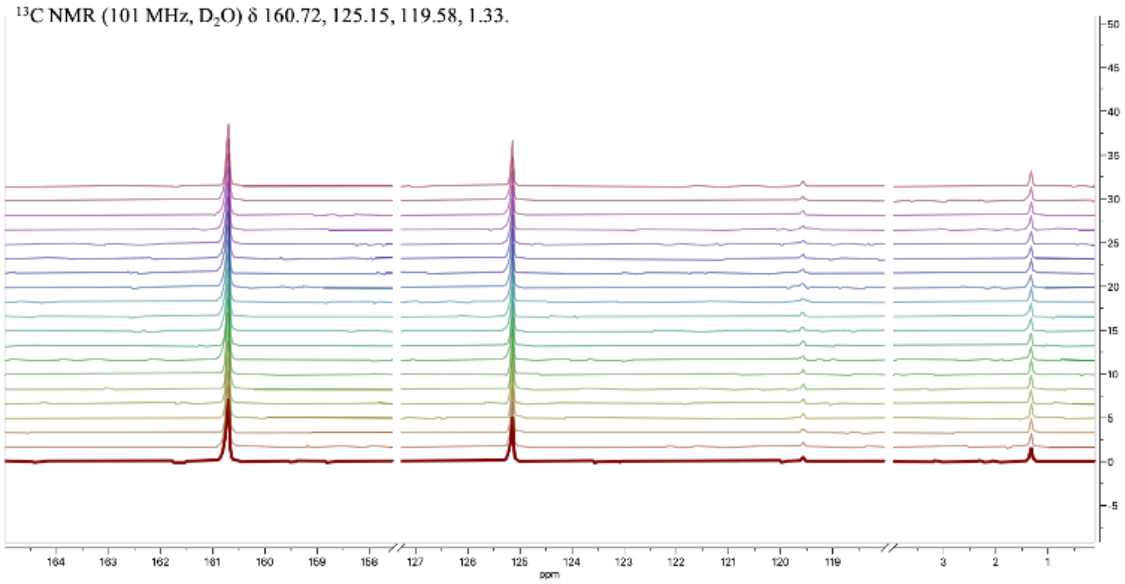

Figure S16. Cytochrome C experiment stacked spectral timeseries, depicting spectra at sixteen minute intervals over the course of 160 minutes of measurement. The bottom-most spectrum is the first measurement, going forward in time to the final measurement, the top-most spectrum.

Appendix II: Glossary

Anabolic: relating to an endergonic (energy-consuming) metabolic process that constructs molecules from smaller units

Carbonyl: a functional group consisting of a carbon atom double-bonded to an oxygen atom containing the strongly electrophilic $\pi^*_{C\text{-}O}$ antibonding orbital

Carboxylation: a reaction in which the addition of CO_2 to a substrate forms a carboxylic acid

Decarboxylation: the opposite of carboxylation; a reaction that removes a carboxyl group to release CO_2

Dehydration: the reverse of hydration; a reaction involving the loss of water from a substrate; also called a condensation reaction

Electrophile/electrophilic: a chemical species that accepts an electron pair to form a chemical bond in a reaction (like a Lewis acid)

Hydration: a reaction in which a substrate combines with water

Hydroxylation: the oxidative addition of a hydroxyl group to a substrate

Nucleophile/nucleophilic: relating to a nucleophile, or a chemical species that donates an electron pair to form a chemical bond in a reaction (like a Lewis base)

pKa: the negative log of the acid dissociation constant of an acid, used to determine the strength of an acid (an acid with a low pKa is strong; a base whose conjugate acid has a low pKa is weak)

Primary amine: an amine species in which one of the three hydrogens bonded to ammonia is replaced by an alkyl or aromatic group (more simply: a nitrogen bonded to two hydrogens and a carbon atom)

Secondary amine: an amine species in which two of the three hydrogens bonded to ammonia is replaced by an alkyl or aromatic group (more simply: a nitrogen bonded to one hydrogen and two carbon atoms)

Sterically hindered: a molecule whose structure inhibits it from participating in chemical reactions due to physical nonbonding interactions between the molecule and substrates

Tertiary amine: an amine species in which three of the three hydrogens bonded to ammonia is replaced by an alkyl or aromatic group (more simply: a nitrogen bonded to three carbon atoms)

Zwitterionic/zwitterion: a compound with one positively charged functional group and one negatively charged functional group such that the net charge is neutral (for example: an amino acid is a zwitterion because it contains positively charged ammonia and negatively charged carboxylate)

Appendix III: Alternative Thesis Titles

A Geoscience Major Pretends To Be a Biochemist for a Year

How To Write A Thesis That Barely Qualifies for an Engineering Degree

From Ocean Farts to Origins of Life: The Evolution of A Thesis in a Pandemic

Please Just Give Me A Degree From Harvard Zoomiversity

How To Write A Musical Instead of A Thesis: A Study in Creative Procrastination

COVID-19: You're the Worst!

School of Rocks: The Sequel

HPT 173: Sit Cohors Prosperatur

I Can't Believe Ann and Susie Left Me Alone with the Vac Line with a Tank of Expensive Pressurized CO_2 and Like Five Dewars of Liquid Nitrogen and I Didn't Blow Up the Entire Lab

The Great Gas Escape

Elida Plays With a Really Big Magnet

Magnets: How Do They Work?!

Elida Spends Way Too Much Time Writing These Hilarious Jokes Instead of Writing Her Thesis

How to Pass Off Carbon Capture Research as Biology 101

Laughing at the Word "Promiscuous Enzyme" for like 10,000 Hours

My Chemical Intuition

How to Convince Your Parents That Studying Obscure Archaea Will Get You Into Med School

Writing A Thesis on Reaction Kinetics: An MCAT Study Guide

How to Turn Your STEM Thesis into Creative Writing: A Masterclass in Science Fiction

Good Grief Charlie Brown, Am I A Scientist Yet?!